GEMS & GEMOLOGY

VOLUME XXXII WINTER 1996

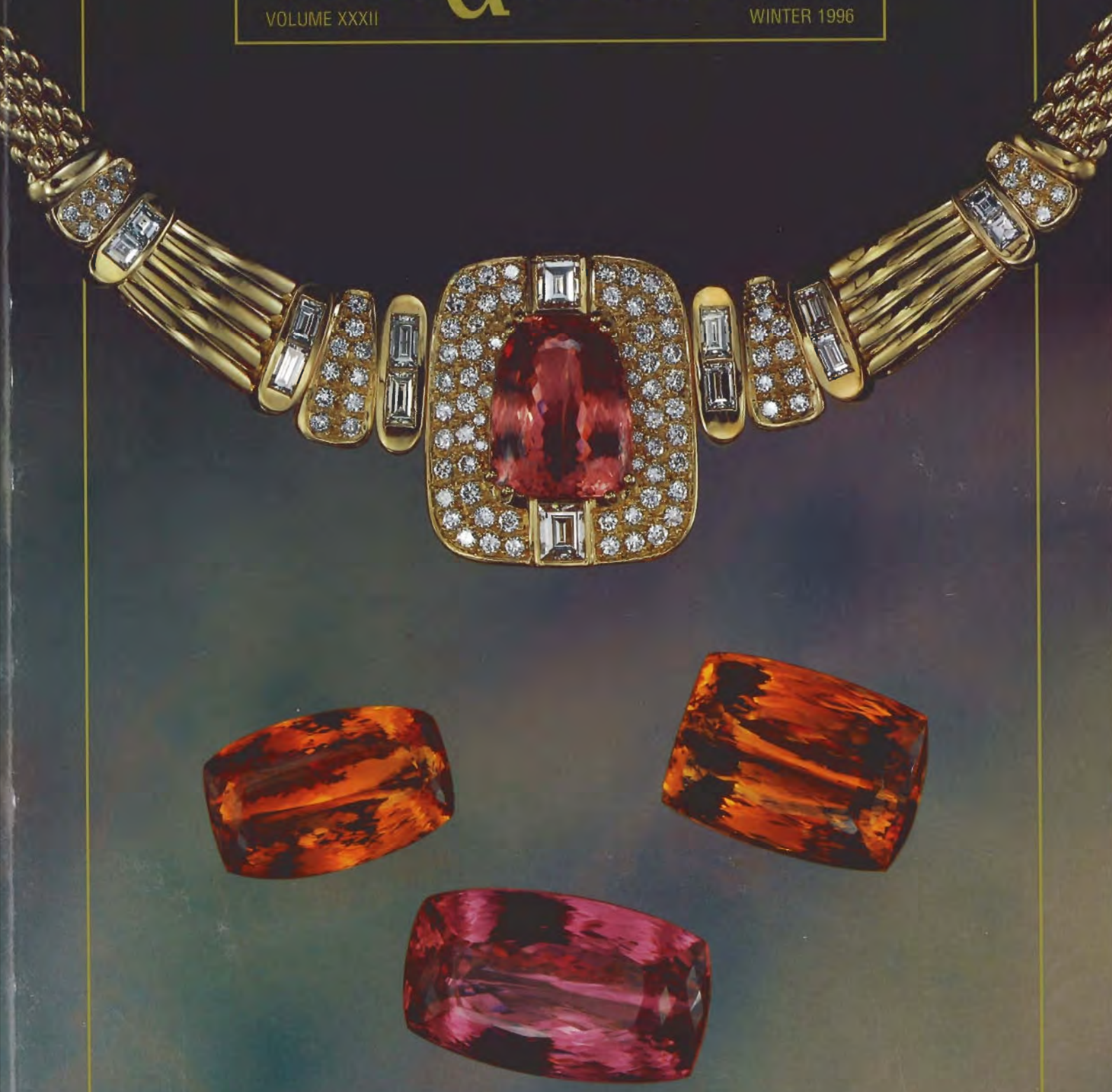

THE QUARTERLY JOURNAL OF THE GEMOLOGICAL INSTITUTE OF AMERICA

GEMS & GEMOLOGY

WINTER 1996 VOLUME 32 NO. 4

TABLE OF CONTENTS

pg. 233

pg. 249

pg. 257

pg. 264

ABOUT THE COVER: The historic Ouro Preto region of Minas Gerais, Brazil, is world-renown for the fine topazes that have been produced there for more than two centuries. Today, the Capão mine is one of the most productive in the region. This mine and the superb topazes produced there are described in the article by D. Sauer and colleagues in this issue. Marketed as "Imperial" topaz in the trade, the Ouro Preto topazes come in a broad range of hues, some of which are illustrated here. The fancy-cut topaz in the necklace weighs 24.13 ct; the three loose topazes weigh (from left to right) 44.11, 71.21, and 66.66 ct, respectively. Courtesy of Amsterdam Sauer Company, Brazil.

Photo © Harold & Erica Van Pelt—Photographers, Los Angeles, CA.

Color separations for Gems & Gemology *are by Effective Graphics, Compton, CA. Printing is by Cadmus Journal Services, Baltimore, MD.*

ISSN 0016-626X

GEMS & GEMOLOGY

SUBSCRIPTIONS

Subscriptions to addresses in the U.S.A. are priced as follows: $64.95 for one year (4 issues), $164.95 for three years (12 issues). Subscriptions sent elsewhere are $75.00 for one year, $195.00 for three years.

Special annual subscription rates are available for all students actively involved in a GIA program: $54.95 to addresses in the U.S.A.; $65.00 elsewhere. Your student number *must* be listed at the time your subscription is entered.

Single issues may be purchased for $16.50 in the U.S.A., $21 .00 elsewhere. Discounts are given for bulk orders of 10 or more of any one issue. A limited number of back issues of *G&G* are also available for purchase. Please address all inquiries regarding subscriptions and the purchase of single copies or back issues to the Subscriptions Department.

To obtain a Japanese translation of *Gems & Gemology*, contact the Association of Japan Gem Trust, Okachimachi Cy Bldg., 5-15-14 Ueno, Taito-ku, Tokyo 110, Japan. Our Canadian goods and service registration number is 126142892RT.

MANUSCRIPT SUBMISSIONS

Gems & Gemology welcomes the submission of articles on all aspects of the field. Please see the Guidelines for Authors in the Summer 1996 issue of the journal, or contact the editor for a copy. Letters on articles published in *Gems & Gemology* and other relevant matters are also welcome.

Gems & Gemology is published quarterly by the Gemological Institute of America, a nonprofit educational organization for the jewelry industry, 1660 Stewart Street, Santa Monica, CA 90404.

Postmaster: Return undeliverable copies of *Gems & Gemology* to 1660 Stewart Street, Santa Monica, CA 90404.

In Honor of Robert C. Kammerling

We are dedicating this issue to the late Robert C. Kammerling. At the time of his tragic death in January 1996, Bob was an associate editor, a member of the Editorial Review Board, co-editor of both the Gem News and Gem Trade Lab Notes sections, and one of *Gems & Gemology*'s most prolific authors. In fact, the Fall 1994 article "An Update on Filled Diamonds," of which he was first author, won both the *Gems & Gemology* Most Valuable Article award and a national award for best scientific article. A superb writer, a brilliant information gatherer, and a true friend to gemology, Bob had a tremendous impact on the journal and on gemology as a whole.

We were very pleased with the response to our request for articles for this *Gems & Gemology* issue honoring Bob. Papers were submitted from all over the world: Brazil, France, Germany, Great Britain, Myanmar, the Netherlands, Russia, Switzerland, and the United States. Although we could not publish all of the articles in one issue because of space and time constraints, this broad involvement speaks to the respect held for Bob internationally.

Indeed, Bob Kammerling was the gemologist's gemologist. He liked gem oddities—whether natural, treated, or manufactured. Such oddities are well-represented in this issue: Unusual gem materials from Sri Lanka (a country Bob visited several years ago) are described by Prof. Pieter Zwaan, several tanzanite imitations are characterized by Drs. Lore Kiefert and Susanne Schmidt, and identification guidelines for black opaque gem materials are provided by Bob's GIA GTL colleagues Dr. Mary Johnson, Shane McClure, and Dino DeGhionno.

Bob also loved to travel to study gem localities, no matter how distant or dangerous. He believed that a true understanding of any gem requires an awareness of the circumstances under which it emerged from the ground and eventually reached the jewelry market. The article by Daniel A. Sauer, Alice S. Keller, and Shane F. McClure—on Brazil's Capão Imperial topaz mine—is the type of locality project he would have pursued personally or encouraged others to go after. In addition, Bob Kammerling brought people of diverse interests together for the common good of gemology. The article on trapiche rubies is a team effort by one of Germany's leading gemologists, Dr. Karl Schmetzer, with fellow experts Dr. Henry Hänni, of the SSEF Swiss Gemmological Laboratory, the Gübelin Laboratory's Dr. Dietmar Schwarz, and Ruhr-University's Dr. Heinz -Jürgen Bernhardt.

Bob Kammerling's first love may have been the Gem News section of the journal, filled with the many small "bytes" of news that he and his co-editors brought to the gemologist. Many readers tell us that this is the section of *Gems & Gemology* to which they turn first, to get the latest information. It is also the place where Bob shared discoveries from his various trips, as well as from his many colleagues in the gemological community.

If the study of gemstones is indeed a blend of art and science, Bob Kammerling epitomized the field he so loved. And, perhaps more than most, he played a primary role in helping us seek the truth about gems in a significant and yet practical way. For this gemologist, Bob Kammerling will be deeply missed and long remembered as one of the heroes of modern gemology.

William E. Boyajian, President,
Gemological Institute of America

AN UPDATE ON IMPERIAL TOPAZ FROM THE CAPÃO MINE, MINAS GERAIS, BRAZIL

By Daniel A. Sauer, Alice S. Keller, and Shane F. McClure

The Capão mine is one of the oldest and most productive fully mechanized Imperial topaz mines in the historic Ouro Preto area of Minas Gerais, Brazil. Bulldozers, water cannons, and dragscrapers are used in two main pits to remove the thick brown overburden for processing to recover topaz crystals in a broad range of sizes and colors. The rarest color is pinkish purple to purple. Heat treatment will turn some brownish yellow or orange Imperial topaz to "peach" or pink. Preliminary testing suggests that there may be a difference in fluorescence between heat-treated and non-heat-treated topaz.

ABOUT THE AUTHORS

Mr. Sauer, a gemologist and geologist, is technical director of Amsterdam Sauer Company, Brazil. Ms. Keller is editor of Gems & Gemology, *Gemological Institute of America, Santa Monica, California. Mr. McClure is supervisor of Identification Services at the GIA Gem Trade Laboratory, Carlsbad, California.*

Acknowledgments: The authors thank Dr. Wagner Colombarolli, Edmar Evanir da Silva, and Fernando Celso Gonçalves, of the Topázio Imperial Mining Company, for the invitation to visit the mine and for providing information. Constantino Psomopoulos of Amsterdam Sauer Co. selected samples for photograph, reviewed the original paper, and helped with subsequent revisions.

Gems & Gemology, *Vol. 32, No. 4, pp. 232–241.*

Topaz has been known from the Ouro Preto area of Minas Gerais for more than 200 years, with the discovery first announced publicly in 1768 (Rolff, 1971). Since then, topaz has been recovered sporadically from a number of deposits within an area of approximately 120 km^2 that lies, for the most part, just west of the colonial city of Ouro Preto. Today, the region known in the world gem market as the Ouro Preto Imperial topaz district comprises two major active mining sites—Capão (formerly Capão do Lana) and Vermelhão (also known as Saramenha)—and a few dozen abandoned mines, occurrences, and alluvial workings. Although Vermelhão and other mining areas have yielded excellent gem topaz (Vermelhão is especially noted for the large crystals found there), the only private, wholly owned, and completely mechanized mine currently in full operation is the Capão mine, in the Rodrigo Silva district. Specimens and information about that mine were gathered by the senior author (DAS) during several visits over the last few years and in a visit by the second author (ASK) in August 1996.

Several articles have been written on the intense orangy yellow-to-orange-to-"sherry" red topazes from Ouro Preto (figure 1) that are called Imperial topaz in the trade (e.g., Atkinson, 1908, 1909; Bastos, 1964, 1976; Olsen 1971, 1972; Fleischer, 1972; D'Elboux and Ferreira, 1975, 1978; Keller, 1983; Cassedanne and Sauer, 1987; Cassedanne, 1989). The present article describes the current mining situation at the Capão mine and describes the topaz found there, both as it is recovered and as it reaches the market. It also reports on the heat treatment of some orange Imperial topaz to produce attractive pink stones.

LOCATION AND ACCESS

Capão is one of several known topaz deposits in the Ouro Preto area (figure 2). It can be visited easily in a day from Rio

Figure 1. The fine Imperial topazes from the region near Ouro Preto, in Minas Gerais, Brazil, are most commonly intense orangy yellow to orange. The most sought-after Imperial topazes are the "sherry" red and saturated pink stones. Bi-colored stones are rare. The stones shown here range from 8.82 to 14.28 ct; the bi-colored topaz at the bottom is 14.10 ct. Stones courtesy of Amsterdam Sauer Co.; photo © Harold & Erica Van Pelt.

de Janeiro, traveling first by air (about 350 air kilometers) to Belo Horizonte, and then by car on Route BR040 (Belo Horizonte–Rio de Janeiro) south for 30 km (19 miles) to Route BR356, then east (toward Ouro Preto) for 53 km (33 miles), at which point a right turn onto a dirt road leads to Rodrigo Silva, about 7 km to the south. From Rodrigo Silva, a village of approximately 1,200 residents, one travels on a dirt road about 3 km west to reach the mining site. Access to the mine area is limited to those who work there or are invited by the principals. Located in one of the highest regions of the country, the Capão mine lies at an altitude of about 1,200 m (3,900 feet). The chief industry in this mountainous area is cattle ranching, both for beef and dairy products.

Since 1972, the mine has been under the ownership of the Topázio Imperial Mining Company (Topázio Imperial Mineração, Comércio e Indústria Ltda.), of which the three partners are Dr. Wagner Colombarolli, Edmar Evanir da Silva, and Fernando Celso Gonçalves. The entire concession is approximately 600 ha (1,500 acres); it consists of the main mine and three reservoirs. The Topázio Imperial Mining Company also has another concession, the Córrego do Cipó complex, which is 2.5 km northwest of Capão (again, see figure 2); it is now under development for possible future mining.

A BRIEF SUMMARY OF THE GEOLOGY

The geology of the Ouro Preto topaz area has been discussed by Keller (1983), Pires et al. (1983), Ferreira (1983 and 1987), Cassedanne and Sauer (1987), Cassedanne (1989), and Hoover (1992). To summarize, the topaz deposits occur in the Ouro Preto quadrangle of the Quadrilátero Ferrífero (a famous iron-producing area) in southern Minas Gerais. The topaz mineralization falls within an

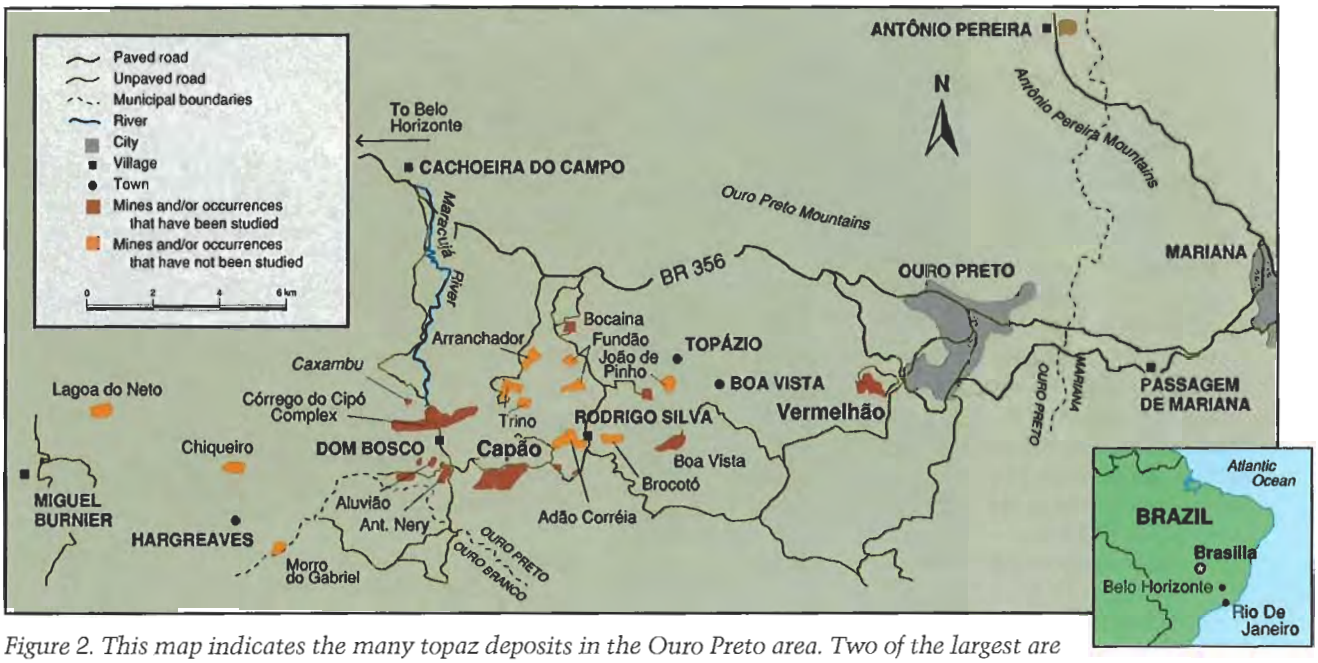

Figure 2. This map indicates the many topaz deposits in the Ouro Preto area. Two of the largest are the Vermelhão mine, near Ouro Preto, and the Capão mine, near the village of Rodrigo Silva. Adapted from a 1987 map produced by the Minas Gerais Light and Power Company.

east-west trending zone that extends from Antônio Pereira village (Antônio Pereira mine) on the east, to Miguel Burnier village (Lagoa do Neto occurrence) on the west, both in the Ouro Preto district (again, see figure 2). Pires et al. (1983) identified four main topaz belts in the region, each of which trends east-west.

The formation of the topaz has been the subject of much debate over the last century (see Olsen, 1971, 1972; Fleischer, 1972; for an informative summary of this debate, see Cassedanne, 1989). The mineralized zone is characterized by intensely weathered (to depths of at least 50 m) rocks underlain by unweathered granitic gneisses, granites, and three series of Precambrian metasedimentary rocks. The Minas series of Precambrian metasediments was subjected to two major intrusive events: (1) about 2,700 million years ago, by a batholith that fractured the sedimentary rocks; and (2) about 1,300 million years ago, by acid intrusions (high-silica igneous rocks). It is believed by Keller (1983) and others that one or both of these intrusions provided the mechanism for the fluorine-rich solutions that entered the rocks through fractures and generated the topaz mineralization. Pires et al. (1983), Oliveira (1984), and Hoover (1992) support the formation of strata-bound topaz deposits from a predominantly hydrothermal process that occurred during or shortly after a period of intense metamorphism.

Regardless of its mode of formation, the mineralized rock comprises a single horizon that varies in thickness from 1 to 6 m (rarely, to 10 m). It is composed of a heavily weathered yellowish to dark brown talc-clay rock called "brown terrain" that is cut by discontinuous kaolinite veins (Cassedanne, 1989) and lenses. Topaz crystals are found within the kaolinite—together with quartz, mica, and specular hematite. They sometimes are associated with rutile and, rarely, with green and blue euclase.

CURRENT MINING OPERATION

At Capão, the mining operation has grown significantly from the single shallow pit last described in this journal by Keller (1983). At the time of the present authors' August 1996 visit, two large open pits were being worked, separated by a narrow access road that will be removed in the near future to make one large pit. The larger pit was 30 m at its deepest point and approximately 350 m long by 150 m wide (figure 3). The smaller pit was 18 m at its deepest point, and approximately 200 m by 80 m (figure 4). The two pits together covered about 7 ha, or 17 acres.

Capão Creek, which runs through the hilly concession area, has been dammed in three places to form reservoirs that serve the mining operation and minimize its environmental impact. One reservoir, for sedimentation control, blocks off an area where the mine tailings are dumped; once the sediments have settled to the bottom of the reservoir, the suspension-free water is released back into the creek. The other two reservoirs provide water for mining and washing the ore.

Because of the depth of the current mining operation, dragscrapers are now used at both pits to recover the topaz. Large buckets are dropped from overhead lines into the pit, where they scoop up the materials comprising the weathered zone (figure 5) and drag them to the top for processing. At the time of our visit, there were two dragscrapers at the larger pit and one at the smaller (newer) one. At both pits, bulldozers work the surface of the pit and push the lateritic soil and rock materials into the path of the dragscraper. This material is then pulled to a large, fixed bucket (washing area) at the top of the pit and washed by water cannons to form a mud pulp. This pulp then flows to a fixed screen, with a quarter-inch (less than 1 cm) mesh, through which the smaller particles pass to the sedimentation reservoir. The remaining gravels are processed to recover topaz. As a secondary operation, water cannons are used at the bottom of the pit both to soften the rock for recovery by the dragscraper and to create a slurry. The slurry is then pumped out of the pit (again, see figure 3) onto the same quarter-inch-mesh fixed screen used to separate the mud pulp.

When the bulldozer uncovers a white kaolinite vein, a good indicator of topaz mineralization, the driver stops. Three people are sent to scrape the vein by hand to look for gem crystals (figure 6). Like all of those who are authorized to pick up crystals, these special miners are identified by their red hats. The remaining minerals recovered from these veins are processed in smaller screens, also with a quarter-inch mesh.

To date, the owners have determined that open-pit mining is the most efficient system for recovery of the topaz. Core drilling has shown that mineralization extends as much as 40–50 m below the lowest part of the larger pit (W. Colombarolli, pers. comm., 1996). Over the last two years—because of the combined effects of a strong currency (which has more than doubled labor costs in U.S. dollar amounts), the deeper workings, and stricter environmental requirements—operating costs for the Capão mine have risen 70%. The sedimentation reservoir will be full after only about 10 years; it must then be restored to its natural state, and another reservoir created.

Figure 3. In August 1996, the larger pit at the Capão mine was 30 m deep and approximately 350 m long. Toward the bottom of the pit, a water cannon softens the weathered host material and creates a slurry that is then pumped out of the pit. One of the mine owners, Dr. Wagner Colombarolli, is standing at the upper edge of the pit with one of the authors. Photo by Daniel A. Sauer.

Recovery. At the washing area at the top of the pits, giant water cannons first push the material removed by the dragscraper through a 4 inch (10 cm) "grizzly" screen (figure 7). Material that does not pass through the screen is rejected. Gravity carries the remaining pulp down through large gutter pipes to the quarter-inch-mesh screen that separates out the smaller particles. The fraction that remains is washed to remove any residual clay, so only rock fragments and minerals are left for further processing.

Next, a conveyor belt transports the washed material to a bucket wheel that tosses the rock fragments and minerals onto a two-tier vibrating screen: One tier has a 1¼ inch mesh and the other is ⅝ inch. Any material over 1¼ inch is put in the waste pile. The fractions that remain—one between 1¼ inch and ⅝ inch and the other less than ⅝ inch—are stockpiled separately into two silos.

Figure 4. The newer, shallower pit at Capão—separated from the original pit by only a narrow access road (on the left)—has proved very productive. Here, a bulldozer pushes the intensely weathered rocks and soils into the center of the pit for washing. Photo by Daniel A. Sauer.

For final processing, crystals and rock fragments from one of the silos are placed on another conveyor belt, where several sorters pick out the topaz by hand (figure 8). By only processing one of the two sizes at a time, the miners reduce the risk of larger stones hiding smaller ones. Any topaz found is placed in a tube that runs alongside the conveyor belt. At the end of the day, a security manager runs water through the tube and collects all of the topaz in a bag at one end. These crystals are then placed in a locked box that has a padlock at the bottom and two "blades" at the top, so the crystals can be inserted easily but will not drop out if the box is turned upside down

Currently, approximately 50 people are involved in the Capão mining and processing operation. Because more ore is mined daily than can be processed, some of the screened gravels are stockpiled for processing during the December-to-April rainy season, when mining slows down considerably.

PRODUCTION

Topaz is found in a broad range of colors at the Capão mine: light yellow, orange-yellow, brownish orange, pinkish orange ("salmon" or "peach"), pink, reddish orange, orange-red, and "sherry" red (again, see figure 1). All of these colors of topaz from the Ouro Preto deposits are traded as "Imperial."

The rarest color is pinkish purple to purple (figure 9). Although this hue was not seen at the Capão mine for almost eight years, approximately 200 grams were found from a single area of the main pit in 1996. Most of these crystals were heavily included, so the total production is expected to yield no more than 15 carats of faceted stones, ranging from 0.5 to 2 ct. Also rare, but seen in finer, less-included, qualities this year, are bi-colored crystals. When cut, these make exquisite gems (again, see figure 1).

After purple, the next rarest color of Imperial topaz is a slightly brownish or "sherry" red. The most sought-after color in the topaz market, "sherry" red topaz represents less than one-half of one percent of the total cuttable material found. Most faceted "sherry" red stones from Capão are 5–10 ct, but 20–30 ct topazes in this color range have been cut. Also rare are the pale-to-saturated pink stones that occur naturally at the Capão mine.

Most common is yellow-to-orange topaz. Capão is the main source for commercial sizes (2–8 ct) in this color range. In addition, many stones in the 10–15 ct range have been cut; 20–30 ct stones are rare but available.

During our visit to the Capão mine, we were shown a half-day's production from the main pit (figure 10). The 3.5–4 kg of topaz crystals represented very good output for one day—according to the mine owners, a half-kilo of crystals is typical. The crystals we examined were predominantly yellow to orange to pink, although we did see at least one 5.5 cm orange-red crystal that would yield about 12 ct of faceted topaz, with the largest stone 7–8 ct. The largest fine crystal was 8 cm and was deep red down the c-axis. We also saw a few bi-colored, orange-and-pink, crystals.

Production from the smaller pit for the same time period was 500–600 grams. We saw more pink stones in this lot than in that from the larger pit.

Only 1%–2% of all the material recovered is faceting quality, according to Dr. Colombarolli. In 1995, from an average of 11,000 m^3 of ore processed every month, fewer than 100 kg of mine-run topaz crystals were recovered. The estimated yield from these crystals, based on experience to date, would be 5,500 carats—a total of 66,000 carats of cut Imperial topaz for the year, or 0.5 ct of topaz per cubic meter of ore processed.

The largest crystal recovered to date at the Capão mine (although broken into four pieces) was 1.3 kg, Dr. Colombarolli noted.

HEAT TREATMENT

Although "peach" to pink (figure 11) Imperial topaz does occur naturally, these colors may be produced in some brownish yellow or orange topaz by heat treatment, which removes the yellow color center. At one operation visited by the second author (ASK), the cut stones are put in a small (about 7.5 cm square) clay tray that is then placed in an oven, and the temperature is brought to 1050°F (565°C; it takes approximately 40 minutes). The oven is then turned off, and the stones are allowed to cool slowly to room temperature, to avoid thermal shock, before they are removed. Although the occasional "peach" stone that results from a partial heating may turn pink on further heating, the pink color obtained at 1050°F is usually the best that can be achieved. Reheating a pink stone or heating it longer will not produce any additional change (see also Nassau, 1994). However, as shown in figure 12, the change is often substantial.

Figure 5. One of two dragscrapers in the larger pit at Capão pulls the saturated, intensely weathered host material to the top for processing. Photo by Daniel A. Sauer.

Figure 6. When the bulldozer uncovers a distinctive kaolinite vein, all other activity stops. Certain miners (denoted by red hats) then search for topaz crystals by hand. Here, the senior author examines a topaz crystal found in this thin white vein. Photo by Alice S. Keller.

Most topaz is not suitable for heating, because topaz typically contains a number of inclusions: liquid-and-gas, breadcrumb-like crystal clusters, needle-like voids, transparent-to-translucent rhombohedral crystals or negative crystals, and fingerprint-like patterns of liquid inclusions. When liquid inclusions, in particular, are present, there is a good chance that the stone will develop large cracks or localized fractures as a result of fluid expansion.

GEMOLOGICAL TESTING

Materials and Methods. We examined a small sample of material that the Amsterdam Sauer Company had obtained directly from the Capão mine office during the last two years and cut in their own facilities. The sample included: five faceted natural-color Imperial topazes, ranging from brownish yellowish orange to pinkish orange (3.09–9.59 ct); two faceted stones (0.65 and 1.19 ct) and three crystals (17.73–67.97 ct) that were pinkish purple; six faceted

Figure 7. The two dragscrapers bring the host material directly to corresponding platforms at the top of the larger pit, where miners wield large water cannons to wash off the finer particles and push the rock fragments through a series of grates. The largest rocks are screened out first. Photo by Daniel A. Sauer.

stones that had been heat treated to purplish pink (0.90–2.61 ct); and one yellowish orange crystal (97.59 ct) that had been sawn in half, with one half then heat treated to purplish pink. All of the heat-treated stones had been treated by the method described in the preceding section.

Refractive index readings were obtained on all of the cut stones with a Duplex II refractometer and a near-sodium equivalent light source. Specific gravity on the cut stones was determined by the hydrostatic weighing method, with three separate measurements taken on each stone. A desk-model Beck prism spectroscope was used to examine the absorption spectra of the cut stones in the study, and a polarizing-filter dichroscope was used to determine the pleochroism on all samples. The ultraviolet fluorescence of all samples was viewed in a darkened environment using four-watt long- and short-wave lamps. The stability to light of two of the heat-treated purplish pink samples and two of the natural-color orange samples was tested with an Oriel 300-watt solar simulator. The four stones were placed in the solar simulator for 145 hours, which is equal to about 290 hours of sun exposure (at noon strength for a mid-latitude location). The temperature was monitored so that it did not exceed 130°F (54°C). Halfway through the test, and at the end, we compared the samples to the other, comparable-color stones in this study.

DESCRIPTION OF THE TOPAZ

We determined refractive indices of n_α =1.630 and n_γ =1.638 (birefringence=0.008) on all of our samples and a specific gravity of 3.52–3.54±0.02. These findings are consistent with published values for topaz (see, e.g., Webster, 1994) and did not vary for any of the colors we examined, including those that were the result of heat treatment.

Also consistent with published values are the absorption spectra and pleochroism. In most stones, the only absorption visible was a general darkening of the far red portion of the spectrum. When viewed down the c-axis, the heated pink stones and the pinkish purple crystals showed a barely discernible line at 682 nm. This line is related to the chromium that produces these colors; it has previously been

Figure 8. In a shed-like structure behind the main pit, miners manually sort through the concentrate, searching for topaz. Any topaz found is placed in tubes along either side of the conveyor belt. Photo by Daniel A. Sauer.

reported in heat-treated pink topaz from Brazil and in natural-color pink topaz from Pakistan (Hoover, 1992; Webster, 1994).

The pleochroism of the predominantly orange material was yellow, yellowish orange, and purplish pink. This changed to shades of pink in two directions, and colorless in the third, after heat treatment. Pleochroism in the pinkish purple samples was purplish pink, pinkish purple, and colorless.

All of the samples were inert or fluoresced moderate orange to long-wave ultraviolet radiation, with a somewhat stronger reaction in the predominantly orange stones. To short-wave UV, the orange and pinkish purple stones fluoresced a very weak to moderate chalky yellow-green. However, the heat-treated pink topazes had a generally stronger fluorescence than the natural-color stones, with a shift in fluorescence hue to a yellowish or greenish white (figure 13). This distinction between the heated and unheated topazes was very evident in the two halves of the sawn topaz crystal (figure 14). To the best of our knowledge, this difference in fluorescence has not been reported previously in the literature. However, our results are based on a small sample and so are only preliminary. The possibility of fluorescence as an indicator of treated or natural color needs to be investigated further with a significant sample of known natural-color pink topazes.

It is interesting that although the internal characteristics of the stones we examined were typical of topaz from this area (liquid inclusions, groups of tiny crystals, some larger rhombic crystals, angular grain plains, and internal fractures), there was no apparent difference in the nature of these inclusions between the heated and unheated stones. This was true even for the sawn crystal (figure 15), which was heavily included; we thought it likely that at least some of the liquid inclusions in such a crystal would have burst. Nevertheless, we caution against heating material that has inclusions, as such stones often do not survive the treatment process.

There was no noticeable loss or change of color in any of the topazes tested with the solar simulator, either the heat-treated purplish pink or the natural-color orange stones.

CUTTING

Because topaz has perfect basal cleavage, the table must always be polished at an angle to the c-axis (12°–15°, according to Webster, 1994); extreme care should be taken to avoid grinding the stone perpendicular to the cleavage plane. Also, inclusions can cause the stone to break on the wheel. At

Figure 9. One of the rarest colors of topaz from the Ouro Preto region are these pinkish purple gems, found in a small area of the Capão mine. This crystal is 36.87 ct; the cut stones are 1.19 and 0.65 ct. Photo by Shane F. McClure.

Amsterdam Sauer, topaz cutters use a 360 grit grinding wheel, a 600 grit faceting disk, and polish the stones on a lead/tin lap with Linde A (Al_2O_3) powder. Recovery depends on the amount of inclu-

Figure 10. For the authors, the mine owners removed the topaz crystals recovered after only about a half-day's work (usually, they are recovered only once a day). The 3.5–4 kg of topaz crystals shown here represent a particularly good yield for a single day from the larger pit. The largest crystal, in the foreground, is approximately 8 cm long. Photo by Daniel A Sauer.

Figure 11. This suite of jewelry is composed entirely of pink topazes from Ouro Preto. They represent some of the superb stones from this historic Imperial topaz locality. The topazes in the necklace weigh a total of 30.36 ct; those in the earrings, 5.50 ct; and the one in the ring is 1.90 ct. Jewelry courtesy of Amsterdam Sauer Co.; photo © Harold & Erica Van Pelt.

sions in each crystal. Well-formed, fairly clean crystals yield up to 2 carats per gram.

SUMMARY AND CONCLUSIONS

Brazil's historic Ouro Preto topaz region continues to produce significant amounts of fine topaz in a broad variety of colors, which are known in the trade as Imperial topaz. The only private, wholly owned, mechanized mine currently in operation there is the Capão mine, which is near the village of Rodrigo Silva. Today, production from this mine represents as much as 50% of the total production of Imperial topaz from Ouro Preto. Although large amounts of ore are mined from the two open pits that constitute the Capão mine today, the recovery is only 0.5 ct of cut topaz per cubic meter of ore processed. Environmental responsibility and the greater depths

Figure 12. This 97.59 ct Imperial topaz crystal was sawn in half and the bottom was heated to 1050°F, which produced the purplish pink color. Photo by Shane F. McClure.

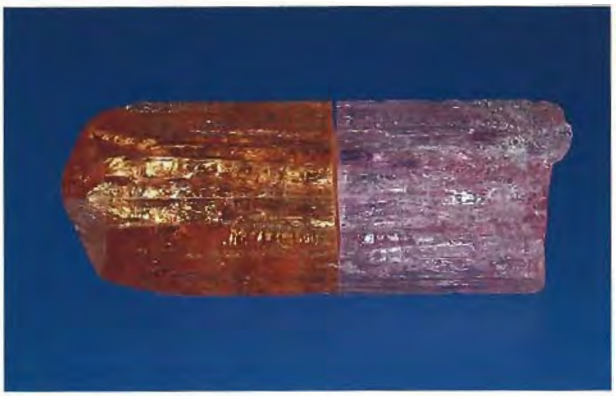

Figure 13. A difference in short-wave UV fluorescence was noted between the unheated and heat-treated faceted topazes examined for this study: here, a weak chalky yellow-green in the two unheated pinkish purple stones (left), as compared to moderate to strong greenish-to-yellowish white in the heat-treated pink stones (right). Photo by Shane F. McClure.

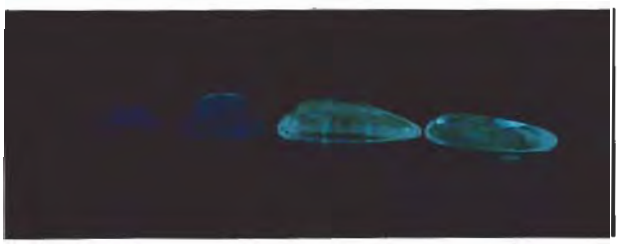

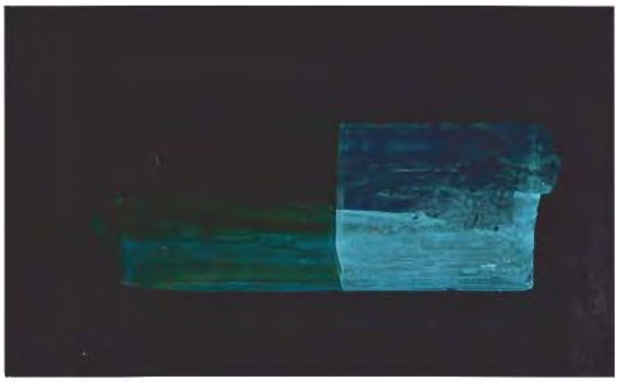

Figure 14. Fluorescence to short-wave UV radiation was the only difference in gemological properties between the unheated (left) and heated halves of the crystal in figure 12. Photo by Shane F. McClure.

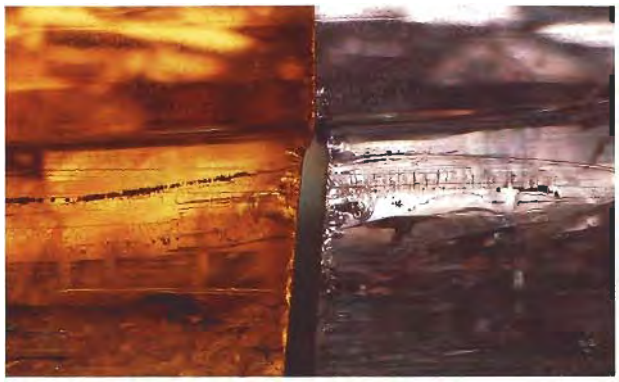

Figure 15. No difference was observed in the nature of the inclusions between the heated and unheated halves of the sawn crystal. Note the undisturbed liquid inclusion plane in the center of the photograph, where it crosses the saw cut. Photomicrograph by Shane F. McClure; magnified 20×.

of the mining operation, together with the strong currency, have significantly increased the costs of extracting the topaz.

The rarest topaz color is purple. "Sherry" red and bi-colored stones are also uncommon. Certain brownish yellow or orange stones can be heat treated to pink, which is stable to light and heat (as evidenced by the fact that further heating or heating at higher temperatures will not change the color). The preliminary observation that heat-treated pink topaz fluoresces a strong yellowish-to-greenish white to short-wave UV radiation, as compared to the weak to moderate chalky yellow-green of their natural-color orange or purple counterparts, deserves further investigation to determine its usefulness as an identification criterion.

Because of the heavily weathered host rocks and the discontinuity of the gem-bearing veins, open-pit mining appears to be the most efficient means to recover these rare gems. The prospects for continued production at the Capão mine are good, inasmuch as core drilling has shown topaz mineralization as deep as 50 m below the current low point of the main pit. However, we do not know what impact the difficulties and related costs of extracting the ore at such depths will have on the general availability of this gem material.

REFERENCES

Atkinson A.S. (1908) Report on topaz in Brazil. *Minerals Yearbook*, U.S. Bureau of Mines, p. 842.

Atkinson A.S. (1909) Mining for gems in Brazil. *Engineering and Mining Journal*, June 19, pp. 1234–1235.

Bastos F.M. (1964) The topaz mines of Ouro Preto. *Lapidary Journal*, Vol. 18, pp. 918–920.

Bastos F.M. (1976) Imperial topaz from Brazil. *Lapidary Journal*, Vol. 30, pp. 1838–1840.

Cassedanne J.P., Sauer D.A. (1987) La topaze impériale. *Revue de Gemmologie*, No. 91, pp. 2-9.

Cassedanne J.P. (1989) Famous mineral localities: The Ouro Preto topaz mines. *Mineralogical Record*, Vol. 20, pp. 221–233.

D'Elboux C.V., Ferreira C.M. (1975) Topazio na região de Ouro Preto. *Boletim do Departemento de Geologia*, UFOP, Publicação Especial No. 1, pp. 73–79.

D'Elboux C.V., Ferreira C.M. (1978) Topazio na região de Ouro Preto. Sociedade de Intercambio Cultural e Estudos Geologicos, *Semanas de Estudos*, Nos. 14 and 15, pp. 14–52.

Ferreira C.M. (1983) Vulcanismo ácido no quadrilátero ferrífero e sua relação com algumas ocorrências e/ou depósitos minerais. *Anais do II Simpósio de Geologia de Minas Gerais*, Belo Horizonte, Brazil, pp. 128-133.

Ferreira C.M. (1987) Geologia da jazida de topázio do Morro de Saramenha. *Revista Escola de Minas*, Vol. 40, No. 3, pp. 15-17.

Fleischer R. (1972) Origin of topaz deposits near Ouro Preto, Minas Gerais, Brazil, discussion. *Economic Geology*, Vol. 67, No. 1, pp. 119-120.

Hoover D.B. (1992) *Topaz*. Butterworth-Heinemann, Oxford, England.

Keller P.C. (1983) The Capão topaz deposit, Ouro Preto, Minas Gerais, Brazil. *Gems & Gemology*, Vol. 19, No. 1, pp. 12–20.

Nassau K. (1994) *Gemstone Enhancement*, 2nd ed. Butterworth-Heinemann Ltd., Oxford, England.

Oliveira C.M.M. de (1984) Composição mineralógica e química do nível topazífero nas proximades de Rodrigo Silva (Ouro Preto, Minas Gerais). *Resumos, Breves Comunicações, Cursos, Excursões e Mesas Redondas*, 33rd Congress of Brazilian Geology, Rio de Janeiro, pp. 265–266.

Olsen D.R. (1971) Origin of topaz deposits near Ouro Preto, Minas Gerais, Brazil. *Economic Geology*, Vol. 66, No. 4, pp. 627–631.

Olsen D.R. (1972) Origin of topaz deposits near Ouro Preto, Minas Gerais, Brazil, a reply. *Economic Geology*, Vol. 67, No. 1, pp. 120–121.

Pires F.R.M., Freitas C.O., Palermo N., Sarciá M.N.G. (1983) Geologia e gênese dos depósitos de topázio do distrito de Ouro Preto, Minas Gerais. *Anais do II Simpósio de Geologia de Minas Gerais*. Belo Horizonte, pp. 283–296.

Rolff A. (1971) Brazilian imperial topaz. *Lapidary Journal*, Vol. 25, pp. 1556–1562.

Webster R. (1994) *Gems*, 5th ed. Rev. by P. G. Read, Butterworth-Heinemann Ltd., Oxford, England.

TRAPICHE RUBIES

By Karl Schmetzer, Henry A. Hänni, Heinz-Jürgen Bernhardt, and Dietmar Schwarz

Ruby crystals from Southeast Asia with a fixed six-rayed star, similar in effect to trapiche emeralds from Colombia, are described. They consist of six transparent-to-translucent ruby sectors separated by nontransparent yellow or white planes. Most samples also have a hexagonal tapered yellow, black, or red core. In the yellow or white arms of the star and in the boundary zones between the core and the six ruby sectors, a massive concentration of tube-like inclusions is seen. These inclusions are oriented perpendicular to the morphologically dominant dipyramidal crystal faces; they contain liquid, two-phase (liquid/gas), and solid fillings identified as magnesium-bearing calcite and dolomite. A trapiche-type sapphire is also described.

ABOUT THE AUTHORS

Dr. Schmetzer is a research scientist residing in Petershausen, near Munich, Germany. Dr. Hänni is director of SSEF Swiss Gemmological Institute, Basel, and professor of gemology at Basel University, Switzerland. Dr. Bernhardt is a research scientist at the Institute for Mineralogy of Ruhr-University, Bochum, Germany. Dr. Schwarz is head of research at the Gübelin Gemmological Laboratory, Lucerne, Switzerland. All photos and photomicrographs are by the authors unless otherwise noted.

Acknowledgments: The authors are grateful to Dr. O. Medenbach of Bochum University for photomicrography of the polished sections and X-ray powder diffraction analysis.

Gems & Gemology, Vol. 32, No. 4, pp. 242–250.

In October 1995, a 6.0 ct cabochon-cut ruby with a distinct sectored appearance—similar to that associated with trapiche emeralds—was shown to one of the authors (KS) by a gem collector who resides near Munich, Germany. This sample was first described by Müllenmeister and Zang (1995) and also briefly mentioned by Henn and Bank (1996). The unusual cabochon consists of six transparent ruby sectors delineated by six nontransparent (i.e., translucent-to-opaque) yellow arms in the form of a fixed six-rayed star. Myanmar was mentioned as country of origin by the Idar-Oberstein gem dealer who originally sold the stone (R. Goerlitz, pers. comm., 1996). Scanning electron microscope (SEM) examination of this sample revealed the presence of what are most probably carbonates—mainly calcite plus some subordinate ankerite—in the arms of the star (Müllenmeister and Zang, 1995), and carbonates were also mentioned by Henn and Bank (1996). SEM-EDS (energy-dispersive spectroscopy) revealed the characteristic peaks of Ca, Mg, Fe, and C (U. Henn, pers. comm., 1996).

In November 1995, subsequent to the 25th International Gemmological Conference in Thailand, three of the authors (KS, HAH, and DS) visited the ruby market of Mae Sai, close to the Myanmar border, where great quantities of rough and some fashioned rubies were offered for sale. The dealers said that the material on display originated from the Mong Hsu mining area in Myanmar (see Peretti et al., 1995). After two days of searching, we obtained one cabochon (figure 1) and about 30 rough samples of sectored ruby similar to the piece seen in Germany. Some days later, one of the authors (DS) acquired more than 70 additional rough sectored crystals from various dealers in Bangkok. For these samples, the suppliers mentioned Vietnam and Myanmar as possible countries of origin. In total, more than 100 trapiche-type rubies were available for the present study. In the course of our research, we also encountered one gray trapiche-type sapphire (Box A).

MATERIALS AND METHODS

All samples were examined macroscopically as well as by conventional microscopic techniques in reflected and transmitted light. Eighteen samples, which represented all of the structural varieties seen, were sawn into three or four slices each.

The slices were oriented three ways: (1) parallel to the c-axis and parallel to one of the arms of the six-rayed stars, (2) parallel to the c-axis and perpendicular to one of the arms of the stars, or (3) perpendicular to the c-axis. From these slices, we had polished slabs about 1.0–1.3 mm thick prepared for each of the 18 crystals, as well as 10 polished sections about 200 μm thick and two approximately 20 μm polished thin sections. We cut an additional 30 pieces of rough in one direction and polished one side to view the internal structure.

We examined the polished slabs with a gemological microscope, first with fiber-optic illumination and then immersed in methylene iodide. The polished sections were examined with conventional petrographic microscopes (Leitz and Zeiss).

To identify the solid inclusions, we used two microanalytical techniques: 10 of the polished slabs were examined by Raman spectroscopy with a Renishaw Raman microscope (see Hänni et al., 1996, for experimental details), and eight of the approximately 200 μm thick polished sections were analyzed with a CAMECA Camebax SX 50 electron microprobe.

For additional chemical characterization of the material forming the arms of the six-rayed stars and comparison with the chemistry of the host ruby, we submitted five natural crystal fragments and six polished slabs to energy-dispersive X-ray fluorescence (EDXRF) analysis using a Philips PV 9500 X-ray generator and detectors with a Spectrace TX-6100 system and software package. We used lead foils with specially prepared holes to restrict analysis to the ruby areas only (without any arm component) and to analyze areas that included part of a yellow arm and some adjacent ruby.

In addition, yellow, nontransparent (translucent-to-opaque), triangular areas with massive inclusions in the outer zones of two samples were examined both by electron microprobe and by X-ray diffraction analysis (using a conventional 57.3 mm diameter Gandolfi camera).

VISUAL APPEARANCE

We first examined the samples with the unaided eye or a 10× loupe. All of the rough samples were fragments of barrel-shaped crystals; they ranged from about 3 to 8 mm in diameter and from 3 to 10 mm in length. Some were water-worn, but others revealed a distinct striated surface structure on planes more or less parallel to the basal pinacoid (figure 2). About 20 of the crystal fragments had natural faces, all with a uniform habit consisting of a single dipyramidal crystal form. These faces were inclined about 5° to the c-axis, which indicates that the dominant form is the hexagonal dipyramid ω {14 14 $\bar{2}\bar{8}$ 3}. Three crystals had one or two additional rhombohedral faces r {10$\bar{1}$1}.

Figure 1. Trapiche-type rubies have been seen in Southeast Asian gem markets. This 1.55 ct cabochon was purchased in Mae Sai, Thailand, from among material that was mined in Mong Hsu, Myanmar. As is the case with trapiche emeralds, the six-rayed star is fixed; that is, it does not move when the stone or light source is moved.

The divided structure of the crystals was best seen in those polished slabs oriented perpendicular to the c-axis. In these hexagonal cross-sections, six red, transparent-to-translucent sectors were subdivided by the yellow- or white-appearing arms of a six-rayed star. In some crystals, the six arms (which, unlike typical asteriated gems, are fixed—that is, they do not move when the stone or light source is moved) intersected at one small point, forming six triangular ruby sectors (figure 3). In many cases, however, the arms extended outward from a hexagonal central core (figure 4), producing trapezoidal ruby areas. The cores of our study samples were usually either opaque yellow or black (figure 5); in some cases, they were transparent red. We also saw thin yellow or (rarely) white zones, similar in color to the arms of the stars, in the boundaries between the black or red cores and the six triangular ruby sectors (see, e.g., figures 4 and 5).

In some samples, only a small intersection point between the six yellow arms of the star was

Figure 2. The six-rayed (hexagonal) star in this 7.5-mm-diameter trapiche ruby separates the ruby into six triangular sectors. Note the surface striations oriented perpendicular to the six dipyramidal faces of this crystal, almost parallel to the basal pinacoid.

observed on both sides of a crystal fragment or polished slab. In most cases, however, distinct cores were seen, revealing a pyramidal or tapered outline (figure 6). That is, the diameters of the red, yellow, or black cores varied between the two ends of the crystal fragments or between the two sides of the polished slabs (figures 3 and 5). In most cases, the cores or intersection points at both ends were the same color; however, we also saw a few barrel-shaped samples with different colors at either end.

In some samples, yellow, nontransparent, feathery structures extended outward from the dividing planes into the transparent ruby sectors, forming triangular areas of massive inclusions toward the edges of the crystals (figure 7). Occasionally, these zones had been weathered out (figure 8).

MICROSCOPIC EXAMINATION

In transmitted light, the yellow or black central cores, the six yellow arms of the stars, and the yellow triangular areas appeared opaque (figure 9). We observed a series of parallel tube-like structures or striations extending outward from the cores or arms into the ruby sectors (figure 10). Where the ruby sectors were transparent, these structures were largely restricted to thin areas close to the central core and the arms (figure 11), although some tubes did run through the full transparent

Figure 3. In some of the trapiche rubies, the six arms intersect at one small point, forming six triangular ruby sectors. This polished slab is about 4.2 mm in diameter.

sectors to the outer dipyramidal faces of the crystal. Those ruby sectors that were semi-transparent to translucent had more of the tube-like inclusions.

Examination of the polished sections revealed the same characteristic patterns noted above, with striations restricted to the arms and boundaries between the cores and transparent ruby sectors (figure 12a, b, c) and a dense concentration of tubes in semi-transparent samples (figure 12e, f). In some samples, the six arms intersected in a small point, that is, without a core (figure 12a, e); others had a small transparent red (figure 12f), a small nontrans-

Figure 4. In many of the trapiche rubies, the arms radiate from a hexagonal central core, so the six ruby sectors are trapezoidal. This polished slab measures about 3.2 mm in diameter.

Figure 5. These trapiche ruby cross-sections illustrate some of the different forms observed in the samples examined. The arms of the stars intersect in a small point (lower right) or extend outward from the corners of a hexagonal black (upper right and lower left) or yellow (upper left) core. The upper left sample (which measures about 4.2 mm in diameter) is the other side of the slab shown in figure 3; note the size difference in the centers on the two sides.

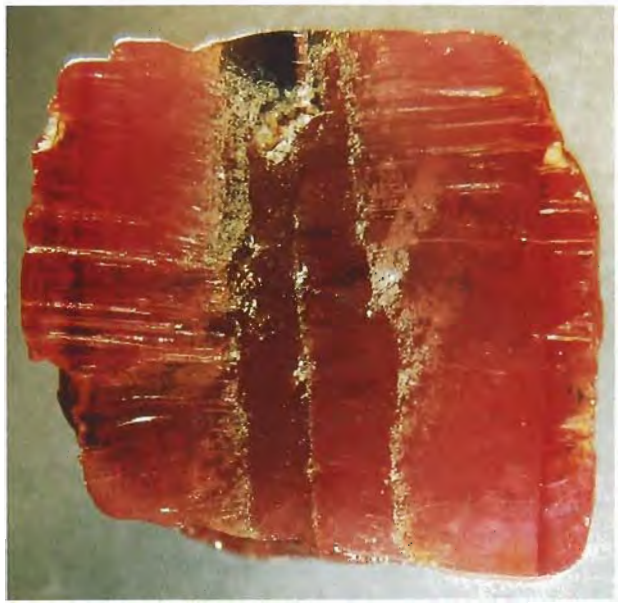

Figure 6. This view, parallel to the c-axis of this 7.2-mm-diameter sample, illustrates the tapered core, which is mostly red but black at one end. Note the strong striations in the outer zones, away from the core.

parent yellow (figure 12c), or an opaque black core (figure 12d). A few had large cores (figure 12b, d). Occasionally, the arms widened toward the edges of the crystals, often with evidence of weathering (figure 12d–f).

With higher magnification, using crossed polarizers, we resolved the striations as thin tubes (figure 13a) that were often filled with birefringent minerals. The arms of the six-rayed stars were formed by massive concentrations of such tubes, which were filled with birefringent minerals (figure 13b), a liquid, or a liquid and gas (figure 13c).

Examination of sections parallel to the c-axis revealed that the tube-like structures are not oriented exactly parallel to the basal plane of the corundum crystals, but rather show a slight inclination, about 5° (figure 14). This indicates that they are oriented perpendicular to the dominant dipyramidal faces ω, which are inclined about 5° to the c-axis.

In the black or yellow cores of some of the polished sections, we observed small birefringent mineral inclusions in the form of tiny round spots (figure 13a). These probably represent cross-sections of tubes oriented perpendicular to the basal pinacoid, which means that the tube-like structures also run parallel to the c-axis in the cores of some samples.

IDENTIFICATION OF THE MINERAL INCLUSIONS

The birefringent mineral inclusions in the tube-like structures were analyzed independently by Raman spectroscopy and an electron microprobe. Two types of Raman spectra were found repeatedly in all of the polished slabs (figure 15). These spectra were consistent with calcite and dolomite, as determined by data in the literature (White, 1974; Pinet et al., 1992) and our own reference spectra.

Electron microprobe analysis of the solids filling the tubes confirmed these results and provided some

Figure 7. The arms in this 4 × 6 mm trapiche ruby slab "feather out" and widen toward the outer edge of the crystal, almost completely absorbing one of the ruby sectors.

Figure 8. In some of the trapiche rubies in which the arms form triangular zones at the rim of the crystal, weathering has created re-entrant angles. This sample is approximately 7 × 8 mm.

additional chemical data. Two mineral phases were present in all of the samples examined (figure 16): a magnesium-bearing calcium-rich mineral (calcite) and a carbonate with higher magnesium and lower calcium contents (dolomite). Quantitative chemical analyses gave a Mg:Ca ratio of 7:93 for the magnesium-bearing calcite (average of five analyses) and a Mg:Ca ratio of 49:51 for the dolomite (average of six analyses). No iron was detected in either of these minerals.

Figure 9. When the slabs are examined with transmitted light, the cores and arms of the trapiche rubies appear opaque. The parallel striations illustrated in figure 2 are clearly seen in this 3.5-mm-diameter cross-section. Immersion, crossed polarizers.

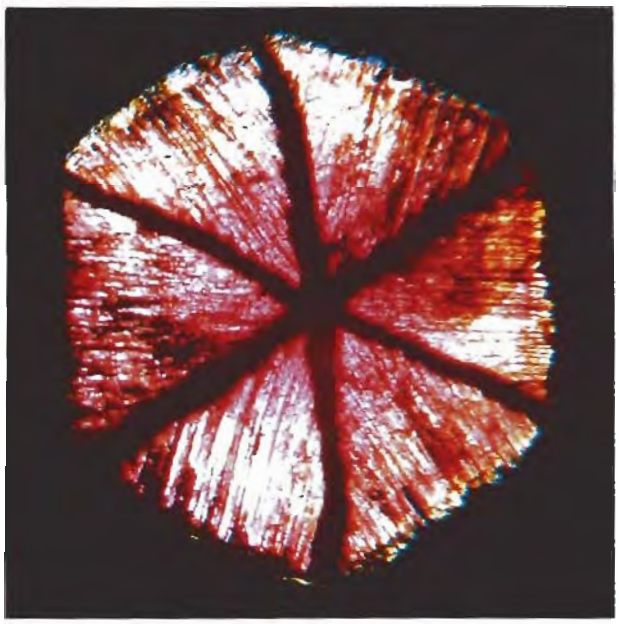

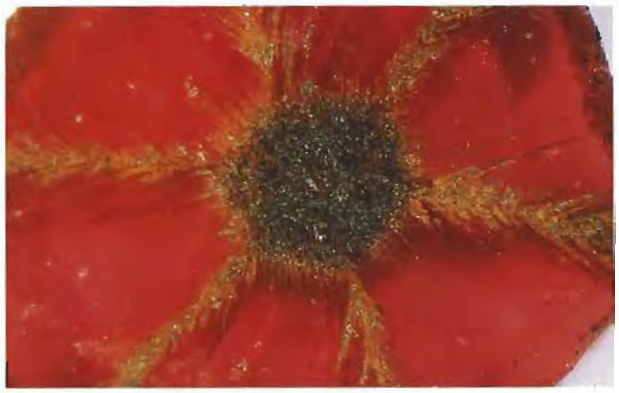

Figure 10. In reflected light, this trapiche ruby slab reveals a series of parallel tube-like structures extending outward from each of the six arms of the star and from the dividing planes between the black core and the six trapezoidal red zones. Magnified 10×.

Because the tube-like structures that extended into the gem-quality ruby sectors were colorless, and the calcite and dolomite inclusions were iron-free, we concluded that the yellow color of the arms and some cores must be due to intense weathering and secondary iron staining of the cavities and tubes. This interpretation was supported by the presence of white arms in some (not deeply weathered) samples and by X-ray fluorescence analyses. In two samples for which we recorded distinct differences, the iron signal in the XRF spectrum of the yellow arm was about four to five times stronger than the iron signal of the adjacent ruby sector (which contained fewer tube-like inclusions).

The massive, nontransparent, yellow triangular areas that broadened toward the outer rim in some samples consist of non-gem-quality corundum, according to X-ray powder diffraction and micro-

Figure 11. In those samples with transparent ruby sectors, most of the tube-like inclusions ended close to the arms or dividing planes with the core. Magnified 50×.

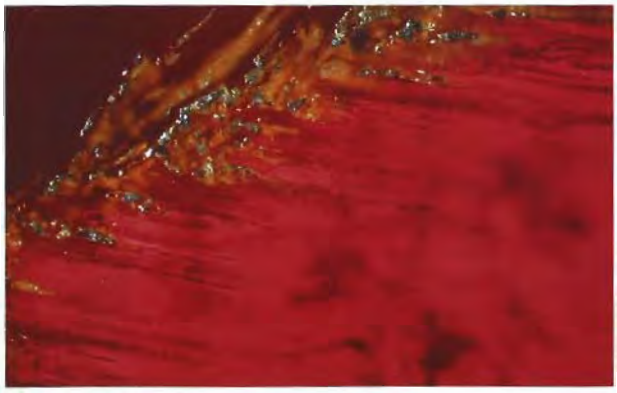

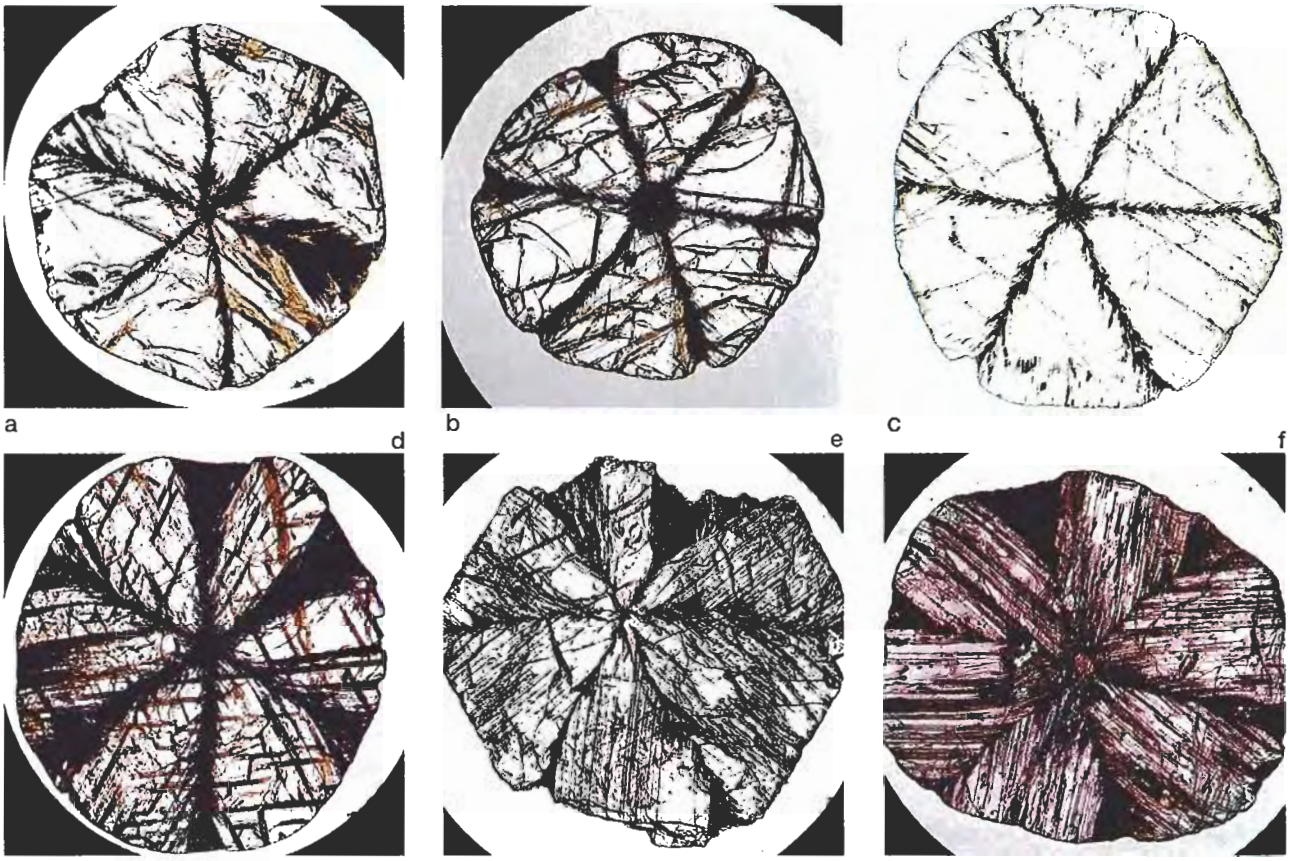

Figure 12. When viewed with transmitted light, the polished basal sections of the trapiche rubies clearly illustrate the different types of star-like structures: (a) the arms of the star in this 3-mm-diameter sample intersect in a small central point; (b) the arms in this 4-mm-diameter section extend outward from the corners of a yellow central core; (c) the arms in this 4.2-mm-diameter section extend outward from the corners of a small yellow central core, with evidence of weathering in the arms at the rim (re-entrant angles); (d) the arms in this 3.2-mm-diameter section, which extend from a black core, get thicker as they approach the outer rim of the crystal, with evidence of weathering at the rim; (e) weathering is more extensive in the arms of this 5-mm-diameter sample, which intersect in a small central point; and (f) the arms in this 4.5 × 5 mm sample extend outward from a red core, ending in partially weathered triangular structures at the rim of the crystal. Note the profusion of tube-like inclusions in the ruby sectors of semi-transparent samples e–f, as compared to the ruby sectors of transparent samples a–c. Polished sections a, b, and d–f are 200 μm thick; sample c is 20 μm thick. Photomicrographs by O. Medenbach.

probe analyses. In the samples we examined, these sectors contained a massive concentration of inclusions, apparently also accompanied by intense weathering and iron staining.

DISCUSSION

Nomenclature. These ruby samples share a number of common structural features with trapiche emeralds from Colombia, as described in the mineralogic and gemological literature (Bernauer, 1926; McKague, 1964; Schiffmann, 1968; Nassau and Jackson, 1970; O'Donoghue, 1971). In both mineral species, corundum and beryl, hexagonal single crystals are divided by included material into six distinct triangular or trapezoidal growth sectors, depending on the presence or absence of a central core. The arms of the six-rayed stars consist of the host (ruby or emerald) with inclusions of other minerals: calcite and dolomite for ruby, albite for emerald. In both gem materials, the central core consists of the host mineral alone or of the host mineral plus inclusions (similar to the composition of the arms), and it is typically tapered.

Oriented striations (tube-like inclusions) occur both at the outline of the core and extending outward from the nontransparent arms into the transparent ruby or emerald sectors. In our ruby samples, these striations were oriented perpendicular to the dominant crystal form, that is, perpendicular to the hexagonal dipyramid ω {14 14 $\bar{2}8$ 3}; in emerald, they are perpendicular to the first-order hexagonal prism m {10$\bar{1}$0}.

In general, most of the structural characteristics that have been described for various trapiche emer-

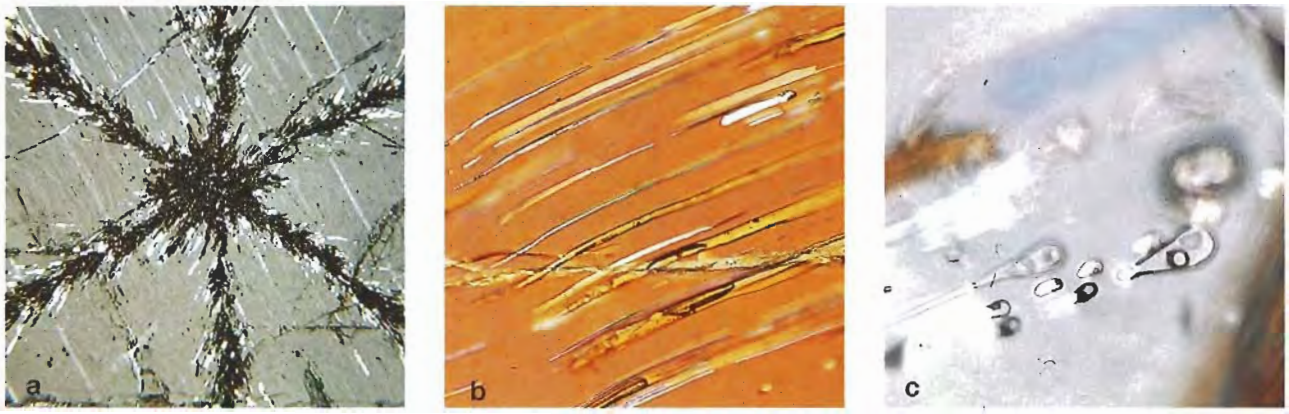

Figure 13. When the polished sections were viewed with higher magnification and crossed polarizers, it became evident that the tube-like structures (a) were filled with birefringent minerals (b), or with a liquid or liquid and gas (c). The tiny round spots in the core of figure a are actually cross-sections of tubes that run perpendicular to the basal pinacoid. Photomicrographs by O. Medenbach; a = magnified 10×, b = 40×, c = 40×.

alds from Colombia (see, e.g., Bemauer, 1926; Nassau and Jackson, 1970) were also found in the sectored rubies described in this article. Thus, it seems reasonable to apply the term *trapiche* not only to sectored emeralds from Colombia, but also to similarly sectored rubies regardless of geographic origin.

Formation Sequence. Discussions as to whether the structural features observed in Colombian trapiche emeralds are primary or secondary in origin (i.e., whether they formed during or after the formation of the host emerald) are ongoing (McKague, 1964; Nassau and Jackson, 1970; Petreus, 1974). However, the arrangement of the tube-like inclusions in our samples suggests that the sectored structure of the trapiche rubies described in this article is primary. Specifically, we believe that the red or black core formed first; then, a change in the growth environment caused the massive formation of tube-like inclusions at the outer edge of the core. Subsequent to this event, new tube-like inclusions formed at the boundaries between the six dipyramidal growth sectors. In the direction along the c-axis, tube-like inclu-

Figure 14. In this view of a 5.9-mm-diameter trapiche ruby crystal parallel to the c-axis, the tube-like inclusions show a small inclination to the basal plane.

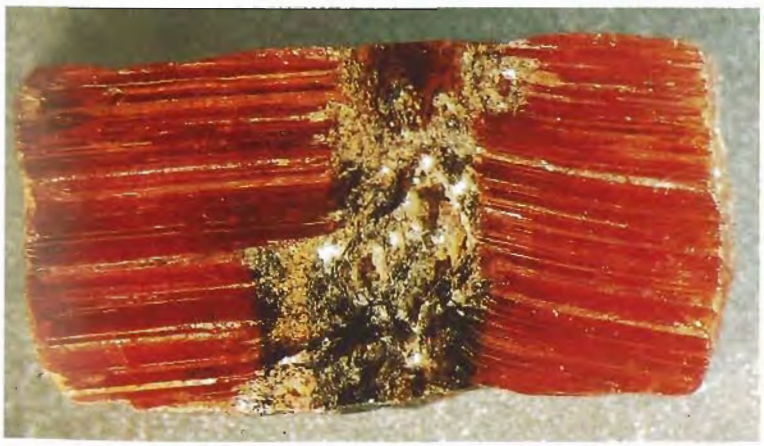

Figure 15. On the basis of these Raman spectra (note that scales are different), the mineral inclusions in the tube-like structures were identified as (A) calcite and (B) dolomite. The lines at 414.8 and 749.7 cm^{-1} (not labeled) are assigned to the corundum host.

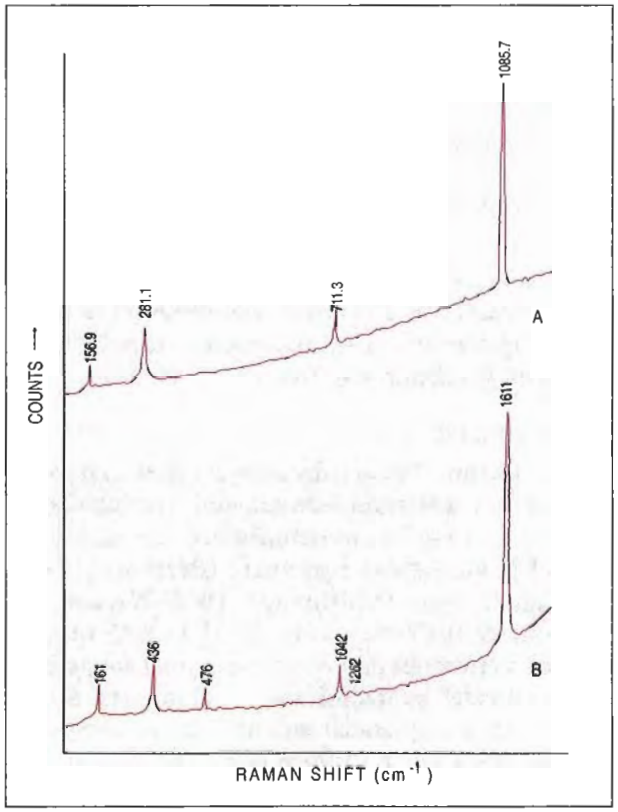

BOX A: TRAPICHE SAPPHIRE

A different type of trapiche emerald, which originated from the state of Goiás, Brazil, was described by DelRe (1994). The samples he examined consisted of a hexagonal central core with dark, trapezoidal, nontransparent areas extending inward from the six prism faces of the crystal; the trapezoidal areas were separated by narrower green transparent zones that extended from the corners of the central core. Consequently, the Brazilian material appeared to be a photographic "negative" of Colombian trapiche emeralds.

Recently, trapiche corundum with a similar "negative" appearance was seen in the gem market. Ten sapphires with a sectored structure were offered at the 1996 Basel fair by a Berlin gem dealer. He had purchased several cabochons and one faceted trapiche sapphire in Myanmar in early 1996; at that time, he was told that the samples originated from the Mong Hsu mining area (H.-J. Engelbrecht, pers. comm., 1996).

A 6.59 ct trapiche sapphire was purchased by one of the authors (HAH). It is whitish gray in color, with six almost triangular white reflective (opaque) areas. Small bands of a darker gray, less translucent material delineate the six triangular zones. The overall effect is of a fixed six-rayed hexagonal star (figure A-1). The white reflective material in the triangular areas closely resembles "silk," and microscopic examination confirmed the presence in these areas of a dense pattern of rutile needles, similar to that which is commonly seen in Burmese rubies and sapphires. In addition, hexagonal growth zoning parallel to prism and/or dipyramidal faces established that the six rays of the star in this sample are oriented perpendicular to the prism and/or dipyramidal faces of the corundum crystal (figure A-2). This indicates that the six arms of the star in this trapiche sapphire are oriented perpendicular to the arms of the stars in the trapiche rubies described in this article.

Microscopic examination also revealed yellow-appearing mineral inclusions that were concentrated in the areas confined by the six arms of the star. After carefully repolishing the back of the sapphire cabochon, we were able to identify these inclusions by SEM-EDS as phlogopite. These phlogopite inclusions, which were undoubtedly concentrated during crystal growth, are responsible for the dark gray appearance of the arms of the star.

Figure A-1. Whitish gray sapphires with a sectored structure have also appeared recently in the gem market. A 6.59 ct trapiche sapphire is shown here with the 1.55 ct trapiche ruby cabochon for comparison.

Figure A-2. These schematic drawings illustrate differences between the trapiche rubies and trapiche sapphire studied. In the ruby (a), the dividing planes between the red sectors are formed by tube-like inclusions oriented perpendicular to dipyramidal crystal faces (see figure 12). In the sapphire (b), the dividing planes are formed by zones with a high concentration of phlogopite inclusions perpendicular to prismatic or dipyramidal growth planes (broken lines); the rutile needles in the whitish reflecting growth zones are oriented parallel to the growth planes, as indicated here by the arms of the small six-rayed stars.

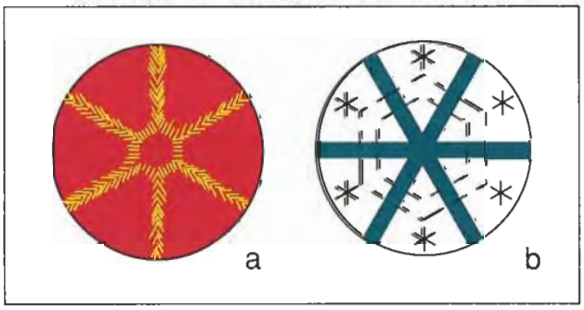

sions also formed in basal growth sectors, with an orientation perpendicular to the basal pinacoid. Where the basal faces were prominent, discrete cores with calcite and dolomite inclusions in tube-like structures formed; where the basal faces were small or absent, smaller cores or intersection points between the arms of the stars formed.

The appearance of the samples described in this article can be explained in terms of their relative position in this trapiche ruby growth sequence: Samples with red and/or black cores on either end of the crystal fragments were grown at an earlier stage, and those with yellow cores or intersection points were grown in a later stage.

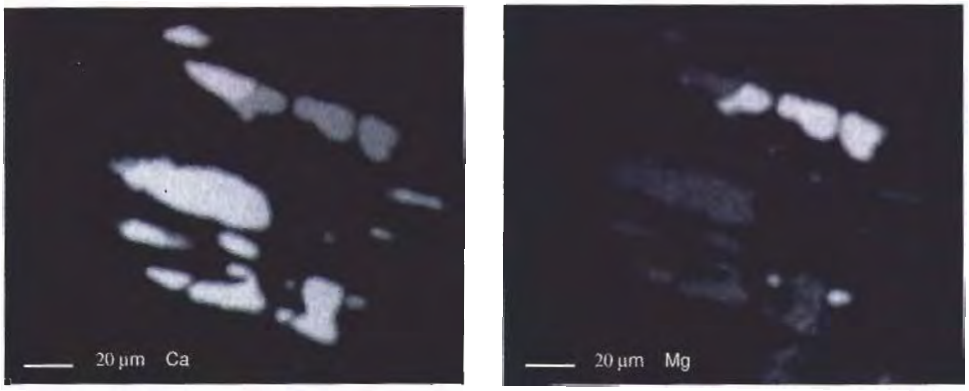

Figure 16. Electron microprobe–generated X-ray scanning images for Ca (left) and Mg (right) confirmed the presence of calcite and dolomite in the tube-like inclusions. The more intense calcite image reflects the higher calcium content in this mineral.

Origin. As mentioned previously, some of the material described in this article was selected by the authors from large parcels of reportedly Mong Hsu rough in Mae Sai, northern Thailand. Certain characteristics of these trapiche rubies are closely related to those of untreated rubies from Mong Hsu (see Peretti et al., 1995): The dominant crystal form is the hexagonal dipyramid $\omega\{14\ 14\ \overline{28}\ 3\}$, typical samples reveal dark violet to almost black central cores and red rims, and an abrupt change of growth conditions is evident in the growth sequence. Furthermore, calcite and dolomite are components of the Mong Hsu host rock; Peretti et al. (1996) described a ruby crystal from Mong Hsu in a calcite vein, embedded in a dolomite marble.

However, there are also some indications that Vietnam might be the country of origin for all or some of the samples. One Bangkok gem dealer mentioned that he had seen rubies of this type coming from Vietnam (K. Siu, pers. comm., 1995). In addition, rubies with sectored growth structures were seen about five years ago in large parcels of material from Vietnam, which probably originated from the Luc Yen mining area (C. P. Smith, pers. comm., 1996), and a purple-pink trapiche sapphire described by Koivula et al. (1994) reportedly came from a parcel of Vietnamese rough.

CONCLUSION

Trapiche rubies represent a new variety of corundum that is similar in appearance to trapiche emeralds. Like trapiche emeralds, these rubies are composed of six triangular or trapezoidal sectors formed by the fixed arms of a six-rayed star, with or without a tapered core. The arms consist of the host material and massive concentrations of inclusions. In trapiche rubies, these inclusions are tube-like structures that are oriented perpendicular to dominant dipyramidal crystal faces. The minerals in these tubes are calcite and dolomite. Although the arrangement of these inclusions suggests that the star pattern formed at the same time as the ruby crystal formed, the detailed growth mechanism of the trapiche ruby pattern cannot be explained at present.

REFERENCES

Bernauer F. (1926) Die sog. Smaragddrillinge von Muzo und ihre optischen Anomalien. *Neues Jahrbuch für Mineralogie, Geologie und Paläontologie*, Supplemental Vol. 54, Part A, pp. 205–242.

DelRe N. (1994) Gem trade lab notes: Emerald, trapiche from a new locality. *Gems & Gemology*, Vol. 30, No. 2, pp. 116–117.

Hänni H.A., Kiefert L., Chalain J.-P., Wilcock I.C. (1996) Ein Renishaw Raman Mikroskop im gemmologischen Labor: Erste Erfahrungen bei der Anwendung [A Renishaw Raman Microscope in the gemmological laboratory: First application experiences]. *Gemmologie. Zeitschrift der Deutschen Gemmologischen Gesellschaft*, Vol. 45, No. 2, 1996, pp. 55–70.

Henn U., Bank H. (1996) Trapicheartige Korunde aus Myanmar. *Gemmologie. Zeitschrift der Deutschen Gemmologischen Gesellschaft*, Vol. 45, No. 1, pp. 23–24.

Koivula J.I., Kammerling R.C., Fritsch E. (1994) Gem news: "Trapiche" purple-pink sapphire. *Gems & Gemology*, Vol. 30, No. 3, p. 197.

McKague H.L. (1964) Trapiche emeralds from Colombia, part I. *Gems & Gemology*, Vol. 11, No. 7, pp. 210–213, 223.

Müllenmeister H.-J., Zang J. (1995) Ein Trapiche-Rubin aus Myanmar (Burma). *Lapis*, Vol. 20, No. 12, p. 50.

Nassau K., Jackson K.A. (1970) Trapiche emeralds from Chivor and Muzo, Colombia. *American Mineralogist*, Vol. 55, No. 3/4, pp. 416–427.

O'Donoghue M.J. (1971) Trapiche emerald. *Journal of Gemmology*, Vol. 12, No 8, pp. 329–332.

Peretti A., Mullis J., Mouawad F. (1996) The role of fluorine in the formation of colour-zoning in rubies from Mong Hsu, Myanmar (Burma). *Journal of Gemmology*, Vol. 25, No. 1, pp. 3–19.

Peretti A., Schmetzer K., Bernhardt H.-J., Mouawad F. (1995) Rubies from Mong Hsu. *Gems & Gemmology*, Vol. 31, No. 1, pp. 2–26.

Petreus I. (1974) The divided structure of crystals, II: Secondary structures and habits. *Neues Jahrbuch für Mineralogie Abhandlungen*, Vol. 122, No. 3, pp. 314–338.

Pinet M., Smith D.C., Lasnier B. (1992) Utilité de la microsonde Raman pour l'identification non-destructive des gemmes. In *La Microsonde Raman en Gemmologie*, Association Française de Gemmologie, Paris, pp. 11–60.

Schiffmann C.A. (1968) Unusual emeralds. *Journal of Gemmology*, Vol. 11, No. 4, pp. 105–114.

White W.B. (1974) The carbonate minerals. In V.C. Farmer, Ed., *The Infrared Spectra of Minerals*, Mineralogical Society Monograph 4, London, pp. 227–284.

BACK ISSUES OF

GEMS & GEMOLOGY

Limited quantities of these issues are still available


Spring 1994


Spring 1995


Spring 1996


Summer 1994


Summer 1995


Summer 1996


Fall 1994


Fall 1995


Fall 1996


Winter 1994


Winter 1995


Winter 1996

Complete your back issues of Gems & Gemology NOW!

	U.S.	Canada & Mexico	Elsewhere
Single Issues*	$ 11.00 each	$ 13.00 each	$ 14.00 each
*Complete Volumes:**			
1987, 1991, 1992, 1993, 1994, 1995, 1996	$ 38.00 each	$ 44.00 each	$ 53.00 each
Three-year set	$105.00 each	$120.00 each	$155.00 each
Five-year set	$170.00 each	$190.00 each	$245.00 each

*10% discount for GIA Annual Fund donors at the Booster's Circle level and above.

TO ORDER: Call toll free (800) 421-7250, ext. 202 or (310) 829-2991, ext. 202
FAX (310) 453-4478 OR WRITE: G&G Subscriptions GIA
P.O. Box 2110, Santa Monica, CA 90404 USA

Fall 1988
An Economic Review of Diamonds
The Sapphires of Penglai, Hainan Island, China
Iridescent Orthoamphibole from Wyoming
Detection of Treatment in Two Green Diamonds

Spring 1989
The Sinkankas Library
The Gujar Killi Emerald Deposit
Beryl Gem Nodules from the Bananal Mine
"Opalite:" Plastic Imitation Opal

Summer 1989
Filled Diamonds
Synthetic Diamond Thin Films
Grading the Hope Diamond
Diamonds with Color-Zoned Pavilions

Fall 1989
Polynesian Black Pearls
The Capoeirana Emerald Deposit
Brazil-Twinned Synthetic Quartz
Thermal Alteration of Inclusions in Rutilated Topaz
Chicken-Blood Stone from China

Winter 1989
Emerald and Gold Treasures of the Atocha
Zircon from the Harts Range, Australia
Blue Feldspar
Reflectance Infrared Spectroscopy in Gemology
Mildly Radioactive Rhinestones

SOLD OUT

Spring 1990
Gem Localities of the 1980s
Gemstone Enhancement and Its Detection
Synthetic Gem Materials in the 1980s
New Technologies of the 1980s
Jewelry of the 1980s

Spring 1991
Age, Origin, and Emplacement of Diamonds
Emeralds of Panjshir Valley, Afghanistan

Summer 1991
Fracture Filling of Emeralds: Opticon and "Oils"
Emeralds from the Ural Mountains, USSR
Treated Andamooka Matrix Opal

Fall 1991
Rubies and Fancy Sapphires from Vietnam
New Rubies from Morogoro, Tanzania
Bohemian Garnet—Today

Winter 1991
Marine Mining of Diamonds off Southern Africa
Sunstone Labradorite from the Ponderosa Mine
Nontraditional Gemstone Cutting
Nontransparent "CZ" from Russia

Spring 1992
Gem-Quality Green Zoisite
Kilbourne Hole Peridot
Fluid Inclusion Study of Querétaro Opal
Natural-Color Nonconductive Gray-to-Blue Diamonds
Peridot as an Interplanetary Gemstone

Summer 1992
Gem Wealth of Tanzania
Gamma-Ray Spectroscopy and Radioactivity
Dyed Natural Corundum as a Ruby Imitation
An Update on Sumitomo Synthetic Diamonds

Fall 1992
Ruby and Sapphire Mining in Mogok
Bleached and Polymer-Impregnated Jadeite
Radiation-Induced Yellow-Green in Garnet

Winter 1992
Determining the Gold Content of Jewelry Metals
Diamond Sources and Production
Sapphires from Changle, China

Spring 1993
Queensland Boulder Opal
Update on Diffusion-Treated Corundum: Red and Other Colors
A New Gem Beryl Locality: Luumäki, Finland
De Beers Near Colorless-to-Blue Experimental Gem-Quality Synthetic Diamonds

Summer 1993
Flux-Grown Synthetic Red and Blue Spinels from Russia
Emeralds and Green Beryls of Upper Egypt
Reactor-Irradiated Green Topaz

Fall 1993
Jewels of the Edwardians
A Guide Map to the Gem Deposits of Sri Lanka
Two Treated-Color Synthetic Red Diamonds
Two Near-Colorless General Electric Type IIa Synthetic Diamond Crystals

Winter 1993
Russian Gem-Quality Synthetic Yellow Diamonds
Heat Treating Rock Creek (Montana) Sapphires
Garnets from Altay, China

Spring 1994
The Anahí Ametrine Mine, Bolivia
Indaia Sapphire Deposits of Minas Gerais, Brazil
Flux-Induced Fingerprints in Synthetic Ruby

Summer 1994
Synthetic Rubies by Douros
Emeralds from the Mananjary Region, Madagascar: Internal Features
Synthetic Forsterite and Synthetic Peridot
Update on Mining Rubies and Fancy Sapphires in Northern Vietnam

Fall 1994
Filled Diamonds: Identification and Durability
Inclusions of Native Copper and Tenorite in Cuprian-Elbaite Tourmaline, Paraíba, Brazil

Winter 1994
Color Grading of Colored Diamonds in the GIA Gem Trade Laboratory
Ruby and Sapphire from the Ural Mountains, Russia
Gem Corundum in Alkali Basalt

Spring 1995
Rubies from Mong Hsu
The Yogo Sapphire Deposit
Meerschaum from Eskisehir Province, Turkey

Summer 1995
History of Pearling in La Paz Bay
An Update on the Ural Emerald Mines
A Visual Guide to the Identification of Filled Diamonds

Fall 1995
Gem-Quality Grossular-Andradite: A New Garnet from Mali
Sapphires from Southern Vietnam
"Ti-Sapphire": Czochralski-Pulled Synthetic Pink Sapphire from Union Carbide

Winter 1995
A History of Diamond Sources in Africa: Part I
A Chart for the Separation of Natural and Synthetic Diamonds

Spring 1996
A History of Diamond Sources in Africa: Part II
Gemological Investigation of a New Type of Russian Hydrothermal Synthetic Emerald
Growth Method and Growth-Related Properties of a New Type of Russian Hydrothermal Synthetic Emerald

Summer 1996
Sapphires from the Andranondambo Region, Madagascar
Russian Demantoid, Czar of the Garnet Family
Opal from Shewa Province, Ethiopia

Fall 1996
De Beers Natural versus Synthetic Diamond Verification Instruments
Analyzing Internal Growth Structures: Identification of the Negative *d* Plane in Natural Ruby
Russian Flux-Grown Synthetic Alexandrite

Winter 1996
Imperial Topaz from the Capão Mine, Minas Gerais, Brazil
Trapiche Rubies
Identifying Black Opaque Gem Materials
Enstatite, Cordierite, Kornerupine and Scapolite from Embilipitiya, Sri Lanka
Some Tanzanite Imitations

Some issues from the 1984–1987 volume years are also available.
Please contact the Subscriptions Office for details.

ORDER NOW!

SOME GEMOLOGICAL CHALLENGES IN IDENTIFYING BLACK OPAQUE GEM MATERIALS

By Mary L. Johnson, Shane F. McClure, and Dino G. DeGhionno

Among the most difficult gems to identify are those that are black and opaque (or nearly so). In general, any gem material can be opaque because of inclusions, any black opaque material can be fashioned, and any porous material can be dyed. Thus, to identify a black opaque material, every possible mineral, and many rocks and manufactured substances, must be considered. Microscopic appearance, refractive index, specific gravity, and other properties (such as magnetism or radioactivity) provide useful clues, but in most cases advanced identification techniques (X-ray diffraction, EDXRF spectroscopy) are necessary, and even these may not be conclusive. Black opaque pyroxenes, amphiboles, and spinel-group minerals are especially challenging to identify.

ABOUT THE AUTHORS

Dr. Johnson is a research scientist, Mr. McClure is supervisor of identification services, and Mr. DeGhionno is staff gemologist at the Gemological Institute of America Gem Trade Laboratory in Carlsbad, California.

Acknowledgments: This article is dedicated to the late Robert C. Kammerling, former vice president of Identification and Research and Development at GIA GTL, Santa Monica, California, for his inspiration. (He also provided the spinel-group mineral samples.) For critical review of the manuscript, the authors also thank Tom Moses and Ilene Reinitz, both of New York GIA GTL, and John I. Koivula, Carlsbad GIA GTL.

Gems & Gemology, Vol. 32, No. 4, pp. 252–261.

One of the most challenging problems in gemology is that of determining the identity of a black opaque gem material—hereafter called a "black opaque." Such materials are a mainstay of the jewelry business, primarily as side stones, decorative elements in multi-stone mosaics, and in men's jewelry. Treated black chalcedony ("black onyx"), black jade, and hematite traditionally have been the black opaques in greatest demand. As a variety of quartz, "black onyx" is probably the most familiar durable black opaque to lapidaries and gem cutters. Today, it is a popular medium for artistic carvings, many of which have been incorporated into fine jewelry (figure 1).

In recent years, various materials have been misrepresented as "black onyx" or "black jade" to meet the trade's need for calibrated goods in high-volume markets. Members of the trade, in turn, have been sending samples to identification laboratories to ensure that the material has been properly represented, so that they can sell it honestly. Usually, individual items sent to the GIA Gem Trade Laboratory (GIA GTL) for identification are representative of larger lots.

The purpose of this article is to provide a set of procedures by which to identify black opaques (that is, materials that are black or almost black and opaque or nearly so). The examples used are drawn primarily from our experience at GIA GTL. Not all black opaques are included here, as that is beyond the scope of a single article (and almost any gem material, by virtue of inclusions, can become a "black opaque"). Because so many materials—both common and exotic—may be used as black opaques, any set of identification procedures must take all possibilities into consideration, not just a few. For example, black jade (nephrite or jadeite), "onyx," and hematite each have many imitations. Also, natural-color black diamonds may be confused with diamond imitations and treated-color diamonds. In the last few years, other black opaque materials have become increasingly available, such as the amphibole ferrohornblende (sold as black "gem barkevikite") and various spinel-group minerals (figure 2). Still another challenging problem is that of identifying black opaque polycrystalline aggregates, or rocks.

This article will examine the applicability of advanced as well as traditional gemological tests in identifying black opaque gem substances. Basic gemological tests can distinguish some common black opaque materials, but they cannot be relied on for unambiguous determination in all cases. Various ancillary methods can also provide useful clues about the nature of black opaques. In most situations, though, only advanced techniques provide the definitive information needed to identify these materials.

Certain black materials (pearl, jet) are distinctive enough to present their own identification challenges, and are outside the scope of this article. The reader should consult Muller (1987) for the separation of jet from other natural and manufactured hydrocarbons; Goebel and Dirlam (1989) provide a good summary of how to identify treatments in black natural and cultured pearls.

TESTING METHODS FOR BLACK OPAQUES

Optical Tests. As Liddicoat (1989) pointed out, the first test used in examining a gem material is visual observation—with a microscope, a loupe, or the unaided eye. For many transparent stones, much of the relevant identification information comes from the stone's interior; that is, transmission of light through the stone is needed to detect characteristic features. In the case of black opaques, however, examination is limited to surface or near-surface features.

The first question to be addressed when identifying black opaques is whether the material is single-crystal (or glass) or an aggregate. An important clue in this regard is the appearance of a fracture surface. With fashioned stones, look for the small chips that are frequently present around the girdle or on the back of cabochons. Most aggregate materials will have a dull, granular fracture, although extremely fine, compact aggregates, such as chalcedony, may appear waxy and conchoidal. In contrast, single-crystal materials may have any of several types of fracture surfaces (including conchoidal, uneven, and splintery with vitreous [glassy] to adamantine luster), but they are never granular. Therefore, if a vitreous conchoidal fracture is observed, it can be surmised that the material is single crystal. Conversely, if a granular fracture is observed, the material must be an aggregate.

Another simple test is to examine the polished material with reflected light, to look for fractures and grain boundaries, differences in relief (figure 3), and differences in reflectivity (figure 4), all of which indicate an aggregate. Contrasts in relief may result from different polishing hardnesses among the minerals present, from directional variations in hardness between grains with different orientations, or from different grain sizes, as in the bands in "black onyx" and black coral. Usually only large differences in refractive index values (and, thus, luster) can be observed.

Figure 1. Because of their dramatic appearance, and the ease with which many can be fashioned, black opaque gem materials are increasingly important in gem carvings and custom-made jewelry. This 9.1 x 3.5 cm piece is composed of carved drusy dyed black chalcedony ("black onyx"), together with carved Oregon opal, a pink tourmaline, mother-of-pearl, and diamonds. Carvings and gold fabrication by Glenn Lehrer, San Rafael, California; photo © Lee-Carraher Photography.

Figure 2. These four opaque black stones, which range from 1.88 to 13.63 ct, are hercynite (the two faceted stones) and magnetite, spinel-group minerals from the Bo Phloi region of Thailand. Photo by Maha DeMaggio.

If a microscope with an analyzer is available, a polarizer can be placed over the light source to obtain additional information. Anisotropic (uniaxial and biaxial) minerals have different refractive indices with different directions of polarized light, so the relative reflectivities of adjacent grains in an aggregate may change as the analyzer is rotated. Some highly reflective materials, such as the black opaque minerals graphite and enargite, may show pleochroism in reflected light.

Observation of the sample's luster can be very important (again, see figure 2). Black opaques can have any type of luster and, in general, "higher" lusters (adamantine or metallic) correspond to high R.I. values. However, the apparent luster also may be affected by the quality of the polish on a fashioned gem.

In many cases, a black opaque is not completely black or opaque when a very thin region is viewed with a strong beam of light. Fiber-optic illumination in conjunction with magnification is ideal for this purpose (Koivula, 1982). Materials that have a black appearance overall may look green, brown, red, blue, purple, gray, or the like, at these intensely lit thin edges. Sometimes growth structures are more visible in thin edges with strong transmitted light (figure 5) than with reflected light. Inclusions—such as gas bubbles in manufactured glass, and stretched gas bubbles and iron-titanium oxide inclusions in natural volcanic glass (obsidian; see, e.g., Gübelin and Koivula, 1986, p. 285)—may also be seen.

Some black opaques display asterism (see, e.g., Kane, 1985 [sapphire]; Liddicoat, 1989 [diopside]; Koivula and Kammerling, 1990a [ekanite]; and Koivula et al., 1993b [irradiated quartz]), which can be an important consideration for identification. Chatoyancy is also seen occasionally (as in opal—Koivula and Kammerling, 1990b). Both of these phenomena may be very weak, so strong pinpoint illumination also should be used to search for them.

In those cases where a material is black because of inclusions, it often helps to try to determine which opaque material is responsible for coloring the unknown. Strong, low-angle oblique illumination can be used, with magnification, to distinguish

Figure 3. The contrast in relief seen in reflected light in this dark green fuchsite (muscovite) mica is due to the presence of harder minerals, such as quartz, in this aggregate material. Photo by John I. Koivula; magnified 15×.

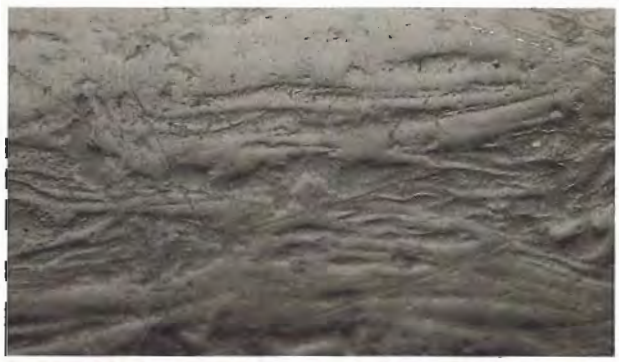

Figure 4. The crystals in this sample of (manufactured) devitrified glass have a higher refractive index than the glass matrix, and so they reflect more light. Photomicrograph by John I. Koivula; magnified 20×.

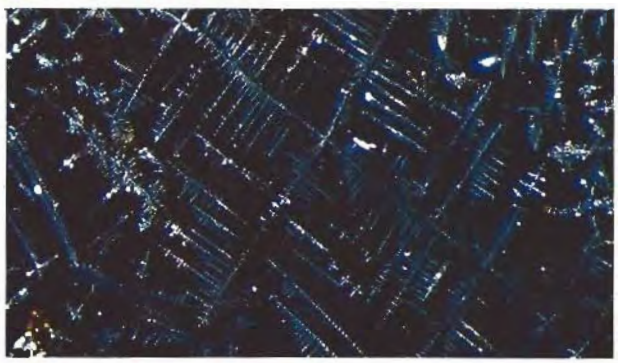

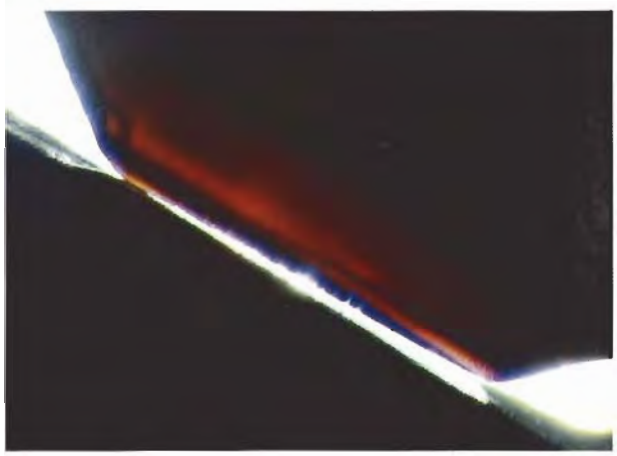

Figure 5. The banding in this "black onyx" cabochon is visible only on a very thin edge with strong fiber-optic illumination. The black chalcedony may have been a banded agate before being treated to produce the black color, or it could have been a chalcedony in which different layers selectively absorbed the coloring agent. Photomicrograph by John I. Koivula; magnified 10×.

(for instance) between metallic iron oxides such as hematite, which appear reddish brown when lit from the side (figure 6), and titanium-bearing oxides such as ilmenite, which may appear white when lit from the side (because of surface alteration into white so-called "leucoxene" [Deer et al., 1966, pp. 418–419], figure 7). Similarly, the opaque iron sulfides pyrite and pyrrhotite look brassy yellow in reflected light. This technique may also provide clues to the identity of a metallic-luster opaque.

Many other optical tests—such as observing the absorption spectrum, checking the optic sign, or looking for pleochroism—are not feasible when testing black opaques. (However, a reflected-light spectrum sometimes can be obtained from opaque samples: Kammerling et al., 1990.) Fortunately, the refractive index (or indices) of an opaque material still can be measured, although many materials, especially those with metallic lusters, have indices that are over the limits of a standard refractometer. Measurements should be taken from several places on a black opaque to check for multiple phases, or to determine if the material is doubly refractive. (As used here, "phases" refers only to solid phases, including distinct minerals, glass, plastic filler, etc.)

Other Physical Tests. Specific gravity can be extremely valuable for distinguishing among single-crystal materials, especially those with refractive indices greater than 1.81. It is somewhat less reliable for aggregates and porous materials. Note that some materials give inconsistent specific gravity values, including the hercynite sample described below. Also, hydrostatic specific gravity measurements are less precise than, for example, refractive index measurements.

Figure 6. The large hematite crystal in this quartz/magnetite/hematite cabochon looks red along a very thin edge; this red color is seen when the sample is examined with low-angle oblique illumination. Photomicrograph by John I. Koivula; magnified 15×.

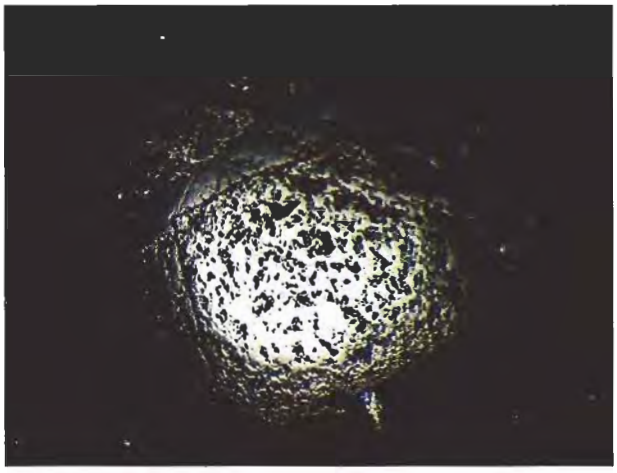

Figure 7. The ilmenite crystal in this black labradorite moonstone cabochon looks white when viewed with low-angle oblique illumination. Photomicrograph by John I. Koivula; magnified 20×.

Various other tests may be useful or even diagnostic for certain materials. One common test is the observation of luminescence to long- or short-wave ultraviolet radiation. For example, some black diamonds fluoresce (Kammerling et al., 1990). Certain black opaques, notably magnetite, are strongly attracted to magnets, as are some other spinel-group minerals (e.g., some hercynite: Johnson, 1994) and some hematite (Fryer et al., 1984). The streak test (scratching an inconspicuous corner of the sample across an unglazed porcelain plate) must be made carefully, as it is a destructive test, but it can provide distinctive information about certain materials. For example, the iron oxides—magnetite, hematite, and goethite—have black, red, and brown streaks, respectively. However, for aggregate materials with small grain sizes, the low-angle oblique illumination test mentioned above provides the same information as a streak test, without the risk of damaging the sample. Some low-luster materials, such as jet and plastics, react to the thermal reaction tester ("hot point") with diagnostic aromas.

Some materials are electrically conductive. These will give a positive response to an electrical conductometer—or even to an electrical multimeter, which is available at most hardware stores. For example, a diagnostic test for manufactured yttrium iron garnet, YIG, is that it does not conduct electricity (Kammerling et al., 1990). However, practically any mineral or rock can appear black and opaque because of included graphite, which conducts electricity; consequently, such a material might give a positive response to an electrical conductivity test even though the host material is not electrically conductive.

Finally, a few materials are innately radioactive, such as pitchblende (uraninite; Fuhrbach, 1987) and dark green to black-appearing ekanite (see, e.g., Kane, 1986a; "Gem News," 1987). Others are radioactive because of treatment, such as treated-color black diamonds (see, e.g., Reinitz and Ashbaugh, 1992; Koivula et al., 1992c). Radioactivity can be detected by means of handheld detectors (such as Geiger counters), by the fogging of photographic film (see, e.g., Fuhrbach, 1987), or with more sophisticated techniques (Ashbaugh, 1992).

In many cases, however, the information provided by the tests described above will not be sufficient to identify a black opaque (figure 8). For these pieces, more advanced testing, requiring more sophisticated equipment, is necessary.

Advanced Tests. Two advanced testing procedures will usually identify any unknown black opaque: X-ray powder diffraction analysis and energy-dispersive X-ray fluorescence (EDXRF) spectroscopy. In X-ray powder diffraction analysis, a minute amount of material is scraped from an inconspicuous spot on the sample. The resulting fine powder is attached to a small glass fiber "spindle" that is then mounted—along with a strip of X-ray sensitive film—in a special diffraction camera. Next, the sample is exposed to a strong beam of nearly monochromatic X-rays. The lattice of atoms (atomic structure) of the rotating powdered sample causes the X-rays to be diffracted and expose arc-shaped regions on the film. By measuring the positions of these arcs, and estimating their relative intensities, we can compare the X-ray powder diffraction pattern of the unknown material to diagnostic patterns for known materials. Because the powder sample is usually taken from only one or a few inconspicuous spots, care must be exercised to ensure that the area sampled is representative of the piece as a whole; this is especially difficult to guarantee for black aggregates.

In the second test, EDXRF spectroscopy, the entire sample is exposed to a strong X-ray source, which induces the elements in the sample to produce (or "fluoresce") secondary X-rays. Because each element in the sample produces X-rays with a characteristic set of energy levels, the sample's chemical composition can be approximated by collecting and counting these X-rays. (Note that the elements within the sample absorb some or all of each other's emitted X-rays, as well as the source X-rays, and can cause one another to fluoresce; consequently, the quantitative or even semi-quantitative determination of a sample's chemistry is much more complicated and, in general, requires appropriate and well-understood standards.)

The combination of X-ray powder diffraction and EDXRF analyses can usually determine both the structure and the chemistry of a sample. Frequently, this information is sufficient to identify the material. However, we may not be able to separate minerals that form groups or series (such as pyroxenes, amphiboles, and spinels) from other members of the same mineral group without further testing, such as the destructive or relatively inaccessible tests described below.

Petrographic and Other Geologic Tests (Not Recommended). Because of their destructive nature, certain standard geologic tests may be inap-

propriate for gemstones. The simplest of these is hardness testing, which requires scratching the sample one or more times. Detailed optical information about transparent minerals can be obtained from thin sections of that material—that is, slices with an ideal thickness of about 30 μm that have been polished on both sides. Many minerals that appear to be opaque at a thickness useful for jewelry are transparent or translucent in thin section; however, most customers do not want a representative slice taken from their valuable gem!

Quantitative chemical techniques, such as electron microprobe analysis and scanning electron microscopy–energy dispersive spectroscopy (SEM-EDS), require costly equipment, trained personnel, and special sample preparation. Some other techniques, such as classical wet chemistry and the more modern gas chromatography/mass spectrometry (GC/MS), require complete destruction of at least part of the sample. Other sophisticated tests—transmission electron microscopy, the "ion probe," single-crystal X-ray diffraction, and the like—require special preparation and/or some sample destruction in order to characterize a mineral completely. Consequently, such tests are usually inappropriate for isolated gem samples, although they may be required to characterize fully a new gem material.

SPECIFIC IDENTIFICATION EXAMPLES

Several examples of black opaque materials that have been seen at GIA GTL are given in table 1, along with an abbreviated list of their properties and some references for further information. This list is certainly not complete, as any gem material may be black and opaque if it contains a sufficient amount of dark inclusions (as is the case with black diamonds, for example). Furthermore, virtually any dark-colored mineral that occurs in aggregates that are large and coherent enough can be fashioned into a cabochon, and any porous material—such as calcite, dolomite, chalcedony, and the like—can be dyed black (figure 9). Three especially challenging identification problems are discussed below: rocks (aggregate materials), pyroxene- and amphibole-group minerals, and black spinel-group minerals.

First Example: Aggregate Materials (Rocks). Inspection with reflected light provides the best clue to the appropriate procedure for identifying a black opaque aggregate material. Are there differences in polishing hardness, relief, or reflectivity, indicating the presence of multiple phases or of multiple orientations of the same mineral phase? If so, what are the relative amounts of the phases present? (Relative amounts are determined by estimating the proportion of different distinct areas, a standard practice in sedimentary petrology.) In most cases, only phases comprising 25% or more of the sample are identified by GIA GTL.

Figure 8. It would probably be necessary to use advanced testing methods, such as EDXRF spectroscopy and X-ray powder diffraction analysis, to determine which black material was used in this carving by Steve Walters. The carving is set with amethyst-citrine and diamonds in a convertible enhancer pin designed and manufactured by David W. Lisky and Christopher Engelken, of Christopher David Designs, Milwaukee, Wisconsin. Photo by John Parish.

Sometimes, the surface areas of individual phases in a rock are large enough so that individual R.I. values can be determined. The specific gravity, on the other hand, is an aggregate property: The specific gravity we determine for an aggregate sample should agree with the weighted average of the S.G. values of the individual phases present. (If it does not, the material may be different below its surface—e.g., hollow, or zoned around a denser

TABLE 1. Gemological properties of some black opaque gem materials.[a]

Name	R.I.	S.G.	Luster	Comments	References
Hematite	2.94–3.22	4.95–5.16	Metallic	Sometimes magnetic	Fryer et al. (1984), Liddicoat (1989), Webster (1994)
Uraninite	Not available	5.2–10.0	Submetallic, resinous	Radioactive	Fuhrbach (1987), Liddicoat (1989), Kammerling et al. (1990)
Diamond	2.417	3.52	Adamantine		Liddicoat (1989), Crowningshield (1990), Kammerling et al. (1990), Johnson (1995)
Irradiated "black" diamond	2.417	3.52	Adamantine	Sometimes radioactive	Liddicoat (1989), Kammerling et al. (1990), Koivula et al. (1992c), Reinitz and Ashbaugh (1992)
Cassiterite	2.006–2.097	6.99	Adamantine to vitreous		Liddicoat (1989), Kammerling et al. (1990)
Hausmannite	> 1.81	4.84	Adamantine		Kammerling et al. (1995b), observation of same material (unpublished)
"Psilomelane" (Mn oxides)	> 1.81	4.35	Metallic to submetallic		Webster (1994)
Spinel Group					
Magnetite	2.42	5.20	Metallic	Magnetic	Deer et al. (1966), Welch (1987), this work
Hercynite	> 1.81; 1.835	4.40	Subadamantine	Sometimes magnetic	Johnson (1994), Webster (1994), this work,
Spinel	1.77	3.83	Vitreous		Fryer et al. (1982), Hurwit (1984), Webster (1994)
Intermediate spinel-hercynite	1.765	3.93	Subadamantine to vitreous		Koivula et al. (1993a)
Garnet Group					
Andradite garnet (melanite)	1.885	3.84	Subadamantine to vitreous		Liddicoat (1989)
Pyrope	1.740	About 3.72	Vitreous		Fryer (1988)
Corundum (star sapphire)	1.760–1.78	3.989–4.0	Subadamantine		Kane (1985), Liddicoat (1989), Webster (1994)
Pyroxene Group					
Augite	1.702–1.728	3.20–3.35	"High" vitreous		Hurwit (1988a)
Diopside (star)	1.675-1.701	3.33	Vitreous		Liddicoat (1989), Webster (1994)
Jadeite jade	1.65-1.67	3.20–3.34	Vitreous		Liddicoat (1989), Hargett (1990)
Tourmaline	1.622-1.655	3.15–3.2	Vitreous		Liddicoat (1989), Webster (1994)
Amphibole Group					
Ferrohornblende	1.60-1.70	3.36	Vitreous		Crowningshield et al. (1994)
Nephrite jade	1.600–1.641	2.90–3.02	Vitreous		Liddicoat (1989), Webster (1994)
Cummingtonite-grunerite	1.54–1.65				Kane (1984)
Jet	1.59–1.66	1.20–1.30	Resinous		Hurwit (1985), Liddicoat (1989), Webster (1994)
Ekanite	1.593–1.595	About 3.30	Vitreous	Radioactive	Kane (1986a)
Labradorite feldspar	1.560–1.568	2.69	Vitreous	Colored by inclusions	Liddicoat (1989), Webster (1994)
Dyed chalcedony (black "onyx")	1.530–1.539	2.57–2.64	Vitreous		Koivula and Kammerling (1991), Webster (1994)
Chalcedony with "Psilomelane"	1.535–1.539	3.0–3.1	Metallic to submetallic	Banded	Liddicoat (1989), Kammerling et al. (1990), Koivula and Kammerling (1989)
Coated quartz	1.54		Vitreous to dull		Hurwit (1988b)
Dolomite	1.51–1.67	2.8–2.9	Vitreous		Koivula et al. (1994), Webster (1994)
Black coral	1.56	1.34	Resinous		Liddicoat (1989), Webster (1994)
Obsidian	1.48–1.52	2.30–2.50	Vitreous		Liddicoat (1989), Webster (1994)
Opal (black opaque)	1.44	2.02	Vitreous		Koivula and Kammerling (1990b)
Rocks (aggregates)					
Dolomite/quartzite rock	1.66 spot	2.74	Vitreous		Hargett (1991)
Basalt rock	n.d.[b]	n.d.	n.d.		Koivula and Kammerling (1989)
Simulants					
Cubic zirconia	2.14	6.14–6.16	Adamantine		Kammerling et al. (1991), Koivula et al. (1992b)
Silicon	> 1.81	2.34	Metallic	Gray	Webster (1994), Johnson and Koivula (1996)
"Hematine"	> 1.81	4.00–7.00	Metallic	Magnetic	Liddicoat (1989), Webster (1994)
YIG (yttrium iron garnet)	not available	about 6	Vitreous to submetallic	Magnetic	Liddicoat (1989), Kammerling et al. (1990)
Barium sulfate/polymer	mid-1.50s	2.26, 2.33	n.d.		Koivula et al. (1992a), Webster (1994)
Plastics	1.5–1.6	1.05–1.55	Vitreous to resinous		Liddicoat (1989), Webster (1994)
Glass	1.35–1.70	2.51–3.21	Submetallic to vitreous		Kane (1986c), Welch (1988), Liddicoat (1989), Moses (1989), Webster (1994)

[a] *Arranged in approximate decreasing order of refractive index.* [b] *n.d.= not determined.*

core.) In general, X-ray powder diffraction analysis of each phase is required to identify that phase conclusively; EDXRF spectroscopy, like S.G. determination, only provides information about the sample as a whole.

GIA GTL identifies black opaque rocks as follows: If one phase comprises 75% or more of the sample, it is described as "a rock, consisting primarily of (name of appropriate phase), and possible additional minerals." If there are two or more phases that each comprises 25% or more of the sample, it is described as "a rock, consisting of (commonest phase, next commonest phase, etc.), and possible additional minerals." In both cases, this comment is added: "Petrographic testing would be necessary to fully characterize this material." Of course, if a black opaque rock has a well-established gemological name (e.g., nephrite), that name is used instead. We do not use common petrologic names for rocks (such as basalt, granite, or conglomerate), because such names imply that we know the history of the rock—such as igneous versus sedimentary origin—which cannot be determined easily with our testing procedures (Kammerling et al., 1995a). Typical descriptions of rocks that have been examined by GIA GTL include "dolomite/quartz rock" (Hargett, 1991) and "a rock consisting of plagioclase feldspar, an amphibole, pyrite, and possible additional minerals."

Figure 9. A uniform black is often achieved by dyeing a porous material. This 8.0 x 5.5 cm set was fashioned from two pieces from the same slab of drusy chalcedony, one dyed black and the other natural light gray. Carvings and photo by Glenn Lehrer.

Second Example: Pyroxene- and Amphibole-Group Minerals. As of 1995, there were 21 accepted species of pyroxene-group minerals and 66 species of amphibole-group minerals (Fleischer and Mandarino, 1995). Common gem examples of these minerals include jadeite, diopside, and spodumene (pyroxenes), and the nephrite variety of tremolite or actinolite (amphibole). Many of the rest are dark colored or black, unfamiliar to gemologists, and separated from one another only with great difficulty (i.e., requiring quantitative chemical analysis and detailed crystal structure determination). The most common dark pyroxene in terrestrial rocks is augite, but the correspondingly common black amphibole, once known as hornblende, has been "subdivided" into many different mineral species.

GIA GTL usually relies on a combination of X-ray powder diffraction and EDXRF to identify the less common pyroxenes and amphiboles. In some cases, the exact mineral species cannot be determined. Examples of unusual gem pyroxenes and amphiboles (not necessarily black ones) seen by GIA GTL include the pyroxenes augite (Hurwit, 1988a, 1989), omphacite (Johnson and Kammerling, 1995), and "orthopyroxene" (Kammerling, 1993); and the amphiboles magnesian hastingsite (as indicated by the X-ray diffraction pattern; see Kane, 1986b), ferrohornblende (Crowningshield et al., 1994), "a member of the cummingtonite-grunerite series" (Kane, 1984), and "orthoamphibole" (Crowningshield, 1993). Two additional stones that we examined could only be identified as "a member of the edenite-hastingsite-pargasite series of the amphibole mineral group" and "a member of the amphibole mineral group."

Because determination of the precise pyroxene or amphibole species may require additional, more-destructive tests than we routinely perform, identification reports on these samples often contain the

comment, "Petrographic testing would be necessary to fully characterize this material." This comment means that some of the "less appropriate" tests mentioned earlier would be needed to determine the exact mineral species. Sometimes the comment, "Additional minerals may be present," is added as well.

Third Example: Black Opaque Spinel-Group Minerals. The black members of the spinel mineral group present significant identification challenges, since the group contains 21 species (Fleischer and Mandarino, 1995), and many of these form complete solid solutions (similar to the garnets). However, only four of these end-members are important components of the black spinels that we have examined: spinel, hercynite, magnetite, and, to a much lesser extent, chromite (Fryer et al., 1982; Hurwit, 1984; Welch, 1987; Koivula et al., 1993a; Johnson, 1994).

Magnetite and hercynite have refractive indices that are over the limit of the standard refractometer (that is, greater than 1.81), but the R.I. of spinel can be measured, as can those of some of the intermediates between spinel and hercynite. When measurable, the R.I. of a spinel-group mineral provides an important clue about that mineral's identity.

For many of the black spinels in our experience, the measured specific gravity values (3.78–3.88 for five hercynites, including the two shown in figure 2, and 4.81–4.83 for the two magnetites in figure 2) are lower than those predicted by Deer et al. (1966) from end-member compositions; however, other authors cite different S.G. values for hercynite (see, for instance, Phillips and Griffen, 1981). At least some of the hercynites that we have examined, and all of the magnetites, proved to be magnetic (e.g., Johnson, 1994).

The unit-cell spacing, *a*, is the fundamental distance between identical groups of atoms in the atomic structure of an isometric crystalline material. In spinel-group minerals, this spacing can be measured by X-ray powder diffraction analysis, that is, by carefully measuring the spacings of arcs on the photographic film, with comparison to a standard, preferably one mixed with the powdered unknown (an "internal" standard).

The general formula for the spinel group is AB_2O_4, where A and B are different cation elements; spinel itself is $MgAl_2O_4$; and other spinel-group minerals contain Fe, Zn, Mn, Cr, V, Ni, Co, Cu, Ti, and Ge. (Hercynite is $FeAl_2O_4$, magnetite is $FeFe_2O_4$, and chromite is $FeCr_2O_4$.) All of these elements (except oxygen) can be detected by the EDXRF instrumentation available at GIA GTL, although special attention must be paid to the lightest elements, Mg and Al, so that they are not overlooked. EDXRF spectroscopy is a necessary step in identifying an unknown spinel-group mineral, to make sure that no important component is overlooked.

Deer et al. (1966, p. 431) provide a calibration chart for R.I., S.G., and *a* for six spinel-group minerals, in the two series spinel-hercynite-magnesiochromite-chromite and spinel-hercynite-magnesioferrite-magnetite. We can identify a spinel-group mineral using this chart, our determined values of R.I. and *a*, and the EDXRF results for chemistry. (Because there is some debate as to the appropriate S.G. values to use, we do not include this information.) Black spinel-group minerals examined by GIA GTL include: spinel (Fryer et al., 1982; Hurwit, 1984), hercynite (Johnson, 1994), magnetite (Welch, 1987), and an intermediate between spinel and hercynite (Koivula et al., 1993a).

SUMMARY AND CONCLUSION

Black opaque gem materials present a special identification problem, because many basic gemological identification techniques require the transmission of light through the sample. In some cases, standard examination techniques are adequate to distinguish among common black opaques, at least to some minimum level of confidence. Certain modifications of these techniques, especially visual observation with reflected light, may provide additional insights. Some specific but less routine tests (such as for magnetism) can also be very useful. By-now-routine advanced testing procedures, such as X-ray powder diffraction analysis and EDXRF spectroscopy, give information that cannot be obtained by standard gemological testing alone. These advanced tests are usually required to positively identify most black opaque materials. With black opaques, as with other gem materials, *all* of the information available should be used to identify a sample. Because they are black and opaque, some uncertainty may remain about their identity even after advanced testing. In such cases, destructive testing techniques may be the only option for positive identification.

REFERENCES

Ashbaugh III C.E. (1992) Gamma-ray spectroscopy to measure radioactivity in gemstones. *Gems & Gemology*, Vol. 28, No. 2, pp. 104–111.

Crowningshield G.R. (1990) Gem trade lab notes: Diamond—Fancy black. *Gems & Gemology*, Vol. 26, No. 3, p. 221.

Crowningshield G.R. (1993) Gem Trade lab notes: Iridescent orthoamphibole, "nuummite."*Gems & Gemology*, Vol. 29, No. 4, p. 281.

Crowningshield G.R., Johnson M.L., Reinitz I. (1994) Gem trade lab notes: Iron-rich hornblende. *Gems & Gemology*, Vol. 30, No. 3, pp. 186–187.

Deer W.A., Howie R.A., Zussman J. (1966) *An Introduction to the Rock-Forming Minerals*. Longman Group, London, 528 pp.

Fleischer M., Mandarino J.A. (1995) *Glossary of Mineral Species 1995*, 7th ed. *Mineralogical Record*, Tucson, Arizona, 280 pp.

Fryer C. (1988) Gem trade lab notes: Black pyrope garnet. *Gems & Gemology*, Vol. 24, No. 2, pp. 116–117.

Fryer C., Crowningshield R.C., Hurwit K.N., Kane R.E. (1982) Gem trade lab notes: Spinel?. *Gems & Gemology*, Vol. 18, No. 3, p. 173.

Fryer C., Crowningshield R., Hurwit K.N., Kane R.E. (1984) Gem trade lab notes: Hematite, magnetic. *Gems & Gemology*, Vol. 20, No. 1, pp. 46–47.

Fuhrbach J. (1987) Editorial forum: Want to buy a "hot diamond"? *Gems & Gemology*, Vol. 23, No. 2, p. 111.

Gem news (1987) Large ekanite found. *Gems & Gemology*, Vol. 23, No. 2, p. 123.

Goebel M., Dirlam D.M. (1989) Polynesian black pearls. *Gems & Gemology*, Vol. 25, No. 3, pp. 130–148.

Gübelin E.J., Koivula J.I. (1986) *Photoatlas of Inclusions in Gemstones*. ABC Edition, Zurich, Switzerland, 532 pp.

Hargett D. (1990) Jadeite of Guatemala: A contemporary view. *Gems & Gemology*, Vol. 26, No. 2, pp. 134–141.

Hargett D. (1991) Gem trade lab notes: Quartzite and dolomite bead. *Gems & Gemology*, Vol. 27, No. 4, p. 251.

Hurwit K.N. (1984) Gem trade lab notes: Black spinel. *Gems & Gemology*, Vol. 20, No. 2, p. 112.

Hurwit K.N. (1985) Gem trade lab notes: Carved jet. *Gems & Gemology*, Vol. 21, No. 4, pp. 234–235.

Hurwit K.N. (1988a) Gem trade lab notes: Augite, Chinese "onyx." *Gems & Gemology*, Vol. 24, No. 3, p. 170.

Hurwit K.N. (1988b) Gem trade lab notes: Imitation dyed black chalcedony beads. *Gems & Gemology*, Vol. 24, No. 4, p. 241.

Hurwit K.N. (1989) Gem trade lab notes: Transparent green augite. *Gems & Gemology*, Vol. 25, No. 1, p. 35.

Johnson M.L. (1994) Gem trade lab notes: Magnetic hercynite, a warning about magnetic cards. *Gems & Gemology*, Vol. 30, No. 1, p. 43.

Johnson M.L. (1995) Gem trade lab notes: Diamond—Fancy black, with iron. *Gems & Gemology*, Vol. 31, No. 4, p. 266.

Johnson M.L., Kammerling R.C. (1995) Gem trade lab notes: Omphacite, rock carving. *Gems & Gemology*, Vol. 31, No. 2, pp. 124–125.

Johnson M.L., Koivula J.I. (1996) Gem news: "Drusy" silicon, a computer-industry by-product. *Gems & Gemology*, Vol. 32, No. 2, pp. 138–139.

Kammerling R.C. (1993) Gem trade lab notes: Orthopyroxene, a carved mask. *Gems & Gemology*, Vol. 29, No. 4, p. 281.

Kammerling R.C., Kane R.E., Koivula J.I., McClure S. F. (1990) An investigation of a suite of black diamond jewelry. *Gems & Gemology*, Vol. 26, No. 4, pp. 282–287.

Kammerling R.C., Koivula J.I., Kane R.E., Fritsch E., Muhlmeister S., McClure S.F. (1991) An examination of nontransparent "CZ" from Russia. *Gems & Gemology*, Vol. 276, No. 4, pp. 240–246.

Kammerling R., Johnson M.L., Moses M. (1995a) Describing aggregate gem materials. *ICA Gazette*, February 1995, p. 7.

Kammerling R.C., Koivula J.I., Johnson M.L., Fritsch E. (1995b) Gem news: "Drusy" hausmannite. *Gems & Gemology*, Vol. 31, No. 3, pp. 207–208.

Kane R.E. (1984) Gem trade lab notes: Cummingtonite-grunerite, a series in the amphibole group. *Gems & Gemology*, Vol. 20, No. 2, pp. 106–107.

Kane R.E. (1985) Gem trade lab notes: Corundum—Black star sapphire doublet. *Gems & Gemology*, Vol. 21, No. 3, p. 171.

Kane R.E. (1986a) Gem trade lab notes: Ekanite, a markedly radioactive metamict gem. *Gems & Gemology*, Vol. 22, No. 1, pp. 47–48.

Kane R.E. (1986b) Gem trade lab notes: Hornblende amphibole, magnesian hastingsite(?). *Gems & Gemology*, Vol. 22, No. 1, p. 49.

Kane R.E. (1986c) Gem trade lab notes: Devitrified glass, cobalt-bearing. *Gems & Gemology*, Vol. 22, No. 2, p. 108.

Koivula J.I. (1982) Pinpoint illumination: a controllable system of lighting for gem microscopy. *Gems & Gemology*, Vol. 18, No. 2, pp. 83–86.

Koivula J.I., Kammerling R.C. (1989) Gem news: Psilomelane and basalt—novel black carving materials. *Gems & Gemology*, Vol. 25, No. 4, pp. 246–247.

Koivula J.I., Kammerling R.C. (1990a) Gem news: Star ekanite. *Gems & Gemology*, Vol. 26, No. 1, p. 101.

Koivula J.I., Kammerling R.C. (1990b) Gem news: Black cat's-eye opal. *Gems & Gemology*, Vol. 26, No. 4, p. 304.

Koivula J.I., Kammerling R. C. (1991) Gem news: Drusy gems in jewelry. *Gems & Gemology*, Vol. 27, No. 1, p. 49.

Koivula J.I., Kammerling R.C., Fritsch E. (1992a) Gem news: Imitations of sugilite and other nontransparent gems. *Gems & Gemology*, Vol. 28, No. 1, p. 66.

Koivula J.I., Kammerling R.C., Fritsch E. (1992b) Gem news: Update on nontransparent CZ. *Gems & Gemology*, Vol. 28, No. 2, p. 138.

Koivula J.I., Kammerling R.C., Fritsch E. (1992c) Gem news: More on irradiated "black" diamonds. *Gems & Gemology*, Vol. 28, No. 4, pp. 276–277.

Koivula J.I., Kammerling R.C., Fritsch E. (1993a) Gem news: Black spinel from Mexico. *Gems & Gemology*, Vol. 29, No. 3, pp. 212–213.

Koivula J.I., Kammerling R.C., Fritsch E. (1993b) Gem news: Irradiated phenomenal quartz. *Gems & Gemology*, Vol. 29, No. 4, p. 288.

Koivula J.I., Kammerling R.C., Fritsch E. (1994) Gem news: "Zebra" stones from Australia. *Gems & Gemology*, Vol. 30, No. 2, pp. 128–129.

Liddicoat R.T. Jr. (1989) *Handbook of Gem Identification*. Gemological Institute of America, Santa Monica, California, 364 pp.

Moses T. (1989) Gem trade lab notes: Chalcedony, imitation "black onyx." *Gems & Gemology*, Vol. 25, No. 3, p. 171.

Muller H. (1987) *Jet*. Butterworth and Company, London, England, 149 pp.

Phillips W.R. and Griffen D.T. (1981) *Optical Mineralogy*. W. H. Freeman and Company, San Francisco, California, 677 pp.

Reinitz I., Ashbaugh III C.E. (1992) Gem trade lab notes: Diamond—Treated "black" diamond. *Gems & Gemology*, Vol. 28, No. 2, pp. 124–125.

Webster R. (1994) *Gems: Their Sources, Descriptions and Identification*, 5th ed. Rev. by P.G. Read, Butterworth-Heinemann Ltd., Oxford, England, 1026 pp.

Welch C. (1987) Gem trade lab notes: Magnetite, lodestone. *Gems & Gemology*, Vol. 23, No. 1, p. 45.

Welch C. (1988) Gem trade lab notes: Unusual glass. *Gems & Gemology*, Vol. 24, No. 2, p. 113.

ENSTATITE, CORDIERITE, KORNERUPINE, AND SCAPOLITE WITH UNUSUAL PROPERTIES FROM EMBILIPITIYA, SRI LANKA

By Pieter C. Zwaan

Gem-quality enstatite, cordierite, kornerupine, and scapolite with unusual properties have been recovered from alluvial deposits in the region of Embilipitiya, Sri Lanka. The occurrence of almost pure, completely colorless, enstatite appears to be unique in the world. The cordierites are also usually colorless and nonpleochroic. The diversity in the properties of kornerupine is mainly due to variations in the ratio of magnesium to iron. The strong "canary" yellow fluorescence of scapolites from this locality has not been observed in scapolites from other sources in Sri Lanka.

Since 1984, a group of mineralogists from Leiden, the Netherlands, have performed systematic field work in Sri Lanka. During the course of this research, they accumulated a representative collection of rocks and minerals from that country.

ABOUT THE AUTHOR

Dr. Zwaan is emeritus professor of gemology (Ph.D. Mineralogy) at Leiden University, The Netherlands, and retired director of the Netherlands Gemmological Laboratory, Leiden.

Acknowledgments: The author is much indebted to Dr. Charles E. S. Arps of the National Museum of Natural History, Leiden, for his cooperation, years of fieldwork in Sri Lanka, and critical reading of the manuscript; and to E. Gamini Zoysa, Mount Lavinia, Sri Lanka, for his valuable information and supply of material from different localities. The author also thanks E. A. J. Burke and W. J. Lustenhouwer, of the Institute of Earth Sciences, Free University of Amsterdam, for the Raman spectroscopy and electron microprobe analyses, respectively. D. van der Marel, of the National Museum technical staff, prepared the geologic map and photographed the cut stones. The financial support of the Foundation Stichting Dr. Schürmannfonds is gratefully acknowledged.

This article was developed in part from a paper presented at the 25th International Gemmological Conference in Rayong Resort, Thailand, October 1995. It was the last conference in which Robert C. Kammerling participated.

Gems & Gemology, Vol. 32, No. 4, pp. 262–269.

Although the well-known gem deposits of Ratnapura are still commercially the most important in Sri Lanka, other localities—such as Okkampitiya and Elahera—have also become interesting. Farther to the southeast, west of Kataragama, the Leiden researchers identified yet another locality of special mineralogic and gemological interest: Embilipitiya. Some gem minerals from this region were briefly described earlier (Zwaan, 1986). The present article discusses specific properties, and special aspects of these properties, for gem-quality enstatite, cordierite, kornerupine, and scapolite (figure 1).

GEM MINERALS FROM EMBILIPITIYA

Geoscientists have examined the geology, in particular the petrology, of Sri Lankan basement rocks for many years. To date, however, there has been no clear explanation for the origins of most of the gem minerals. The best summary of the results obtained thus far are the recent article by Dissanayake and Rupasinghe (1995) and the book by Gunaratne and Dissanayake (1995). Most important gems are recovered from alluvial deposits; the few gem minerals that have been traced to their *in situ* sources are not commercially important (i.e., of cutting quality).

Embilipitiya is a small village about 70 km (1.5 hours) by road southeast of Ratnapura. The village has a population of about 300 and is situated in a flat valley, about 2.5 km^2, surrounded by distant hills. The region is tropical, with both wet and dry seasons. Petrologically, it is in the Highland Complex, which contains Precambrian rocks of the metamorphic granulite facies (figure 2). Most of the gem deposits in Sri Lanka are located within this complex.

A variety of gem-quality minerals are found in the Embilipitiya region, in an area of about 6 km^2, primarily in alluvial deposits. Locals engage in small-scale primitive mining, digging narrow pits in the alluvium to a depth of 1.5–2 m (figure 3) to reach the gem-bearing gravels.

Of special interest, because of their unusual gemological properties, are scapolite and the Mg-rich minerals enstatite, cordierite, and kornerupine. Other gem minerals from this area include garnets, mainly almandine, and spinels. Since our first trip in 1984, we have visited the area several times and obtained several hundred carats of these unusual minerals from local inhabitants. During the last five years, however, greater demand by cutters and decreasing production have made it difficult to obtain more samples. These minerals are found mostly as broken and corroded fragments, seldom as rounded pebbles. Kornerupine is the most common of the four gems discussed in this article.

Figure 1. These four gem materials—cordierite (left, 3.75 ct), enstatite (top, 7.69 ct), scapolite (right, 3.08 ct), and kornerupine (bottom, 1.52 ct)—from the Embilipitiya area of Sri Lanka were found to have unusual gem properties. Photo by Shane F. McClure.

MATERIALS AND METHODS

During fieldwork in 1984, the author and his colleagues discovered Embilipitiya on the way from Ratnapura to gem localities in the southeast. At a lunch stop in the village, native people showed us *dullam*, pieces of rough gem minerals, that they were offering for sale. According to these villagers, the minerals came from the Embilipitiya area. At that time, we purchased about 3 kg of material, with a preponderance of colorless specimens. When we inspected these materials at the Netherlands Gemmological Laboratory in Leiden, we found that most of the samples were garnets and spinels, but we also identified a number of much less common gem minerals. During subsequent trips to Sri Lanka, we visited the village regularly and purchased almost every lot that was available.

Within the sample minerals were many fragments without crystal faces but with a recognizable—though usually corroded—prismatic habit. Using a polarizing microscope, we were able to group hundreds of specimens by species. The enstatites were selected for further study because of their range of color, from colorless to deep brown. About 20 rough specimens with a prismatic habit, approximately 10 to 30 mm long, were confirmed to be enstatite by their absorption spectra. In addition, we examined 10 cut enstatites; the largest was a 10.67 ct colorless specimen.

From among the cordierites, we selected about 40 rough samples (15 to 20 mm each) for further study. Most of these were nearly colorless, but some were pale blue. They were easily distinguished from the enstatites by their behavior in ethylene dibromide, in which the cordierites are almost invisible. Five cut stones, the largest of which was 3.75 ct, were available for examination.

A total of 56 rough kornerupines, varying in size from 5 to 20 mm and in weight from 0.91 ct (dark green) to 13.03 ct (dark brown), were selected for detailed study on the basis of their colors, inclusions, and physical properties (specimens with low and high refractive indices and specific gravities were represented). In addition, nine cut stones, the largest of which was 4.56 ct, were examined.

We examined 10 rough scapolites in detail. These were irregular, long prismatic, colorless-to-yellow pieces that ranged from 3.66 to 7.06 ct in weight and from 12 to 16 mm in their longest dimension. In addition, we studied seven cut scapolites from Embilipitiya, ranging from 0.80 ct (yel-

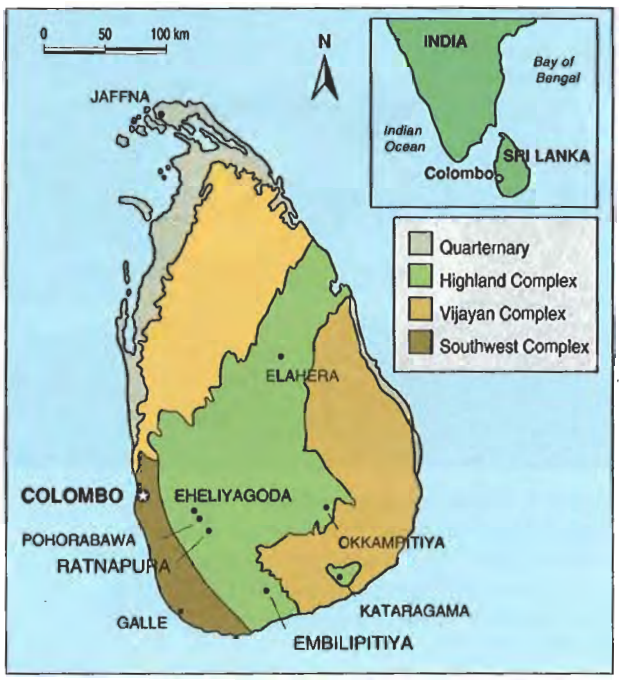

Figure 2. The village of Embilipitiya is about 70 km southeast of Ratnapura. It is in the Highland Complex, one of the main Precambrian geologic complexes that comprise the island nation of Sri Lanka.

low) to 17.79 ct (colorless), and compared their properties to those of 17 cut scapolites from elsewhere in the world. *Scapolite* is the name given to an isomorphous series in which marialite and meionite are the Na-rich and Ca-rich end members, respectively. The intermediate members are usually indicated by their molecular percentage (mol.%) of meionite.

The physical properties of all specimens were measured by standard gemological methods; for this purpose, two flat parallel faces were polished on each, thus forming a window. A Rayner refractometer with an yttrium aluminum garnet (YAG) prism was used to measure the refractive indices and birefringence. Specific gravity was determined with a hydrostatic balance.

The absorption spectra of all specimens were observed with both an Eickhorst handheld prism spectroscope and a Philips UV/ViS spectrometer (model PU 8730). X-ray powder diffraction photographs were taken on representative samples of all gem minerals using a Debye-Scherrer camera on an Enraf-Nonius Diffractis 582 apparatus. Chemical analyses were performed on eight kornerupines and six scapolites using an electron microprobe (JEOL model JXA-8800M), with three to five analyses per sample and the results averaged. The inclusions, mainly in the kornerupines and scapolites, were identified with a laser Raman microspectrometer (Dilor S.A. model Microdil-28).

ENSTATITE

The enstatites ($Mg_2Si_2O_6$) varied from colorless to deep brown (figure 4). The colorless stones had exceptionally low refractive indices (as low as n_α =1.650 and n_γ =1.658) and specific gravities (as low as 3.194). Microprobe analysis of one colorless stone revealed that 99.4 mol.% of the magnesium sites in this stone were occupied by Mg. This composition is very near the magnesium end-member of the enstatite-ferrosilite series. In fact, these were

Figure 3. The gems are recovered from shallow (about 1.5–2 m) alluvial pits in the Embilipitiya area. Photo by Pieter C. Zwaan.

Figure 4. The high-Mg enstatites from Embilipitiya are among the purest natural enstatites known. The enstatites shown here were all part of the study sample; the colorless 10.67 ct oval in the center is 20.5 mm in longest dimension.

the purest natural enstatites ever examined at the Netherlands Gemmological Laboratory.

The sample specimens had a distinct to very strong narrow absorption band at 506 nm, due to ferrous iron. The intensity of this band—which was present, though weak, even in the colorless stones—increased with the saturation of the brownish color, that is, with the Fe content. This absorption band was found to be characteristic of this material and, therefore, of diagnostic value. Most of the stones were relatively inclusion free, but some contained well-developed quartz crystals and two-phase inclusions. (For additional information on enstatites from this locality, see Zwaan, 1987.)

CORDIERITE

We prefer the mineral name *cordierite* ($Mg_2Al_4Si_5O_{18}$), instead of the gem names *iolite* or *dichroite*, for these colorless stones. All the crystals we examined had a prismatic habit and were broken and corroded. We found little variation in their physical properties (refractive indices and specific gravity). Their refractive indices varied from 1.520 (lowest n_α) to 1.541 (highest n_γ), and they had an average specific gravity of 2.570. Pleochroism, usually a diagnostic property for cordierite, was not visible because of the lack of color. In most cordierites, iron (and other trace elements) can substitute for Mg, producing color. However, microprobe analyses showed that these cordierites were very rich in Mg, up to 95 mol.% of the possible Mg sites. These confirm earlier microprobe analyses of some specimens (Zwaan, 1986), which also showed relatively high Mg content.

To the unaided eye, when cut these cordierites (see, e.g., figure 5) strongly resembled colorless enstatites from the same locality. Immersion in ethylene dibromide, however, was sufficient to separate the two gem minerals easily, because the R.I. of the liquid is very similar to that of cordierite. In addition, the cordierites do not have the 506 nm absorption band in the blue that is found in enstatite. Liquid inclusions were common but not of any diagnostic value.

KORNERUPINE

Although considered rare (see, e.g., Webster, 1994), hundreds of carats of kornerupine [$Mg_4(Al,Fe^{+3})_6(Si,B)_4O_{21}(OH)$] have been found in the Embilipitiya deposits (see also Zwaan, 1986, 1992). The author and colleagues saw large quantities of crystal fragments, varying from light brownish yellow, brown, or green to dark brown and dark grayish green (see, e.g., figure 6). Most of the specimens we examined were irregular in shape, because of fractures, and were corroded. Because we did not observe any crystal faces, we could not identify a typical habit. Note that chatoyant kornerupine has not yet been reported from this area.

Specific gravity, ranging from 3.283 to 3.346, generally increased with color intensity (table 1).

Figure 5. Also very high in Mg, the cordierites from Embilipitiya strongly resemble colorless enstatites from this locality. Here, the largest cordierite weighs 3.75 ct and is 11.8 mm long.

Figure 6. Kornerupine is usually considered a rare gem material. However, the author saw hundreds of carats of gem-quality kornerupines in Embilipitiya, which ranged from light brownish yellow to the dark brown and dark green stones shown here (the 4.56 ct stone at the center top is 12.3 mm in longest dimension).

Light brown specimens rose in methylene iodide (S.G. = 3.32), while dark brown samples slowly sank in this liquid. This behavior in methylene iodide, together with the very strong pleochroism in tones of greenish yellow and brownish yellow, appears to be a reliable test for kornerupine specific to this locality: Every green-to-brown strongly pleochroic gemstone from Embilipitiya that either rose or sank slowly in methylene iodide was kornerupine. The refractive indices varied from the lowest n_α of 1.665 (for a light brown specimen) to the highest n_γ of 1.690 (for a medium brown sample). The birefringence, however, was usually 0.012.

Electron microprobe analyses of eight rough specimens, onto which one or two flat faces had been polished, indicated that the color intensity tended to be directly proportionate to the Fe content (again, see table 1). In general, pale kornerupines have distinctly lower S.G.'s and R.I.'s than dark kornerupines, but hue (that is, whether the stone is brown or green) has no effect on these properties.

Most of the Embilipitiya kornerupines we examined had interesting inclusions. The solid inclusions were identified by Raman spectroscopy. Well-crystallized black inclusions with a submetallic luster, seen in about 25 samples, were found to be rutile. One specimen also had red crystals of rutile (figure 7). Another common inclusion was colorless zircon, often with beautiful haloes in polarized light (figure 8). Rounded apatite crystals occurred frequently. However, elongated quartz

TABLE 1. Properties, including electron microprobe analyses, of eight rough kornerupines [$Mg_4(Al,Fe^{+3})_6(Si,B)_4O_{21}(OH)$] from Embilipitiya, Sri Lanka.

	Sample							
Properties	A 1	A 2	A 3	A 4	A 5	A 6	A 7	A 8
Color	Light green	Brown	Dark brown	Light brown	Green	Dark green	Medium brown	Green
Weight (ct)	1.91	3.17	13.03	4.63	3.39	0.91	1.59	1.79
Oxides (wt.%)								
SiO_2	31.87	31.36	30.23	31.79	30.98	31.35	30.95	31.51
TiO_2	0.00	0.05	0.10	0.04	0.05	0.01	0.06	0.04
Al_2O_3	42.36	44.75	44.71	44.15	43.37	43.08	43.36	42.05
Fe_2O_3	1.85	2.51	6.61	1.63	5.40	5.13	5.17	4.60
MgO	19.55	18.49	15.82	19.52	17.21	17.62	17.39	17.80
MnO	0.01	0.02	0.05	0.03	0.07	0.10	0.05	0.05
CaO	0.01	0.01	0.01	0.01	0.01	0.02	0.01	0.02
Na_2O	0.02	0.03	0.02	0.02	0.02	0.03	0.02	0.02
Total[a]	95.67	97.22	97.55	97.19	97.11	97.34	97.01	96.09
S.G.	3.288	3.283	3.346	3.284	3.337	3.339	3.335	3.332
n_α	1.668	1.669	1.672	1.665	1.678	1.672	1.678	1.668
n_γ	1.679	1.681	1.685	1.677	1.687	1.684	1.690	1.680
Birefringence	0.011	0.012	0.013	0.012	0.009	0.012	0.012	0.012

[a] *Note: The element B and the OH group could not be detected by the analytical method employed; hence, the totals are less than 100%.*

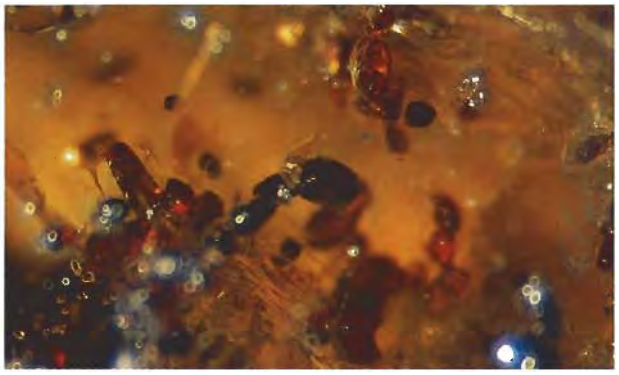

Figure 7. This Embilipitiya kornerupine specimen was observed to have red as well as black rutile crystals. Photomicrograph by Pieter C. Zwaan; magnified 35×.

and tourmaline inclusions, observed parallel to one another, were seen only occasionally. Some kornerupines revealed red-orange hexagonal plates of hematite. Many liquid and liquid-and-gas inclusions were also seen.

To summarize, kornerupines from Embilipitiya can be easily identified by their strong pleochroism and their behavior in methylene iodide. Pale-colored specimens contained considerably less iron than dark-colored samples. There were no distinctive differences between the optical (R.I.) and physical (S.G.) properties of brown and green kornerupines. Rutile appears to be a typical inclusion in kornerupine from this locality.

SCAPOLITE

The crystal fragments and faceted scapolites [$Na_4Al_3Si_9O_{24}Cl$—$Ca_4Al_6Si_6O_{24}(CO_3,SO_4)$] we examined were, for the most part, colorless to pale yellow (figure 9). We found that scapolites from Embilipitiya have mean refractive indices of n_ε = 1.550 and n_o = 1.578, an average specific gravity of 2.694, and an average meionite content of 59.4 mol.% (table 2). They fluoresce a strong "canary" yellow to long-wave UV radiation, comparable to the well-known fluorescence of scapolite (wernerite) from Quebec, Canada. This UV reaction is generally ascribed to sulfur (Webster, 1994).

Although most of these samples were remarkably clean, some contained yellow needle-shaped crystals, which Raman spectroscopy identified as pyrrhotite (figure 10). Pyrrhotite inclusions in scapolite have been mentioned by others (Graziani and Gübelin, 1981; Gübelin and Koivula, 1986).

The pale yellow faceted scapolites from Embilipitiya resemble some other gemstones from Sri Lanka, such as citrine and feldspar. However, the scapolites can be differentiated readily by their strong yellow fluorescence and their much stronger birefringence (0.028).

X-ray diffraction patterns were obtained from six samples. As expected, these patterns were almost identical to one another and were characteristic of scapolites in general.

Electron microprobe analyses were made of two scapolites from Embilipitiya and four scapolites from other sources (one each from Pakistan and Brazil, and two from Pohorabawa, a small village in the Eheliyagoda area that is the major source of colorless scapolite in Sri Lanka; figure 9). As evident in table 2, there were remarkable differences in chlorine content, and thus the marialite/meionite ratio, among the various scapolites.

Note also in table 2 that the one violet scapolite has the lowest specific gravity, refractive indices, birefringence, and meionite content (7.66 mol.%). Previously, the scapolites from East Africa were thought to have the lowest meionite content (10.80 mol.%; Zwaan, 1979). However, the meionite content of this violet scapolite from Pakistan was even lower. The properties of Embilipitiya scapolite, on the other hand, are very similar to those reported for scapolite from Madagascar (n_ε = 1.550, n_o = 1.571; S.G. = 2.686: Bank and Nuber,

Figure 8. In addition to the black rutile crystals, this Embilipitiya kornerupine specimen revealed zircon crystals with haloes visible in polarized light. Zircon is a common inclusion in this material. Photomicrograph by Pieter C. Zwaan; magnified 35×.

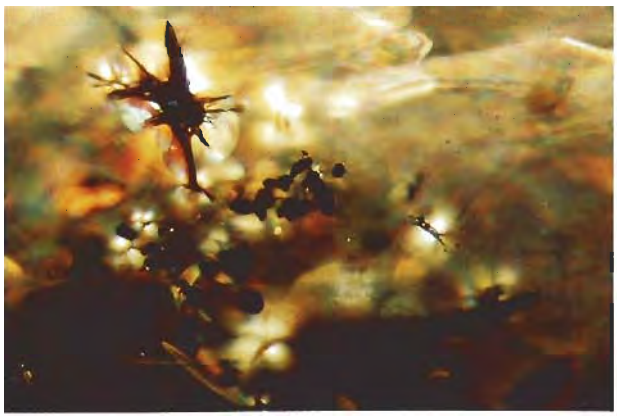

Figure 9. The study of Embilipitiya scapolites included stones from different localities. For example, the 1.58 ct violet triangle-cut scapolite is from Pakistan; the 3.01 ct yellow triangle cut is from Pohorabawa, Sri Lanka, as is the 17.79 ct colorless emerald-cut stone; and the 3.08 ct yellow marquise cut is from Embilipitiya.

1970; Zwaan and Arps, 1980), although the latter do not have the strong yellow fluorescence.

DISCUSSION: SPECIAL ASPECTS OF THE EMBILIPITIYA GEM MINERALS

All four of these gem materials are of special interest both mineralogically and gemologically. The enstatites have very uniform chemical compositions, which is consistent with the fact that they came from a very limited area. The extremely high Mg content of these truly colorless enstatites has not been reported in gem enstatites from any other locality. It is of particular interest that all the enstatites from Embilipitiya can be readily identified with a simple hand spectroscope, by the presence of the 506 nm absorption band.

Like the enstatites, the cordierites also showed little variation in chemical composition from one sample to the next; they, too, were found to have a very high Mg content. The refractive indices and specific gravities of the specimens tested were extremely low. The complete lack of color in most of the samples is exceptional for cordierite, as is the resulting absence of pleochroism.

Kornerupine occurs abundantly in different tones of green and brown. The extremely strong pleochroism, combined with a number of very interesting inclusions (in particular rutile, zircon, and apatite), make it an attractive collector's gemstone.

The chemical composition of the Embilipitiya scapolites varied little from stone to stone. The strong "canary" yellow fluorescence is a very interesting property that has not been found in other Sri Lankan scapolites (although it has been seen in scapolites from other localities).

The Mg-rich minerals in this area are probably derived from originally high-Mg rocks that have been subjected to deep-seated high-grade metamorphism. These are now represented by metamorphic rocks (i.e., metamorphic granulite facies of the Highland Complex), such as hypersthene gneisses (charnockites), sillimanite-garnet gneisses (khondalites), biotite-garnet gneisses, and crystalline limestones (marbles).

Orthopyroxenes, particularly enstatite, are typical minerals of the granulite facies (Deer et al., 1978). They also occur together with cordierite in medium-pressure/high-temperature metamorphosed pelitic rocks. Kornerupine is a typical mineral in high-grade regional and contact metamorphic rocks, whereas scapolite is commonly found in marbles, calcareous gneisses, and granulites. Petrologic studies have shown that many granulite facies rocks elsewhere in the Highland/Southwest Complex are also Mg rich. However, those in the Embilipitiya area seem to be inordinately so.

The gem minerals in Embilipitiya are mined from alluvial deposits. Strongly weathered granulites that contain enstatite were encountered in the field. These might be the host rocks in which

Figure 10. Some of the Embilipitiya scapolites contained needle-like pyrrhotite crystals. Photomicrograph by Pieter C. Zwaan; magnified 35×.

TABLE 2. Properties, including electron microprobe analyses, of six scapolites [$Na_4Al_3Si_9O_{24}Cl$—$Ca_4Al_6Si_6O_{24}(CO_3,SO_4)$] from Sri Lanka and elsewhere.

Properties	Sample					
	1004	RGM 164299	3.01	1006	98-5	R9
Origin	Pakistan	Brazil	Pohorabawa Sri Lanka		Embilipitiya Sri Lanka	
Color	Violet	Yellow	Yellow	Colorless	Yellow	Yellow
Form	Cut	Rough	Cut	Cut	Cut	Rough
Weight (ct)	1.58	19.88	3.01	8.03	1.13	4.47
Oxides (wt.%)						
SiO_2	62.11	55.96	55.16	55.35	48.56	49.15
TiO_2	0.05	0.02	0.04	0.01	0.02	0.03
Al_2O_3	19.07	22.83	22.47	22.71	26.00	26.16
Fe_2O_3	0.06	0.07	0.16	0.10	0.05	0.08
MnO	0	0.03	0.04	0.02	0.01	0.01
MgO	0	0	0.02	0	0.04	0.04
Na_2O	12.06	9.55	8.64	8.59	4.91	4.94
K_2O	1.45	1.24	1.40	1.32	1.04	0.95
CaO	1.87	6.88	7.55	8.16	14.55	14.77
SO_3	0.11	0.03	0.62	0	0.06	0.07
F	0	0.01	0.09	0.07	0.03	0.01
Cl	3.92	3.44	2.72	2.87	0.99	1.00
F=O	0	0	−0.04	−0.03	−0.01	0
Cl=O	−0.88	−0.78	−0.61	−0.65	−0.22	−0.23
Total[a]	99.82	99.28	98.26	98.52	96.03	96.98
Meionite (mol.%)	7.66	27.07	30.92	32.51	59.21	59.69
S.G.	2.584	2.622	2.651	2.632	2.694	2.694
n_ε	1.533	1.540	1.544	1.542	1.550	1.550
n_ω	1.540	1.557	1.560	1.559	1.578	1.578
Birefringence	0.007	0.017	0.016	0.017	0.028	0.028

[a]*Note: The carbonate (CO_3) content of the samples could not be detected by the analytical method employed; hence, the totals are less than 100%.*

the gem minerals originally formed. In other parts of Sri Lanka, gem minerals that occurred in secondary deposits were found *in situ* in basement rocks; with the exception of some almandine garnets, however, none of the minerals found *in situ* thus far have been of gem quality.

REFERENCES

Bank H., Nuber B. (1970) Durchsichtiger Skapolith aus Moçambique. *Zeitschrift der Deutschen Gemmologischen Gesellschaft*, Vol. 19, No. 2, pp. 47–54.

Deer W.A., Howie R.A., Zussman J. (1978) *Rock-Forming Minerals*, Vol. 2A. Longman Group Ltd., London.

Dissanayake C.B., Rupasinghe M.S. (1995) Classification of gem deposits of Sri Lanka. *Geologie en Mijnbouw*, Vol. 74, No. 1, pp. 79–88.

Graziani G., Gübelin E. (1981) Observations on some scapolites of central Tanzania. *Journal of Gemmology*, Vol. 17, No. 6, pp. 395–405.

Gübelin E.J., Koivula J.I. (1986) *Photoatlas of Inclusions in Gemstones*. ABC Edition, Zürich, Switzerland.

Gunaratne H.S., Dissanayake C.B. (1995) *Gems and Gem Deposits of Sri Lanka*. Publication of the National Gems and Jewellery Authority of Sri Lanka, Unigraphs (Pte) Ltd., Colombo, Sri Lanka.

Webster R. (1994) *Gems, Their Sources, Descriptions and Identification*, 5th ed. Rev. by P. G. Read, Butterworth-Heinemann Ltd., Oxford, England.

Zwaan P.C. (1979) More data on violet gem scapolite, probably from Eastern Africa. *Journal of Gemmology*, Vol. 16, No. 7, pp. 448–451.

Zwaan P.C. (1986) Gem minerals from the Embilipitiya and Kataragama areas in Sri Lanka. *Australian Gemmologist*, Vol. 16, No. 2, pp. 35–40.

Zwaan P.C. (1987) Orthopyroxenes from the Embilipitiya area in Sri Lanka. *Schweizerische Mineralogische und Petrographische Mitteilungen*, Vol. 67, pp. 119–125.

Zwaan P.C. (1992) La kornérupine d'Embilipitiya, Sri Lanka. *Revue de Gemmologie*, No. 110, pp. 5-6.

Zwaan P.C., Arps C.E.S. (1980) Properties of gem scapolites from different localities. *Zeitschrift der Deutschen Gemmologischen Gesellschaft*, Vol. 29, No. 1-2, pp. 82–85.

SOME TANZANITE IMITATIONS

By Lore Kiefert and Susanne Th. Schmidt

Since at least 1995, various materials have been manufactured to imitate tanzanite in the gem trade. These include two glasses, two different YAGs (yttrium aluminum garnet), and a synthetic corundum. These imitation tanzanites can be readily separated from the natural gem by standard gemological tests, such as refractive indices, optical character, specific gravity, UV-visible spectra, fluorescence, and the presence or absence of pleochroism. The identifications were confirmed by chemical analysis and Raman spectroscopy.

Tanzanite, the blue-to-violet gem variety of zoisite, was first discovered in Tanzania in the 1960s (see, e.g., Bank et al., 1967). It has increasingly gained popularity as a result of its unusual color and the attractiveness of the cut stones. Most of the material that enters the gem trade is actually brown zoisite that has been heat treated to blue to violet (Nassau, 1994). Although a number of gem materials, including spinel and iolite, may resemble tanzanite, manufactured imitations of this material have also started to appear on the market (figure 1). These recent tanzanite imitations were mentioned by Kammerling et al. (1995) and in the ICA Gazette ("Gem news," 1996). Johnson and Koivula (1996) describe one of the imitations in more detail. However, rumors of Russian imitations, and of efforts by Russian manufacturers to produce synthetic tanzanite, were mentioned as early as 1991 (Koivula and Kammerling, 1991).

The present article characterizes and provides identification criteria for some of the imitations that have recently appeared on the market, including: (1) a doped heavy glass marketed under the trade name U.M. Tanzanic and produced by U.M. Science Company, Glendale, California; (2) a YAG (yttrium aluminum garnet, a manufactured material) from Lannyte Company, Houston, Texas, which has been sold under the trade name Purple Coranite (figure 2); and (3) a synthetic corundum, also from Lannyte, marketed as Blue Coranite (figure 1). Also included are another glass and another YAG, with slightly different properties, that could be mistaken for tanzanite without gemological testing.

For the gemologist, these materials are easy to distinguish from tanzanite (see Box A) on the basis of specific gravity, refractive indices, optic character, internal features, and—to a lesser extent—their spectroscopic characteristics. To characterize these simulants fully, they were also analyzed chemically and by Raman spectroscopy.

ABOUT THE AUTHORS

Dr. Kiefert is a research scientist at the SSEF Swiss Gemmological Institute, Falknerstrasse 9, CH-4001 Basel, Switzerland. Dr. Schmidt is a research scientist at the Mineralogisch-Petrographisches Institut, Universität Basel, CH-4056 Basel.

Acknowledgments: The authors thank the Lannyte Co., Houston, Texas, for providing samples of Purple Coranite, and Prof. B. Lasnier, of the University of Nantes, France, for the loan of the calcium phosphate glass. Dr. H. A. Hänni, of the SSEF Swiss Gemmological Institute, took the photos in figures 1 and 2, provided comparison material, and contributed helpful information. Mr T. Osterlag, University of Freiburg, Germany, helped with the Raman spectra. Special thanks to Mr. J-P. Chalain, of SSEF, for reviewing the paper. All photomicrographs are by the senior author.

Gems & Gemology, Vol. 32, No. 4, pp. 270–276.

CHARACTERISTICS OF THE TANZANITE IMITATIONS

Materials and Methods. The three imitations noted above—U.M. Tanzanic, Blue Coranite, and Purple Coranite—were readily available at the February 1996 Tucson gem shows. The authors purchased

five faceted samples (0.59–2.89 ct) of the heavy glass (U.M. Tanzanic) and one 1.64 ct faceted synthetic corundum (Blue Coranite) for investigation purposes. In addition, the Lannyte Company kindly supplied us with one rough (112.54 ct) and one 0.72 ct faceted piece of their YAG (Purple Coranite).

We also included in our study a 1.99 ct blue YAG from Russia and a 6.90 ct bluish purple Ca-phosphate glass (again, see figure 1). Although these two samples do differ somewhat in color from tanzanite, they are sufficiently close to be mistaken for it.

We determined refractive index, optic character, and specific gravity using standard gemological instrumentation and techniques. S.G. was determined hydrostatically; the values reported are the average of at least two measurements per sample. Microscopic investigations were carried out with darkfield illumination in air with a Gemolite binocular microscope, as well as with immersion in methylene iodide using a Nachet horizontal microscope. We tested the fluorescence to short- and long-wave UV radiation using a commercial gemological UV lamp, and we tested spectroscopic properties with a laboratory spectroscope (both instruments by System Eickhorst).

Semi-quantitative chemical analyses of all samples were performed by energy-dispersive X-ray fluorescence (EDXRF) spectroscopy on a Tracor Northern TN 5000 system. In addition, quantitative chemical data for samples of the heavy glass (U.M. Tanzanic) and the synthetic corundum (Blue Coranite) were obtained using a JEOL 8600 electron microprobe. Raman spectroscopy was carried out on all samples with a Renishaw Raman System 1000 with a 25 mW air-cooled Argon Ion Laser (Omnichrome) lasing at 514 nm. Analysis times were between 60 and 100 seconds, depending on peak intensities and background fluorescence; the spectral range covered was between 100 and 1900 cm^{-1} (see also Hanni et al., 1996).

U.M. Tanzanic. In their advertising brochure for this material, U.M. Science Co. claims that it was created by means of a high-temperature flux process. The material is described as a mix of amorphous and microcrystalline phases, with a refractive index of 1.66–1.67 and a specific gravity of 3.8–4.0. The brochure also lists a number of other properties, such as the absence of internal stress.

Gemological Properties. Our results for the five faceted samples that we tested did not correspond to those published by the producer. The refractive indices varied between 1.600 and 1.605 (isotropic).

Figure 1. Several manufactured materials have appeared on the gem market as tanzanite imitations. A number of these are shown here together with two natural tanzanites. From left to right: (top row) two tanzanites (3.03 ct and 5.89 ct) and a 6.90 ct sample of Ca-phosphate glass; (bottom row) a 1.64 ct synthetic corundum (called Blue Coranite), a 1.99 ct synthetic garnet from Russia, and two samples (2.89 ct and 0.92 ct) of heavy glass (U.M.Tanzanic). Photo by H. A. Hänni.

The specific gravity ranged from 3.36 to 3.48. All specimens showed a poorly polished surface. Three of the five samples were virtually free of any internal features, but two showed diffuse, syrup-like flow structures. One of these two samples also had an irregularly shaped milky white inclusion, probably a microcrystalline portion of the surrounding glass, with syrup-like flow structures (figure 3). The samples fluoresced chalky white to both short- and long-wave UV. They showed weak absorption bands at approximately 490, 550, and 590 nm.

Chemical Composition. We recorded an inhomogeneity in chemical composition among the five samples (see table 1), as well as within the samples. PbO contents between 38.5 and 51.2 wt.% were measured, which appear to be extremely high. The products of other heavy-glass manufacturers only go up to 30 wt.% PbO (Swarogem, pers. comm., 1996). Perhaps U.M. Science Co. uses a light element such as B or Li in their glasses, neither of which is detectable using the microprobe or X-ray fluorescence units available to the authors. SiO_2 contents varied between 46.3 and 58.3 wt.%. The K_2O content ranged between 2.3 and 3.2 wt.%, and the trace elements Mn and Fe were 0.08–0.14 wt.% and 0.03–0.07 wt.%, respectively, expressed as oxides (see table 1). For the two major elements, Si and Pb, SiO_2 and PbO concentrations within one

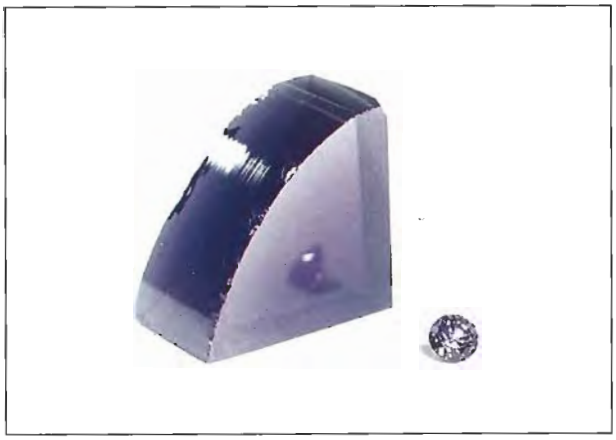

Figure 2. Purple Coranite is a YAG manufactured by the Czochralski method that is marketed as a tanzanite imitation. The unfashioned section weighs 112.54 ct; the faceted piece is 0.72 ct. Photo by H. A. Hänni.

Figure 3. Solid inclusions and a syrup-like flow structure are evident in this heavy glass manufactured as a tanzanite imitation by U.M. Science Co. Immersion, magnified 35×.

stone varied by up to 7 wt.% (see table 1). Al_2O_3 levels were below the detection limits of the EDXRF apparatus and the microprobe.

The Raman spectra of this material showed broad peaks at Raman shifts of 505, 777, 989, and 1064 cm^{-1} (figure 4), as well as a considerable fluorescence to Argon laser light at 514 nm, as can often be observed in glass (Chemarin et al., 1996; Sharma and Wang, 1996).

Coranite. The Lannyte Company offered two tanzanite imitations: a YAG marketed as Purple Coranite and a synthetic corundum sold as Blue Coranite. The manufacturer reported that both materials are grown using the Czochralski-pulling method.

Purple Coranite. The manufacturer's brochure reported that "the material is garnet based, with a hardness of nearly 9 and a refractive index of over 1.80. Our investigations confirmed that the R.I. is over 1.80, and we measured a specific gravity of 4.58, which is slightly higher than published data for YAG (e.g., Nassau, 1980). We saw no pleochroism in the samples, but we did see some strain with the polariscope. Spectroscopic observation showed a broad band at approximately 540 nm.

The material fluoresced a strong chalky orange to short-wave UV radiation (figure 5). Similar data were obtained by Johnson and Koivula (1996) on a 7.07 ct tanzanite imitation purchased in 1995. EDXRF analysis of their specimen revealed yttrium, aluminum, and europium; all three elements were found in the EDXRF analyses of our two purple coranite samples.

The piece of unfaceted Purple Coranite was polished on one side for microscopic examination. However, we saw no bubbles or other internal features. Color zoning was apparent with the unaided eye: The core was a distinctly darker purple than the rim, and the color faded gradually from core to rim. The orange fluorescence corresponded to the zoning, but inversely; that is, it was brightest near the colorless rim (figure 5). Microscopic examination of the small faceted sample showed no growth

TABLE 1. Chemical composition of five glass imitations of tanzanite from U.M. Science Co.

Oxide (wt.%)	Sample 1[a] (2.89 ct)	Sample 2[b] (1.84 ct)	Sample 3[a] (0.92 ct)	Sample 4[a] (0.76 ct)	Sample 5[b] (0.59 ct)
SiO_2	51.26–58.30	51.39–55.77	50.25–55.50	46.32–51.55	46.49–50.13
K_2O	2.87– 3.09	2.66– 3.15	2.89– 2.94	2.29– 2.84	2.29– 2.62
MnO	0.09– 0.10	0.08– 0.09	0.11– 0.13	0.11– 0.13	0.10– 0.14
FeO	0.04± 0.002	0.03– 0.04	0.05± 0.002	0.05– 0.07	0.04– 0.05
PbO	38.47–45.53	40.96–45.68	41.39–46.69	45.50–51.20	47.17–51.06

[a] *Range of 3 microprobe analyses.* [b] *Range of 4 microprobe analyses.*

BOX A: CHARACTERISTICS OF TANZANITE, THE BLUE-TO-VIOLET VARIETY OF ZOISITE

Zoisite is an orthorhombic silicate mineral of the epidote group with the chemical formula: $Ca_2Al_3Si_3O_{12}(OH)$. Crystalline zoisite is found in various hues, including colorless, brown, yellow, blue, purple, green, and pink. Certain ornamental rocks, such as anyolite and sausserite, contain massive zoisite (Webster, 1975). The best known zoisite is the transparent blue-to-violet variety, tanzanite, a name first promoted by Tiffany and Company in the late 1960s.

The specific gravity of tanzanite is 3.35, with a hardness of 6–7 and refractive indices of $n_\alpha = 1.692$, $n_\beta = 1.693$, and $n_\gamma = 1.700$, with a birefringence of 0.008 (Webster, 1975). There is one perfect cleavage. Tanzanite typically exhibits trichroism of *a* = violet blue, *b* = violet, and *c* = brownish red, and it shows broad absorption bands at approximately 535 and 595 nm in the spectroscope (*Gem Reference Guide*, 1995). Tanzanite is inert to ultraviolet radiation (see, e.g., Malisa et al., 1986; Barot and Boehm, 1992).

Inclusions. A variety of inclusions have been identified in tanzanite: calcite, gypsum, graphite, hematite, ilmenite, staurolite, rutile, titanite, xenotime, quartz, diopside and tremolite-actinolite, as well as fluid inclusions in healed "feathers" (Gübelin and Koivula, 1986; Malisa et al., 1986). As noted by Barot and Boehm (1992), however, faceted tanzanites are often flawless, because most inclusions are removed in the cutting process.

Chemical Composition. In 1967, Bank et al. reported on strontium-containing blue zoisite crystals. In 1969, Hurlbut described this Tanzanian material more comprehensively, published a chemical analysis, and attributed the blue color to its vanadium content: 0.03–0.44 wt.% V_2O_3. For more information about trace elements in tanzanite, refer to Schmetzer (1978; 1982), Barot and Boehm (1992), and Traber (1995).

Tanzanite also has a characteristic Raman spectrum (figure A-1), so that it can be easily separated from simulants or imitations by Raman spectroscopy alone.

Figure A-1. This Raman spectrum of a tanzanite crystal loaned by Th. Ostertag, Freiburg, Germany, is consistent with the Raman spectra of other tanzanites seen in the SSEF laboratory.

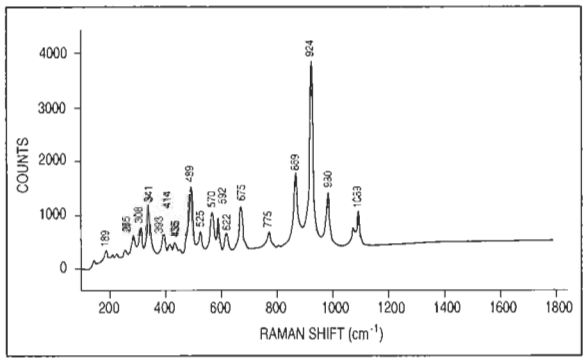

structures, but it did reveal small bubbles that were arranged in a circular pattern.

The Raman spectra of the two Purple Coranite samples that we examined were very distinct, with a large number of peaks; some of these were at positions different from those in the Raman spectra of the other YAG investigated and described below (figure 6). Additional Raman studies of various colors of YAG showed that their peak intensities, and some peak positions, vary depending on the doping element. The Raman spectrum of a colorless YAG reproduced in Pinet et al. (1992) corresponds to that of the colorless YAG we analyzed.

Blue Coranite. The gemological properties of this synthetic corundum are consistent with the known properties for corundum and are similar to those reported by Kammerling et al. (1995) for comparable material. The 1.64 ct oval cut that we examined had a specific gravity of 4.02 ± 0.02 and refractive indices of $n_\varepsilon = 1.764$, $n_o = 1.771$, with a birefringence of 0.007. In contrast to tanzanite, corundum is uniaxial, and this material showed much weaker pleochroism from purplish blue (ordinary ray) to light grayish blue (extraordinary ray). No lines were observed in the spectroscope. The sample was inert to both short- and long-wave UV radiation. Microscopic examination revealed no inclusions or growth features.

The chemical composition of this sample of Blue Coranite is similar to that of synthetic sapphire, with few trace elements and no V or Ga. The only elements we detected were Al (in a major amount) and Ti and Fe (each in the same amount, as trace elements). The TiO_2 content varied slightly within the sample. The Raman spectrum of our sample of Blue Coranite corresponds to the Raman spectra of other corundum samples, with only weak peaks at 375, 416, 577, 644 and 750 cm^{-1} (see Pinet et al., 1992).

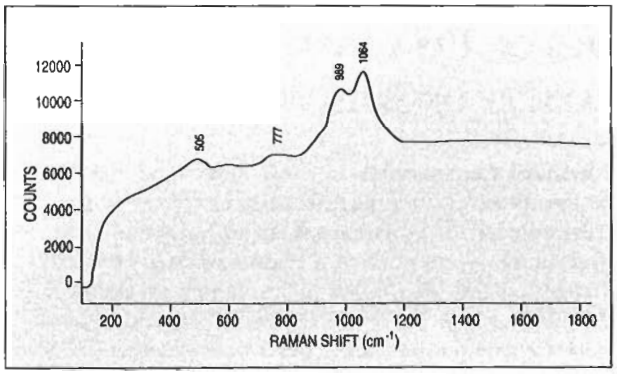

Figure 4. This Raman spectrum of the heavy-glass imitation of tanzanite illustrated in figure 3 shows broad peaks at Raman shifts of 505, 777, 989, and 1064 cm^{-1}.

YAG from Russia. A 1.99 ct round-brilliant-cut synthetic garnet from Russia (again, see figure 1) was available from the collection of Dr. H. A. Hänni, SSEF Swiss Gemmological Institute, who purchased it in 1991 from Mr. P. Hollenstein of Zurich, Switzerland. It had an S.G. of 4.56 and an R.I. over 1.80. As with the Purple Coranite, this sample showed no pleochroism, but we observed some strain with the polariscope. Also, it fluoresced a moderate orange to short-wave UV radiation. We also saw minute inclusions on an irregular plane throughout the piece. They resembled the rutile particles frequently observed in corundum.

The chemical composition of this synthetic was found to be mainly Y and Al, with traces of Yb. The Raman spectrum differed distinctly from the one obtained for Purple Coranite because of the different trace elements (again, see figure 6). We observed no characteristic spectrum in the spectroscope.

Figure 5. This sample of Purple Coranite, a YAG manufactured to imitate tanzanite, fluoresced a strong, chalky orange to short-wave UV radiation. Note that the fluorescence is strongest near the near-colorless rim. Photo by L. Kiefert.

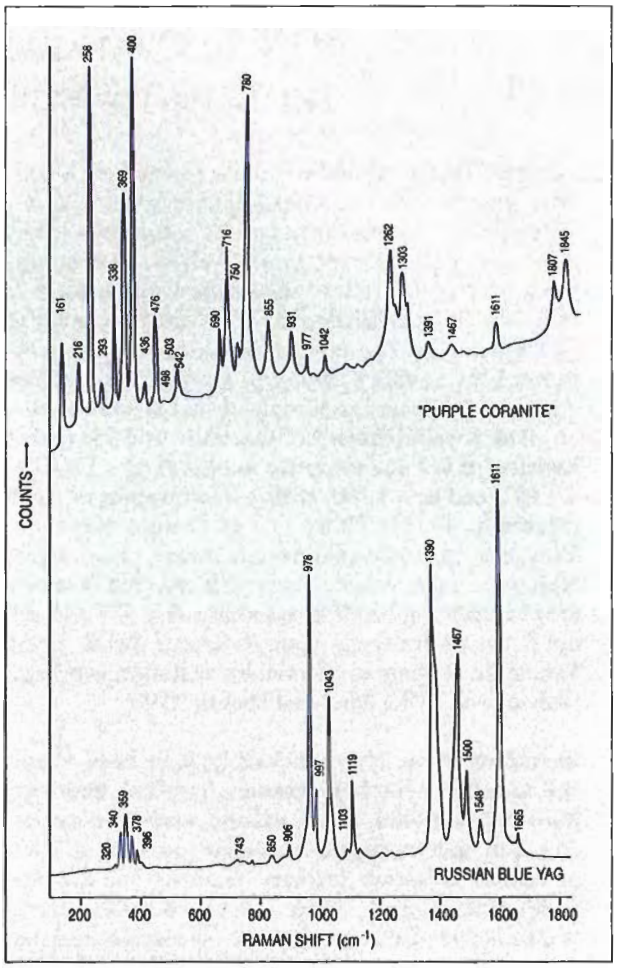

Figure 6. The Raman spectra of these two YAGs manufactured by the Lannyte Co. (top) and in Russia (bottom) differ from each other because of different trace elements, but neither resembles the spectrum of tanzanite.

Ca-phosphate Glass. The mineral display at the University of Nantes contains a 6.90 ct bluish purple brilliant-cut that was described to one of the authors by Dr. E. Fritsch, Nantes, as synthetic Ca-phosphate glass (again, see figure 1). It had been purchased several years earlier at a Tucson Gem Show. Testing revealed a refractive index of 1.537 for this isotropic material, a specific gravity of 2.64, and no reaction to either long- or short-wave ultraviolet radiation. In the spectroscope, we observed a moderate band in the yellow at 580 nm.

When viewed with the microscope, the piece revealed the irregular flow structures and large number of bubbles frequently observed in glass (fig-

Figure 7. Bubbles and devitrification crystals help identify this sample as a purple Ca-phosphate glass. Immersion, magnified 35×.

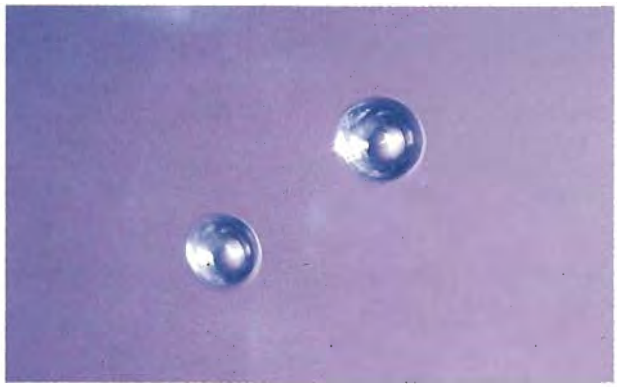

Figure 8. Bubbles help show that this is a Ca-phosphate glass. Note also the needle-like devitrification features on the large bubble. Magnified 100×.

ures 7 and 8). Raman spectra of the bubbles gave no specific peaks, which suggested that they might contain air. We observed devitrification effects around some of the bubbles, which had the appearance of needle-like crystals forming a radial pattern (figure 8). Various crystalline phases, such as that illustrated in figure 9, and an apparently orthorhombic crystal inclusion were also seen.

This sample was very similar in chemistry to apatite, with high amounts of Ca and P. We also recorded minor amounts of Mg, K, Fe, Co, Sr, and Zr, as well as traces of Zn.

The Raman spectrum showed a curve similar to that of other amorphous materials, with broad peaks (figure 10). The spectrum of the needle-like inclusions, however, had much more discrete peaks, at the same position as the broad peaks from the larger sample; whereas the orthorhombic crystal revealed peaks that were not observed in either the host or the crystallized areas around the bubbles. The Raman spectrum of apatite, however, is distinctly different (again, see figure 10).

The measured properties of this unusual stone contain no conclusive evidence as to the nature of the material, other than the fact that it is a Ca-phosphate glass.

Figure 9. Various crystal phases were seen in this Ca-phosphate glass. Magnified 100×.

Figure 10. Raman spectra of a purple Ca-phosphate with glass structure (A), devitrification area (B), and crystal inclusions (C) help characterize this tanzanite imitation, which was chemically similar to apatite (D).

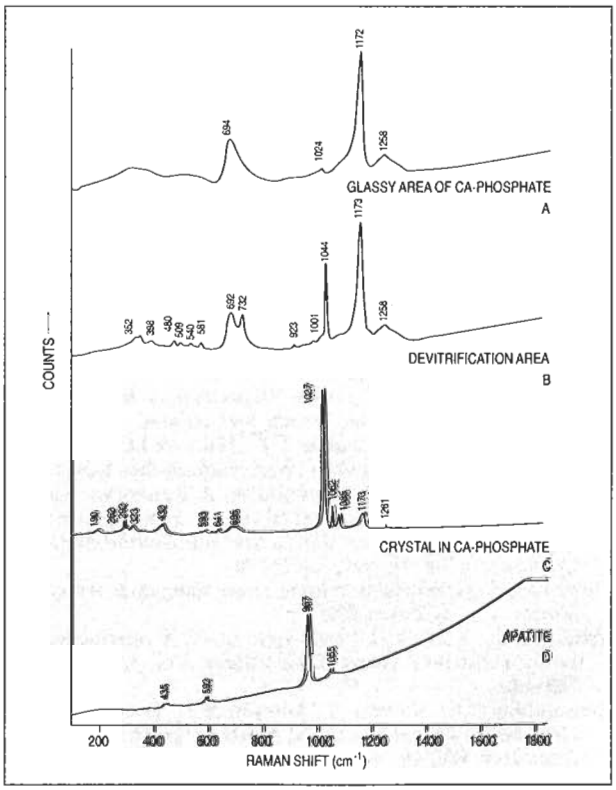

TABLE 2. Gemological properties of tanzanite and some imitations.

Trade name	Identification	Number of samples	Refractive index	Birefringence	Specific gravity	UV fluorescence	
						Short-wave	Long-wave
Tanzanite	Zoisite	NA[a]	1.688–1.696 to 1.691–1.700	0.008 – 0.009	3.35	None	None
U.M. Tanzanic	Heavy Pb-glass	5	1.600–1.605	Isotropic	3.36 – 3.48	Chalky white	Chalky white
Purple Coranite	YAG	2	> 1.80	Isotropic	4.58	Strong chalky orange	Weak, chalky orange
Blue Coranite	Synthetic corundum	1	1.764(n_ε)–1.771(n_o)	0.007	4.02	None	None
Russian YAG	YAG	1	> 1.80	Isotropic	4.56	Moderate orange	None
None	Ca-phosphate glass	1	1.537	Isotropic	2.64	None	None

[a] *Not applicable; properties quoted for tanzanite are from literature sources referenced in the text.*

DISCUSSION AND CONCLUSIONS

Various tanzanite imitations are gradually entering the gem market. Three of the most convincing in appearance are the heavy glass manufactured by U.M. Science Co. and marketed under the name U.M.Tanzanic, the YAG manufactured by the Lannyte Company (and marketed as Purple Coranite), and the synthetic corundum by Lannyte that is sold as Blue Coranite. For the gemologist, tanzanite imitations are easily detectable because of differences in refractive index and specific gravity (table 2). Pleochroism and optic character are also helpful, as tanzanite has a relatively strong pleochroism compared to the only other pleochroic imitation, Blue Coranite. However, Blue Coranite is uniaxial, whereas Tanzanite is biaxial. The tanzanite imitations can also be identified with a handheld spectroscope, provided good spectra are obtained. Chemical composition and Raman spectra are useful to confirm that these are indeed imitations.

REFERENCES

Bank H., Berdesinski W., Nuber B. (1967) Strontiumhaltiger trichroitischer Zoisit von Edelsteinqualität. *Zeitschrift der Deutschen Gesellschaft für Edelsteinkunde*, No. 61, pp. 27–29

Barot N.R., Boehm E.W. (1992) Gem-quality green zoisite. *Gems & Gemology*, Vol. 28, No. 1, pp. 4–15.

Chemarin C., Panczer G., Champagnon B. (1996) Structural modifications in silica geoglasses related to their formation process. *TERRA Abstracts*, Abstract supplement No. 2 to *TERRA Nova*, Vol. 8, p. 14.

Gem news (1996). *ICA Gazette*, April 1996, pp. 4-5.

Gem Reference Guide (1995) Gemological Institute of America, Santa Monica, California.

Gübelin E.J., Koivula J.I. (1986) *Photoatlas of Inclusions in Gemstones*. ABC Edition, Zurich, Switzerland.

Hänni H.A., Kiefert L., Chalain J.-P., Wilcock I.C. (1996) Ein Renishaw Raman Mikroskop im gemmologischen Labor: Erste Erfahrungen bei der Anwendung (A Renishaw Raman Microscope in the gemological laboratory: First experiences of application). *Zeitschrift der Deutschen Gemmologischen Gesellschaft*, Vol. 45, No. 2, pp. 55–70.

Hurlbut C.S. (1969) Gem zoisite from Tanzania. *American Mineralogist*, Vol. 54, p. 702.

Johnson M.L., Koivula J.I. (1996) Gem news: A convincing tanzanite substitute. *Gems & Gemology*, Vol. 32, No. 2, pp. 138–139.

Kammerling R.C., Koivula J.I., Johnson M.L., Fritsch E. (1995) Gem news: Tanzanite-colored synthetic sapphire. *Gems & Gemology*, Vol. 31, No. 3, pp. 215–216.

Koivula J.I., Kammerling R.C. (1991) Gem news: More Soviet synthetics. *Gems & Gemology*, Vol. 27, No. 1, p. 55.

Malisa E., Kinnunen K., Koljonen T. (1986) Notes on fluid inclusions of vanadiferous zoisite (tanzanite) and green grossular in Merelani area, Northern Tanzania. *Bulletin of the Geological Society of Finland*, Vol. 58, No. 2, pp. 53–58.

Nassau K. (1980) *Gems Made by Man*. Gemological Institute of America, Santa Monica, California.

Nassau K. (1994) *Gemstone Enhancement*, 2nd ed. Butterworth-Heinemann, Oxford, England.

Pinet M., Smith D., Lasnier B. (1992) Utilité de la microsonde Raman pour l'identification non destructive des gemmes. In *La Microsonde Raman en Gemmologie, Revue de Gemmologie*, Association Française de Gemmologie, special edition, pp. 11–61.

Schmetzer K. (1978) Vanadium III als Farbträger bei natürlichen Silikaten und Oxiden--ein Beitrag zur Kristallchemie des Vanadiums. Ph.D. Dissertation, Universität Heidelberg, Germany, p. 209–225.

Schmetzer K. (1982) Absorptionsspektroskopie und Farbe von V^{3+}-haltigen natürlichen Oxiden und Silikaten--ein Beitrag zur Kristallchemie des Vanadiums. *Neues Jahrbuch für Mineralogie, Abhandlungen*, Vol. 144, pp. 73–106.

Sharma S.K., Wang Z. (1996) A confocal micro-Raman system with oblique excitation for weakly scattering materials. *TERRA Abstracts*, Abstract supplement No. 2 to *TERRA Nova*, Vol. 8, p. 23.

Traber D. (1995) Eine mineralchemische und spektroskopische Studie an Zoisiten aus Merelani, Tansania. Diplomarbeit, Mineralogisch-Petrographisches Institut der Universität Basel, Switzerland.

Webster R. (1975) *Gems: Their Sources, Descriptions and Identification*. Butterworth & Co., London.

GIA GEM TRADE
LAB NOTES

CORUNDUM and PLASTIC, A Surprising Assemblage

A charming dark-red Buddha statuette (figure 1) was submitted to the East Coast lab by a client who wanted to know if it was artificially colored. When exposed to long-wave ultraviolet radiation in a darkened room, the statuette appeared splotchy orangy red, with some areas of slightly greenish blue (the ears, for example); on the back, just above the base, were two lines of what appeared to be raised Thai lettering that also fluoresced greenish blue (figure 2). When we examined the item with a desk-model spectroscope, we saw a spectrum typical of ruby in some areas but no spectrum at all in others.

Following these observations, we quickly turned to the microscope to determine better what material(s) we were dealing with. An examination of the most transparent area (the right arm) immediately showed the reason for the splotchy appearance to UV radiation: The Buddha was clearly made of a variegated—near-colorless to pink—matrix embedded with small pink-to-red fragments. The morphology of the fragments suggested that they were natural corundum. Higher magnification showed fractures and fluid-filled inclusions in the fragments. Although the spectrum seen in some areas matched that of ruby, we could not determine if all the corundum chips had the prerequisite depth of color to be classified as ruby. Small globules and numerous gas bubbles in surface areas of the matrix (figure 3) indicated plastic. Therefore, we concluded that the piece was an assemblage consisting of natural corundum fragments in plastic.

Figure 1. Testing revealed that this Buddha statuette (about 41.60 × 21.40 × 16.20 mm) is an assemblage of ruby and pink corundum chips in plastic.

Figure 2. Two rows of raised Thai letters along the base, seen here under long-wave UV, could only have been formed in this fashion if the statuette was produced in a mold.

A Thai staff member informed us that the script was the name of a well-known Buddhist monk. The piece may have been a way of honoring him and providing a "good luck" talisman for its owners. In addition to the monk's name, the date "Sat 5" was present, which represents an important spiritual day for Buddhists.

It is intriguing to speculate how the piece was manufactured. Indications are that it was made in a mold, since corundum could not be polished while embedded in such soft material, and the raised script could not have been produced as it was except in a mold.

Similar assemblages that we have seen include a necklace of barrel-shaped beads (amber fragments in plastic; Fall 1983 Lab Notes, pp. 171–172), a drilled "amber" tablet (Winter 1987 Lab Notes, p. 232), and an imitation anyolite plaque (Gem News, this issue). Once again, we cannot say whether this statuette is a one of-a-kind piece or another mass-manufactured tourist bauble from some gem-producing country.

GRC and TM

Editor's note: The initials at the end of each item identify the contributing editor(s) who provided that item.

Gems & Gemology, *Vol. 32, No. 4, pp. 277–281*

Figure 3. With long-wave UV radiation, the individual fragments and gas bubbles in the "matrix" are readily apparent on the base of the statuette shown in figure 1.

DIAMOND

Fracture Filled

Although we have been aware of fracture-filled diamonds for many years, we continue to see new or different aspects to the appearance of filled diamonds. In most cases, when a fracture-filled diamond is noteworthy, it is because the flash effect is very subtle. Examples include a 0.88 ct heart-shaped brilliant with low-angle filled fractures (Summer 1993 Lab Notes, p. 123) and a 1.07 ct diamond in which the orange darkfield flash was masked by the stone's yellowish orange body color (Winter 1995 Lab Notes, pp. 266–267). However, a 2.03 ct heart-shaped brilliant seen in the West Coast laboratory was notable for the opposite reason: The flash effects were so pronounced that we discerned an additional feature.

One of our staff members (whose background includes petrology) keeps the analyzing filter (top polarizer) attached to the microscope. In general, flash-effect colors are more difficult to see with such an arrangement. However, the flash-effect colors in this diamond were readily seen, even with the analyzing filter. In addition, and to our surprise, the flash colors changed as the polarizing filter was rotated, without any movement of the stone, in both darkfield and brightfield illumination (figure 4). For each polarization direction, the darkfield colors continued to be the "subtractive" opposites of their respective brightfield colors. This reaction suggests that, for at least this stone, either the filler itself or optical effects resulting from the filling process behaved in an anisotropic fashion; that is, the flash colors acted as if the filler was pleochroic. Another possibility is that strain in this diamond caused the "flash pleochroism."

Qualitative chemical analysis by energy-dispersive X-ray fluorescence (EDXRF) spectroscopy revealed lead, bromine, and thallium, the same trace elements identified in the filled diamond described in the aforementioned Winter 1995 Lab Note. Subsequent EDXRF examinations revealed thallium in many diamonds that we believe were treated by the Goldman Oved Diamond Company in the early 1990s (see R. C. Kammerling et al., "An Update on Filled Diamonds: Identification and Durability," *Gems & Gemology*, Fall 1994, pp. 142–177). *MLJ*

Unusual Cause of Uneven Color Distribution

A 1.15 ct octagonal modified brilliant-cut diamond submitted to the East Coast lab presented an unusual example of a colored diamond with uneven color distribution. In the color grading of colored diamonds, color distribution is defined as the perceived evenness or unevenness of color seen in the diamond in its face-up position (J. King et al., "Color Grading of Colored Diamonds in the GIA Gem Trade Laboratory," *Gems & Gemology*, Winter 1994, pp. 220–242). In most colored diamonds, uneven color distribution is an effect of cutting (for instance, the tips of a marquise brilliant may show color, while the center of the stone may appear near-colorless), although occasionally the diamond is actually color zoned. In the case of this diamond, a large cleavage (and its reflection) concentrated color in some areas, while other areas appeared nearly colorless. Consequently, the color distribution of this stone was classified as "uneven."

The cleavage not only influenced the perceived distribution of color, but it also affected the apparent strength of color. As we have noted before (Winter 1985 Lab Notes, p. 234), in some cases the way a diamond is cut may intensify the color appearance. In this stone, the cleavage performed a similar role, by internal reflection and refraction (figure 5). When examined table-down, the dia-

Figure 4. By changing the direction of polarization of the light by 90° (below, left to right), the shift in darkfield (top) and brightfield (bottom) flash colors was readily seen in this filled fracture in a 2.03 ct diamond. Magnified 20×.

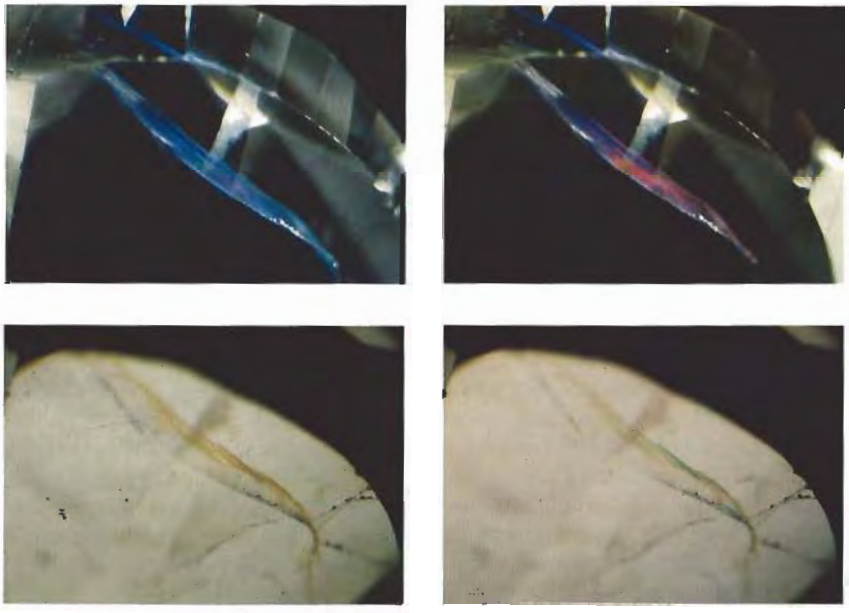

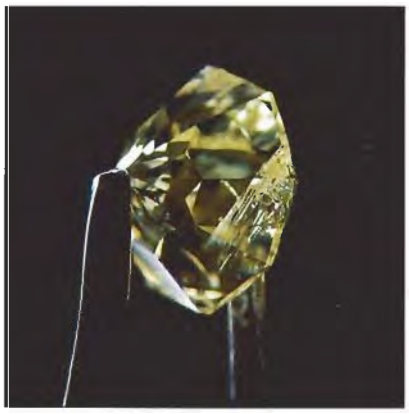

Figure 5. There is no foreign substance in the cleavage of this 1.15 ct round brilliant-cut diamond; the presence of the cleavage is enough to profoundly affect its face-up color. Magnified 10×.

mond appeared to be in the W–Z range, that is, Light Yellow. Face up, however, the angle of the cleavage intensified the color so that it appeared deeper than the "Z" master stone (figure 6). In accordance with GIA GTL policy to assess a diamond's color face up in such a situation (see p. 225 of the King et al. article cited above), this stone was graded Fancy Light Yellow.

Thomas Gelb

Figure 6. When viewed face up next to the "Z" master stone on the left, the 1.15 ct diamond in figure 5 appears more intense, which resulted in a Fancy Light Yellow color grade. The color appears to be concentrated in regions where the cleavage and its reflection are visible.

SYNTHETIC EMERALD

The Fall 1985 issue of *Gems & Gemology* carried a definitive article (by R. E. Kane and R. T. Liddicoat) about the Biron hydrothermal synthetic emerald, at the time a challenging newcomer. GTL staff members on the East Coast have not seen many of these stones submitted for routine testing in recent years. However, our initial examination of a small, relatively inclusion-free marquise brilliant mounted in a lady's cluster ring (figure 7) prompted another look at that enlightening article.

It is important to remember how much the properties of this product overlap those of some Colombian emeralds. For example, Biron hydrothermal synthetic emeralds do not fluoresce to long-wave ultraviolet radiation because of the quenching effect of vanadium; in natural emeralds, iron usually suppresses the fluorescence. Although the birefringence is lower, the refractive indices of this synthetic are very close to those of Colombian stones: n_ε=1.569, n_o=1.573. The specific gravity of 2.68–2.71 reported for the Biron synthetics in the Kane and Liddicoat article also does not help: This range almost exactly overlaps that of emeralds from Colombia. (In some other cases, S.G. provides a useful clue for separating unmounted stones.)

As for using magnification to help with the separation, some inclusions in these synthetics can be confused with those in natural stones. In this case, a very small, highly reflective "crystal" was at first thought to be pyrite, a mineral seen in emeralds from some Colombian localities. With higher magnification (figure 8), however, the yellowish inclusion was clearly not equant, but rather appeared platy—calling to mind the gold inclusions reportedly seen, albeit rarely, in the Biron synthetic. A few needle-like inclusions further confused the matter, as they resembled the needles sometimes seen in natural stones. With the aid of fiber-optic illumination, however, their true nature was revealed: a series of closely spaced linear "dashes," not single solid needles. On further examination, we saw a two-phase "nail-head" spicule, similar to the one shown in figure 9, which is

Figure 7. The marquise brilliant (8.00 × 4.10 mm) in this woman's closed-back cluster ring proved to be a hydrothermal synthetic emerald.

Figure 8. At lower magnification, this gold-colored plate-like inclusion in the synthetic emerald in figure 7 resembled pyrite, a mineral found in some Colombian emeralds. Magnified 200×.

Figure 9. A two-phase "nail-head" spicule, similar to this one, positively identified the stone in figure 7 as hydrothermal synthetic emerald.

Figure 10. A blister pearl (20 × 15 × 10 mm) can be seen at the top of this red abalone (Haliotus rufescens) *shell.*

Figure 11. The blister pearl shown in figure 10 was produced from the irritant provided by the burrowing of a small bivalve mollusk, the shell of which is seen here embedded in the outer surface of the abalone shell.

typical of hydrothermal synthesis. For further corroboration, we had an infrared spectrum of the stone taken. As expected, the spectrum showed water peaks typical of hydrothermal growth. *GRC and TM*

PEARL,
An Unusual Natural Abalone Blister

Irritants that find their way into a mollusk's shell can induce the animal to form calcareous concretions. If layers of nacre are then deposited on the surface of this concretion, it is properly called a pearl. The irritants can take many forms. They can be organic, even another living organism. Or they can be inorganic—sand, for example. The pearls formed from these concretions can be loose in the mollusk or attached to the shell. If attached to the shell, they are called blisters.

Our laboratories see many varieties of pearls. Although once relatively uncommon, abalone pearls are now appearing in the lab more frequently. Most natural abalone pearls seen in the trade are loose and irregular in shape (see, e.g., Fall 1984 Lab Notes, p. 169). However, they can also occur as blister pearls, where they are a continuation of the inner nacreous part of the shell. Abalone blister pearls have been cultured, too, often with a specially shaped nucleus to control the shape of the finished product. The blister is then cut from the shell and processed to make a "mabe," an assembled cultured blister pearl (see, e.g., Winter 1994 Lab Notes, p. 268; Spring 1996 Gem News, p. 55).

Recently, the East Coast lab examined a red abalone shell (*Haliotus rufescens*; figure 10), which presented an opportunity to view a sizable natural blister pearl and the irritant that caused it. In this case, the irritant was a mollusk that made its home by burrowing into the outside of the shell (figure 11). It appears that the rate of pearl formation kept pace with the excavation of the burrow in the shell; the invader never reached the tissue of the abalone.

Nicholas DelRe

Imitation STAR RUBY

In recent years, the most convincing star-ruby imitations have been synthetic (or natural) rubies that were diffusion treated to induce the oriented rutile needle inclusions that produce asterism (see, e.g., Fall 1985 Lab Notes, pp. 171–172). In these pieces, the star appears very close to the cabochon's surface. We have also seen assembled pieces where the star appears to come from deep within the cabochon. One such doublet, described in the Fall 1993 Lab Notes (p. 205), had a nonasteriated synthetic ruby top and what was probably a poor-quality natural star ruby—sometimes called "mud ruby"—bottom. Last fall, the West Coast lab encountered a different type of assemblage imitating a star ruby that we had not seen in recent years.

The ring shown in figure 12 was set with a red oval double cabochon that measured 11.98 × 10.33 × 6.25 mm. Diaphaneity varied from transparent to opaque. It had a uniaxial optic figure, a spot R.I. of 1.76, and a typical ruby spectrum (when viewed with the desk-model spectroscope). It fluoresced medium chalky red to long-wave UV radiation, and medium-to-strong chalky red to short-wave UV. With magnification and immersion of the piece in methylene iodide, we discerned three distinct layers (figure 13): a top transparent-to-translucent layer with gas bubbles and curved striae, but no silk (synthetic ruby); an opaque, highly reflective middle layer; and a bottom layer that could not be characterized unless the cabochon was unmounted.

The asterism appeared to originate from the middle, opaque layer. Although this material was difficult to test because the piece was mounted, we did reach one area which we indented with a sharp needle—as would be the case with a metallic foil. Close examination revealed that the foil had been scored with fine parallel lines in three directions (figure 14), producing the asterism. The con-

Figure 12. The star in this double cabochon (11.98 × 10.33 × 6.25 mm) occurs deep within the doublet.

clusion on our report stated that it was "an assemblage, consisting of a synthetic ruby top and an unidentified back with a central engraved foil layer which produces the asterism of the material."

MLJ and SFM

Imitation SPINEL, An Unusual Assemblage

The jewelry trade first encountered a certain type of assembled stone, made to resemble either ruby or sapphire, in the early 1980s. Close observation of this material, even with the unaided eye, reveals a reflection from the joining plane, a strong indication that such a piece is an assemblage. When these stones are immersed in methylene iodide, it is easily seen that the crowns are green and joined by colorless cement to the pavilions, which are either blue (for imitation sapphire) or red (for imitation ruby). The iron line

Figure 13. When we examined the cabochon illustrated in figure 12 with 34× magnification, we noted a shiny foil layer in the middle of the assemblage.

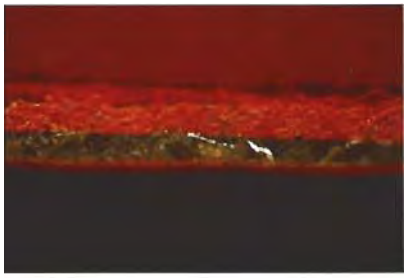

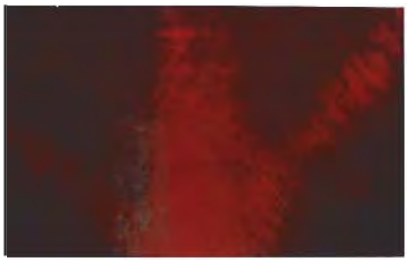

Figure 14. Three arrays of parallel lines, which appear to have been scored into the foil layer, produced the asterism in the assemblage shown in figure 12. Magnified 17×.

(or lines) in the absorption spectrum, as revealed with a handheld spectroscope, prove that the green crowns are natural sapphire. Typically, the blue pavilions are synthetic sapphire; the red pavilions are synthetic ruby, with an accompanying ruby spectrum.

Over the years, we have seen a few variations in the composition of these types of assemblages. One had a colorless synthetic spinel crown and synthetic ruby pavilion (Winter 1984 Lab Notes, pp. 231–232). Another had a green synthetic spinel crown and a blue synthetic sapphire back (Spring 1985 Lab Notes, pp. 46–47).

Last summer, the East Coast laboratory identified yet another variation of this genre, a 6.28 ct "stone" with a beautiful purplish red hue. Because the

Figure 15. Coarse polish lines (or scratches) on one of the surfaces that interfaces with the cement layer in this 6.28 ct assembled stone resemble needles that might be found in a natural ruby. Magnified 10×.

crown's refractive index matched that of spinel, the piece was being offered as a natural spinel. Some coarse polish lines (figure 15), apparently in the joining plane, resembled the needles that are frequently seen in natural corundum, but not in natural spinel. However, these lines were actually on the surface of the crown (or pavilion) at the interface with the cement layer; they could easily have misled someone into assuming the stone was natural.

Because we do not know the manufacturer's intent, we cannot explain why this assemblage was made with a synthetic spinel crown instead of the usual natural green sapphire. However, the color of the crown (figure 16) does resemble that of the natural green

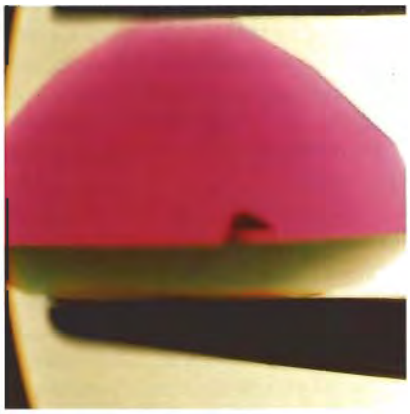

Figure 16. Immersion revealed the green crown of the assembled stone in figure 15. Magnified 5×.

Australian sapphire crowns that are usually used, so the manufacturer may have simply mistaken this material for green synthetic sapphire during the creation of this piece (the pavilion was synthetic ruby). Alternatively, inasmuch as the piece was being sold as natural spinel, this may have been an attempt to imitate fine red Burmese spinel, which itself can have significant value.

GRC

PHOTO CREDITS

Nicholas DelRe supplied the pictures used in figures 1–3, 6–8, 10, 11, 15, and 16. The photomicrographs in figure 4 were taken by John I. Koivula. Figure 5 is by V. J. Cracco. Figure 9 is courtesy of the Richard T. Liddicoat Library and Information Center, photographer unknown. Figures 12–14 are by Shane F. McClure.

GEM N·E·W·S

DIAMONDS

Diamonds from Kelsey Lake, Colorado. More than 1,000 carats of diamonds from the mine at Kelsey Lake, Colorado, were examined by Thomas Hunn of Thomas Hunn Co., Grand Junction, Colorado, during his October 1996 visit to this newly active locality (see, e.g., figure 1). Mr. Hunn provided the following report based largely on his examination of these diamonds and on conversations with Howard Coopersmith, manager, North America, for Redaurum Ltd. of Toronto, Ontario, Canada, which owns the mine.

When the Kelsey Lake mine officially opened on June 1, 1996, it became the only active commercial diamond mine in the United States. (Although Crater of Diamonds State Park in Arkansas is well known as a primary diamond occurrence in this country, we know of no significant commercial production from that source in recent years.) Mr. Coopersmith spent 20 years tracking indicator minerals and geologic clues to locate the heavily weathered kimberlite pipes at Kelsey Lake. With approximately 16.9 million tons of ore reserve (that is, not proven but potential ore), and a monthly production of 2,000 to 4,000 carats, the mine has an estimated life of at least seven years.

The mix of "mine-run" (i.e., not specially selected) stones that Mr. Hunn examined contained both gem-quality and industrial crystals. Of the more than 1,000 carats of rough diamonds that Mr. Hunn examined, 20%–25% were one carat and over, 50%–75% were 0.25 to 1 ct, and 10%–20% were smaller than 0.25 ct. Some crystals weighed more than 9.5 ct, and a 28.3 ct diamond from Kelsey Lake was sold recently (*Rapaport Report*, October 11, 1996, p. 5). Most of the crystals were dodecahedra or octahedra, with a few macles; well-shaped transparent octahedra ("glassies"), twinned crystals (interpenetrant and multiple twins), and modified dodecahedra were also present.

Figure 1. These diamonds (3.28 ct total weight) are from Kelsey Lake, Colorado. Photo © 1996 Thomas Hunn Co.

Figure 2. This 0.27 ct round brilliant (about 4.08 mm diameter × 2.60 mm deep) was cut from one of the "copper" brown diamond crystals found at Kelsey Lake, Colorado. Photo © 1996 Thomas Hunn Co.

The crystals varied from near-colorless to very dark brown. Most were faint to light brown, but about 10%–20% were in the near-colorless range. Only a very few crystals were yellow. Mr. Hunn noted a subtle "copper" tint in some of the brown crystals (figure 2).

With regard to clarity, about half the crystals were cuttable quality; this was true for stones of all sizes, shapes, and colors. "Feathers" (fractures or cleavages) and some inclusions were common throughout the rough; a garnet crystal was identified in one stone. Most crystals displayed fine growth striations on the surface.

Some of the Kelsey Lake diamonds already have been sold (again, see the previously mentioned *Rapaport Report*). Redaurum Ltd. is currently discussing (with various firms) the possibility of bringing the mine's entire production onto the U.S. market.

Update on synthetic diamonds in jewelry. In the Summer 1996 Gem News section (pp. 128–129), we presented information on the marketing of synthetic diamonds in jewelry. At that time, we believed that these synthetic diamonds were being produced by the joint-venture company Tairus. Recently, Dr. Vitaly Efremov, deputy director of the United Institute of Geology, Geophysics and Mineralogy, Siberian Branch of the Russian Academy of Science, Novosibirsk, Russia, clarified this information. (Dr. Efremov also provided the technical information presented in the Summer 1996 issue.) Although Tairus was involved in the early marketing of these synthetics, they actually were grown at the United Institute in Novosibirsk. They are currently being marketed—through Superings, Los Angeles—as "Superdimonds."

COLORED STONES AND ORGANIC MATERIALS

Natural "carvings." For several years now, we have witnessed the creation of increasingly attractive and detailed carvings in various gem materials, including beryl, tourmaline, and quartz. The gem artisans who carve these works of art are usually highly skilled, having labored many years to perfect their craft. Kevin Lane Smith of Tucson, Arizona, has shown a special ability to create pieces that blend nature with artistic vision.

His latest endeavors involve transparent gem crystals with picturesque natural etch or growth patterns that are works of art in themselves. When he locates such a crystal, Mr. Smith works the natural pattern into a fashioned gem, using cabochon or faceting methods, so that light hitting the stone casts shadows that enhance the effect of the pattern. One such natural scene in rock crystal quartz (figure 3) looks like the rugged crags of a mountain range. Most who saw this "carving" thought that the "mountain scene" had been artificially produced. Perhaps the only immediate clue that it is natural is the myriad of tiny red iron oxide diskettes that paint the concave surfaces of the "mountain range" a subtle red.

Figure 3. The detailed mountain scene in this 48.7-mm-long fashioned rock crystal quartz by Kevin Lane Smith is the result of natural "carving." Photo by Maha DeMaggio.

A number of other artists are incorporating the surface texture of natural crystal faces into the pavilions of their faceted stones. The distinctive optical effects that result make every stone unique. This past year, the editors have seen the unusual works of some talented Idar-Oberstein artisans, including the designers of the Philipp Becker Company, who work primarily in beryls (aquamarine, morganite, and heliodor; figure 4), and Klaus Schäfer.

Figure 4. To produce the unusual optics in these two faceted beryls, a 50.66 ct heliodor and a 67.51 ct aquamarine, artists of the Philipp Becker Company incorporated natural faces of the original crystals into the pavilions. Courtesy of James Alger Co., Manchester, New Hampshire; photo © Harold & Erica Van Pelt.

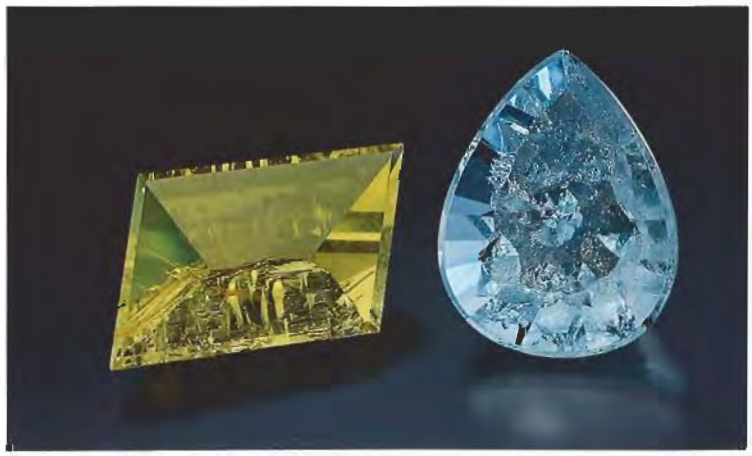

Figure 5. A new deposit in Nevada is the source for this 26.59 ct blue chalcedony cabochon, the polished nugget, and the piece of rough. Photo by Maha DeMaggio.

A new chalcedony locality. A new source for gem-quality blue-to-purple chalcedony was discovered in summer 1994 by geologist Chris Rose, of High Desert Gems and Minerals, Walker Lake, Nevada. The new deposit is located on Mount Airy, near the town of Austin in central Nevada.

Mining, which started in 1996, is currently done by hand. Initial exploration indicated that the site is a typical geode ("thunder egg") deposit; in some areas, the chalcedony nodules are only four inches (10 cm) apart. Eight full claims have been staked out along a mile-long (1.6 km) zone that shows continuous mineralization. The thunder eggs removed so far are typically a few centimeters in diameter, but some nodules over a meter (as large as four feet) across have been found. To date, Mr. Rose has recovered approximately 150–200 kg (330–440 pounds) of nodules, approximately 20% of which contained gem-quality chalcedony. Minerals commonly associated with the chalcedony are calcite and the rock crystal and amethyst varieties of quartz.

Mr. Rose supplied some of the newly discovered material to lapidary Kevin Lane Smith, who provided the Gem News editors with three samples for examination: a large piece of rough, a 474 ct polished "nugget" and a 26.59 ct polished oval cabochon (figure 5).

The Mount Airy chalcedony ranges from a slightly grayish blue (the most common color) to a more purple hue, according to Mr. Rose. The finest specimens are translucent. Energy-dispersive X-ray fluorescence (EDXRF) spectroscopy of the cabochon in figure 5, performed by Sam Muhlmeister in GIA's Research Department, provided no clue as to a possible coloring agent; only silicon and a very small trace of iron were detected. Even at 200× magnification, with pinpoint fiber-optic illumination, we could not resolve any inclusions in the cabochon. We saw only the fine fibrous texture typical of chalcedony.

On the basis of his exploration activities to date, Mr. Rose believes that there are significant reserves of chalcedony in this area.

Cat's-eye emerald from Colombia . . . Chatoyant emerald has been found at the historic Coscuez mine, in the Muzo region of Colombia. Ron Ringsrud, of the Constellation Colombian Emerald Company, Saratoga, California, supplied us with two pieces from this new source: a 22.21 ct oval double cabochon and a 6.75 ct piece of rough (figure 6). In the past, we have seen both cat's-eye and star emeralds from Santa Terezinha de Goiás, Brazil (Gem News, Spring 1992, p. 60; Spring 1995, pp. 60–61; Fall 1995, p. 206); this is the first report of cat's-eye emerald from Coscuez.

The cabochon measured 18.97 × 15.80 × 11.20 mm. Its properties were consistent with those of natural emerald: spot R.I. of 1.58, doubly refractive optic character, typical emerald absorption spectrum when viewed with a desk-model spectroscope, and inert to both long- and short-wave UV radiation. The inclusions that caused the chatoyancy occurred as hazy linear "clouds." Irregular and conical black inclusions were seen at either end of the cabochon.

To date, according to Mr. Ringsrud, chatoyant emerald has been found in only one vein in the Coscuez mine,

Figure 6. Reportedly from Colombia's Coscuez mine, this cat's-eye emerald weighs 22.21 ct. The inset shows part of the chatoyant emerald rough; note the dark carbonaceous shale matrix on the upper and lower faces. Cabochon photo by Shane F. McClure; inset photo by Maha DeMaggio.

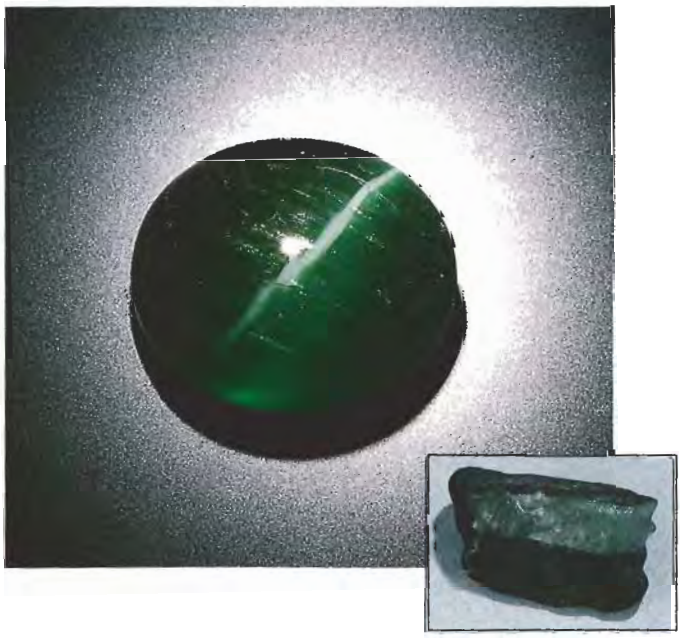

embedded in carbonaceous shale (figure 6, inset) rather than calcite. Discovered in 1996, this vein was depleted within a month. Most of the rough crystals were suitable for fashioning into flattened elongated cat's-eyes; the 22.21 ct stone shown here is the largest that was cut.

. . . And an update on emerald mining at the Muzo mine. On August 16, 1996, *Gems & Gemology* editor Alice Keller and William Rohtert, manager of gemstones for the Kennecott Exploration Company, visited the historic Muzo emerald mine in the state of Boyacá, Colombia. They provided the following account of current activities there.

The Tecminas lease to mine at Muzo was renewed for 25 years in 1995. The three principals are Juan Beetar, Victor Carranza, and Miller Molina. Mr. Rohtert and Ms. Keller were accompanied on their trip to the mine, 100 km north of Bogotá (about a half-hour ride by helicopter from a private airport on the outskirts of the capital), by Tecminas general manager Germán Bernal and geologist Adolpho Pacheco. They spoke with Mr. Beetar and Mr. Carranza at the mining complex in Muzo, and Mr. Carranza conducted the tour of the tunneling operation. At the mining complex, Mr. Carranza brought out a large group of fine emerald crystals—approximately 3,000 carats of rough—that represented the production from a particularly good day (figure 7).

The large mining complex has formal accommodations for dozens of technical staff and has both television and cellular phone capabilities, with power supplied by on-site diesel generators. There is also a small mining village and trading area a few hundred meters down the valley.

Currently, 350 people are working the main Muzo mine, with all organized mining underground, although Tecminas has helped approximately 1,000 local residents form cooperatives for small-scale surface mining and the re-processing of dump material throughout the Muzo area. Most of the tens of thousands of *guaqueros* (independent miners) who once worked the hills and streams at Muzo have moved on to Coscuez, about 10 km to the north, which is responsible for about 85% of Colombia's current emerald production. Tecminas has two concessions (85 ha and 115 ha) at Muzo and a 73 ha concession at Coscuez.

There are two major shafts at the main mine at Muzo—125 m deep and 95 m deep at the time of the August visit—approximately 1.5 km apart. The visitors descended through the 125 m shaft, which measures 5 m in diameter, in a dual-compartment skip (a small open elevator). This shaft is connected to the other, smaller shaft by an intricate network of reinforced tunnels, with a total length of about 2,000–2,500 m. Every 3 m down is a new horizontal level. The mineralized (strike) zone in the district is 1 km wide by 15 km long, and trends north-south. The actual ore zone developed at the Muzo mine measures about 100 m wide by 3 km long. It is discontinuous, so exploration is difficult. The miners look

Figure 7. William Rohtert, Juan Beetar, and Victor Carranza (from left to right) examine approximately 3,000 carats of emeralds recently recovered from the historic Muzo mine, in Boyacá, Colombia. Photo by Alice S. Keller.

for calcite veins and breccias, usually than 1 m thick, with evidence of green beryl and pyrite in the highly carbonaceous black shale. When dolomite bodies are encountered, this signals the end of the emerald mineralization zone.

Blasting is used to move the waste rock. An average of 30 tons of ore a day is shoveled into half-ton ore cars, which are pushed by hand through the tunnels and then taken to the surface in skips for processing in a trommel operation set up a few meters from one of the shafts. When a calcite vein is encountered while tunneling, the miners remove it with handheld pneumatic chisels in a careful and meticulous search for emeralds. About half the emeralds produced are collected by hand from underground, with the remainder recovered from the trommel at the surface. At the time of the visit, a large calcite vein was encountered toward the ceiling of one of the tunnels; four or five miners worked the heavy chisel in rapid succession.

To date, the best stones have come from a small area on the surface called *La Tequendama*. According to Victor Carranza, efforts are now under way to tunnel under the Tequendama area. If the results are not satisfactory, they will return to open-pit mining in this region. Mr. Carranza believes that this is the richest "fringe" of the emerald area. Although the Muzo district has been mined for emeralds for more than a thousand years, Mr. Carranza believes that the reserves are excellent, and his company has identified a number of new mining prospects.

A second Sri Lankan locality for color-change garnet. Garnets that exhibit different colors in incandescent and

daylight-equivalent fluorescent light are known from at least three localities: Umba and Tunduru, Tanzania (Spring 1996 Gem News, pp. 58–59), and Embilipitiya, Sri Lanka. Similar garnets—with a color change strongly reminiscent of alexandrite chrysoberyl—have now been found at a second locality in Sri Lanka, according to Gordon Bleck of Radiance International, San Diego, California. This new locality, Athiliwewa, consists of about 25 acres (10.1 ha) of alluvium, approximately 1.5 miles (2.4 km) east of the Kirindi Oya (stream), near Telulla, in the Monaragala district of southern Sri Lanka. The gem-producing area lies about 4 km east of highway A2 (between the 298 km and 302 km signs), which runs between Tissamaharama and Wellawaya, the nearest large town. Because Athiliwewa is on government land, all mining there is illegal and so is usually done at night.

The garnets are found in alluvial gravels, usually less than a meter below the surface, although one productive hole was reported by Mr. Bleck to be about 3 m deep. The alluvial material, or *illum*, differs from most Sri Lankan *illum* in that it has less clay. The garnets were supposedly discovered by a vegetable farmer in the course of planting. Production as of May 1995 was estimated at 1 kg of garnet rough. Mr. Bleck was told that the largest piece of rough weighed 173 ct, but he did not actually see it. He did see a 40 ct piece of rough (that was later fashioned into a 9.75 ct color-change garnet with a six-rayed star) and a particularly gemmy 32.9 ct piece. As with other color-change garnets that have similar colors (see Spring 1996 Gem News, p. 53), some buyers have mistaken this material for alexandrite.

Gemological properties were acquired for two oval stones, a 1.92 ct modified brilliant (figure 8) and a 0.82 ct mixed cut. In both, the color was evenly distributed and changed from gray-green (in daylight-equivalent fluorescent light; grayish yellowish green in the 0.82 ct stone) to purple (in incandescent light; see again, figure 8). Both also had strong anomalous double refraction when viewed between crossed polarizers, and both were inert to long- and short-wave UV. The large stone had an R.I. of 1.760 and a specific gravity of 3.89; the smaller one had values of 1.768 and 3.91, respectively. Both showed similar absorption spectra with the desk-model spectroscope—435 nm cutoff; 460, 480, 504, and 520 nm lines; and a wide band at 573 nm—typical for color-change pyrope-spessartines. Visible with magnification were iridescent needle-like inclusions (roughly parallel in the larger stone), "fingerprints" (with a two-phase inclusion in the smaller stone), and fractures with iron-oxide stains. EDXRF analysis of these two garnets revealed Al, Si, Mg, Mn, and Fe, as well as lesser amounts of Ca, V, Y, Zr, and Ti.

It is interesting that the color change in these stones was much more obvious when viewed with transmitted light (an effect described by C. M. Stockton in "Two Notable Color-Change Garnets," Summer 1982 *Gems & Gemology*, pp. 100–101; see also "Pyrope-Spessartine Garnets with Unusual Color Behavior," D. V. Manson and C. M. Stockton, Winter 1984 *Gems & Gemology*, pp. 200–207).

SYNTHETICS AND SIMULANTS

Composite tablets, imitation "anyolite." While in Thailand for the International Gemmological Conference in November 1995, the late Robert Kammerling acquired two inexpensive plaques, each representing a seated religious figure (in pink) against a green background (figure 9). Mr. Kammerling suggested that the materials used in these plaques were meant to imitate so-called anyolite—ruby in a green-and-black zoisite matrix. Each plaque was tablet shaped; one measured 35.8 × 24.5 × 9.1 mm, and the other measured 35.3 × 24.3 × 9.5 mm. With magnification, we resolved individual grains of various colors (pink and near-colorless grains in the pink regions; near-colorless, yellow, blue, and green grains in the green regions) set in a pale yellow polymer. Bulk properties included an R.I. of 1.55 (for both tablets; a poor spot R.I. off the polymer filler material) and S.G.'s of 2.54 and 2.51, respectively. The pink regions fluoresced a weak, uneven red to long-wave UV radiation and a faint, uneven red to short-wave UV; the green regions were either inert or fluoresced a very faint bluish white to both short- and long-wave UV.

Both the pleochroism of the grains and the spectrum seen with the handheld spectroscope suggested that most

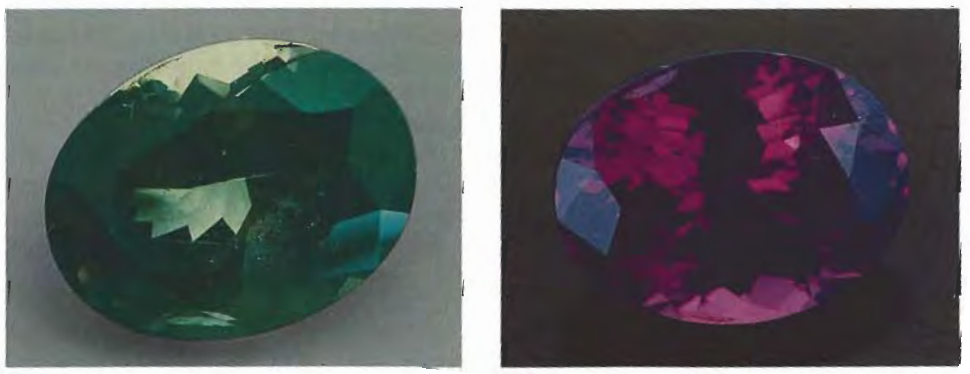

Figure 8. The color change in this 1.92 ct garnet from Athiliwewa, Sri Lanka, is apparent in different lighting conditions (left, daylight-equivalent fluorescent light; right, incandescent light). Photos by Maha DeMaggio.

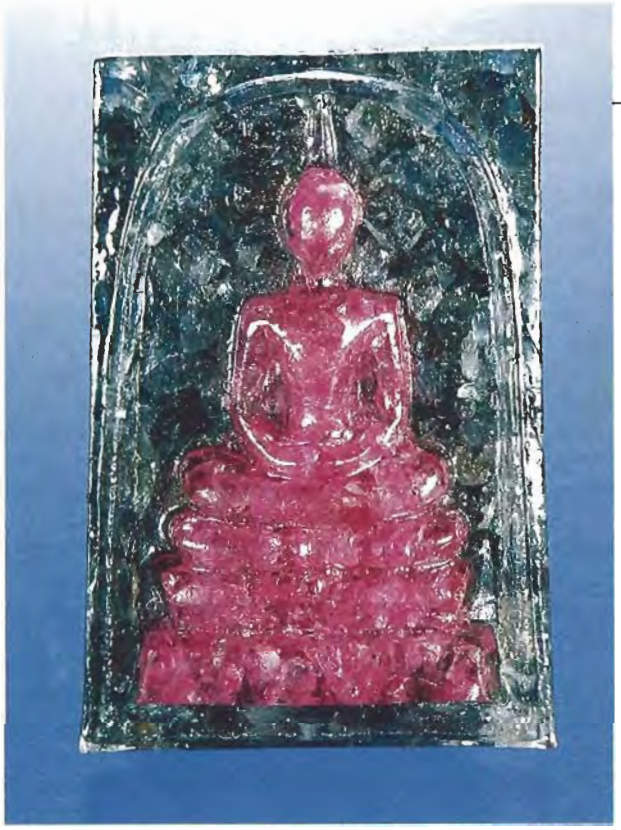

Figure 9. This molded tablet resembles a ruby-in-zoisite ("anyolite") carving. Photo by Maha DeMaggio.

of the grains, in areas of both colors, were corundum. For example, the spectrum of the green area showed readily discernible bands at 450, 460, and 470 nm. The polymer-like material in which the grains were set had many spherical gas bubbles (figure 10). In some of the ruby/pink sapphire chips, we saw clouds of gas bubbles, which indicate synthetic origin. In fact, we could not identify any of the grains in the pink region as natural corundum. Some grains in the green region showed evidence of heat treatment. Some yellow and near-colorless grains appeared to be of a different material, but we could not identify them by standard gemological testing.

UV-visible spectroscopy for the pink region of one plaque revealed a typical ruby spectrum, with an additional absorption edge at about 400 nm, possibly caused by the polymer-like binder. The UV-visible spectrum of the green region showed a band at about 450 nm (resolvable into the 450, 460, and 470 nm peaks seen with the hand spectroscope by looking at the sharp edges) and broad bands centered at about 560 and 820 nm; the latter are related to Fe-Ti and Fe-Fe charge-transfer phenomena. Infrared spectra (between 6000 and 440 cm^{-1}) resolved for both the pink and green regions of one tablet were virtually identical to each other. They were consistent (in the range between 4000 and 1000 cm^{-1}) with the polymer being a mixture of polymethyl methacrylate and alkyd resin (by comparison with the Hummel polymer library).

Bahamian beauties. One tourist now knows that the old adage "let the buyer beware" is more than an idle warning. Susan Hendrickson of Seattle, Washington, an expert and dealer in conch "pearls," was recently shown two beads that had been sold to a friend as conch "pearls." They were purchased during a visit to the Bahama Islands, off Florida's southeast coast.

As is typical with conch "pearls," the two beads were not perfectly spherical (figure 11). Their colors were also somewhat convincing: One (18.49 ct) was an intense slightly brownish red, and the other (18.89 ct) was somewhat more orange. However, the presence of eye-visible swirls in the beads—rather than the flame structure characteristic of conch "pearls"—was immediate cause for suspicion.

Subsequent gemological testing revealed that each bead had a spot refractive index of 1.49 and a specific gravity of 2.52. When the beads were examined with 10× magnification, small spherical gas bubbles were easily seen beneath the surface of each. All of these properties

Figure 10. With magnification, gas bubbles can be seen in the polymer matrix. The grains in the pink region appear to be synthetic ruby and synthetic pink sapphire; in the green region, some of the corundum grains show evidence of heat treatment. Photomicrograph by John I. Koivula, magnified 5×.

Figure 11. These 14.2 mm (red) and 14.3 mm (orange) glass beads were sold in the Bahamas as conch "pearls." Photo by Maha DeMaggio.

proved that the two beads were actually glass.

On further investigation, Ms. Hendrickson learned that such glass imitations were being sold as conch "pearls" by local Bahamian fishermen. Apparently, at least some of the fishermen were convinced that these glass beads actually were conch "pearls." Ms. Hendrickson was not able to find out who was manufacturing and distributing the glass beads.

An ancient Tibetan pendant, represented as a meteorite. Nickel-iron meteorites have long been a source of iron metal, especially in times and regions that lacked easily processed or acquired iron. The Ahnigito meteorite, for example, now at the American Museum of Natural History in New York City, was used as a source of metal by early Greenlanders. So it seemed plausible that a gray metal pendant in the form of a dog (figure 12) could be meteoritic iron that was fashioned in 15th century Tibet (as was represented to its newest owner).

Close examination of the piece, however, revealed various features that made such a composition improbable. Specifically, the piece looked brown in reflected light, not steel gray. In addition, it appeared to be developing a green patina (figure 13), whereas nickel-iron meteorites alter to brown rust in most climates. On the other hand, the green patina could be residual polishing compound, and perhaps the metal surface was brown because it was only slightly rusty. Magnification (again, see figure 13) revealed no evidence of exsolution into a lattice of lath-like metal grains (Widmanstätten structures—Summer 1992 Gem News, p. 133), but only certain nickel-iron meteorites—those with the appropriate composition and cooling history—show these patterns. Etching with a caustic compound is usually needed to expose the pattern when it is present. Ultimately, EDXRF spectroscopy provided the definitive evidence: It revealed copper, tin, zinc, lead, only a trace of iron, and no nickel. Consequently, the material was a bronze (copper-tin) or brass (copper-zinc) alloy, but not a nickel-iron alloy.

University geology departments often are called on by members of the public to determine whether particular samples are meteorites; most of these unknown materials turn out to be "meteor-wrongs." Although this pendant is not a meteorite, it is an unusual and attractive piece. (For more on meteorites and jewelry, see Spring 1995 Gem News, pp. 62–63.) Its age, and whether it came from Tibet, are beyond the scope of our normal identification process.

Figure 12. The gray metal dog-shaped pendant, or tokcha, *around which this pin was built was represented to the owner as manufactured in 15th-century Tibet from meteoritic iron. The brooch (40.7 × 30.9 mm) is courtesy of David Humphrey, Pacific Palisades, California; photo by Maha DeMaggio.*

Figure 13. With magnification, the metallic brooch in figure 12 appeared brown, with a greenish patina in some regions. Chemical analysis confirmed that the material was not a nickel-iron meteorite but rather a copper alloy. Photomicrograph by John I. Koivula; magnified 10×.

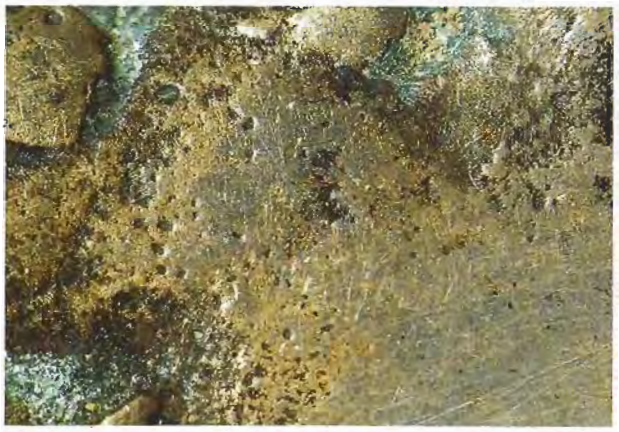

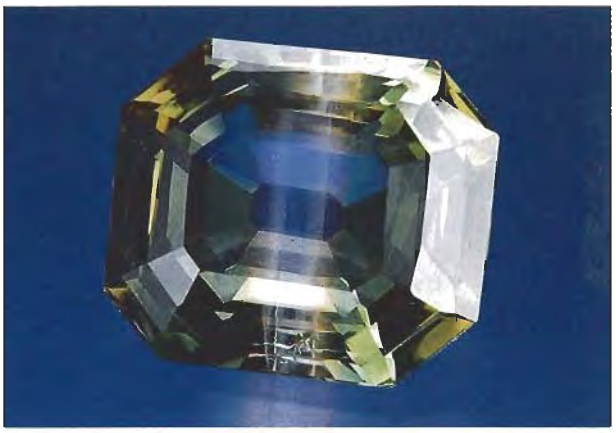

Figure 14. This 45.45 ct synthetic quartz was fashioned to emphasize the near-colorless seed plane. Stone courtesy of Paddie Harris, Santa Monica, California; photo by Maha DeMaggio.

An unusual fashioned "tricolor" synthetic quartz. Last summer, *Gems & Gemology* editor-in-chief Richard T. Liddicoat examined a particularly interesting example of a color-zoned synthetic quartz (figure 14). Most of the synthetic materials that we see have been fashioned in ways that disguise their manufactured origin, but this 45.45 ct emerald cut flaunted its synthetic nature: The near-colorless seed plane formed an obvious stripe through the center of the table. Thin bands of synthetic yellow citrine flanked both sides of the stripe, and the balance of the sample was grayish green. The piece was acquired, already fashioned, in an inexpensive bag of mixed, predominantly rough material purchased at an auction. (For gemological information on a more typically fashioned color-zoned—green and yellow—synthetic quartz, see Winter 1995 Lab Notes, pp. 268–269.)

Figure 15. The 4.01 ct modified brilliant pear shape and 3.84 ct triangular modified brilliant shown here are synthetic spinel triplets, imitating tanzanite. Photo by Maha DeMaggio.

Another tanzanite imitation: Synthetic spinel triplets. So far, we have seen no examples of synthetic tanzanite, although rumors of its existence have circulated since the early 1990s. However, several tanzanite imitations were available at Tucson in February 1996, including synthetic sapphire; a compound of yttrium, aluminum, and europium; and glass (see the article by L. Kiefert and S. Th. Schmidt in this issue, pp. 270–276). Another imitation, marketed as "Tanzation," consisted of synthetic spinel triplets (figure 15). Max Schuster of Los Angeles gave two samples of this material to contributing editor Dino DeGhionno for examination.

We recorded the following gemological properties for these triplets: color—violet; color distribution—even (face up), but all color was contained in the middle "glue" layer; diaphaneity—transparent; optic character—weak anomalous double refraction, manifested as cross-hatching; color-filter reaction—red; refractive indices—1.727 (top and bottom of larger sample), 1.729 (top and bottom of smaller sample); and specific gravity—3.73 (probably unimportant, as the imitation is likely to be successful only when mounted). Each triplet was inert to long-wave UV radiation, but the top and bottom layers fluoresced a strong chalky even greenish yellow to short-wave UV. The "glue" layer was inert to short-wave UV, but was a weak red transmitter to visible light ("transmission luminescence"). When viewed with a desk-model spectroscope, each sample showed three diffuse absorption bands, the strongest at 570–590 nm and the other two at 520–540 nm and 630–650 nm.

With magnification, the "glue" layer in each piece was seen to extend from midway down the girdle into the upper pavilion (figure 16). This layer showed gas bubbles, flow structure, and mottled color distribution, with the color occurring in "thready spots." EDXRF spectroscopy revealed major Mg and Al in the top and bottom layers—consistent with synthetic spinel; the middle layer also contained Si, Pb, Nd, and Co. Therefore, we believe that the "glue" in the middle is, in fact, a silicate

Figure 16. In profile, the bottom of the "glue" layer of the pear-shaped triplet in figure 15 can be seen as a faint line near the top of the pavilion. Photo by Maha DeMaggio.

Figure 17. The bright red stones in this historic cross from Basel Cathedral were identified as dyed red quartz by means of Raman spectroscopy. Photo by P. Portner, Museum for History, Basel, Switzerland.

glass that owes its color to cobalt and neodymium chromophores. The glass is fused to the synthetic spinel crown and pavilion layers.

INSTRUMENTATION

International conference on Raman spectroscopy and geology. Prof. Emmanuel Fritsch of the Institut des Matériaux, University of Nantes, France, provided the following report on the Georaman 96 conference held in Nantes last June. The conference focused on applications of Raman spectroscopy to geologic objects. One session concentrated on applications to gemology, with many of the talks related to the identification of inclusions.

Prof. Paul Dhamelincourt and his colleagues from Villeneuve d'Ascq, France, have identified—using Raman spectroscopy—the following inclusions in Vietnamese rubies: rutile, apatite, muscovite, margarite, phengite, zircon, dolomite, calcite, labradorite, goethite, pyrite, chalcopyrite, and quartz. It is unusual to get good Raman spectra from sulfides (pyrite, chalcopyrite), and quartz was unexpected as an inclusion in ruby, as it should react with corundum to form aluminosilicates. Prof. Dhamelincourt et al. also identified carbon dioxide as an inclusion in an African ruby, and kaolinite and hydrocarbons in fractures in a Burmese (Myanmar) ruby. Finally, they studied in extreme detail an inclusion in a diamond from Liaoning Province, China: The core of the inclusion was a pure forsterite (olivine) crystal that itself contained a microscopic diamond. The forsterite crystal was surrounded by silicate glass and black dendritic plates of graphite and majorite garnet; calcite and a possible sulfate mineral were also found in the inclusion.

Dr. Lore Kiefert, from the SSEF Swiss Gemmological Institute in Basel, reported that organic fracture fillings in filled emeralds can be recognized easily using Raman spectroscopy, as their Raman spectra are distinctive. In another study, grains of albite were detected as a minor rock component in a cabochon of deep violet jadeite jade.

Professors B. Lasnier, Fritsch, and Serge Lefrant from the University of Nantes identified—using Raman spectroscopy and scanning electron microscope data—a spectacular "golf ball" inclusion in a heat-treated sapphire as the product of incongruent melting of zircon.

Another topic was the ability of Raman spectroscopy to characterize samples in geometrically obstructed environments. For instance, Prof. Lasnier demonstrated Raman spectroscopy's ability to document many small stones set in a large ring. Dr. Kiefert reported on identifying diamonds set in a watch face, testing through the transparent synthetic corundum watch "glass."

Raman spectroscopy is now routinely used for the nondestructive identification of archaeological or museum objects, the subject of another session. Using this technique, Prof. Lasnier characterized a neolithic bead from Western Brittany as a sericitic mica; Dr. Kiefert identified red dyed quartz set in a crucifix from Basel Cathedral (figure 17); and Prof. David Smith, from the Paris Museum of Natural History, identified the component minerals of eclogite, gabbro, and jade rocks in pre-Colombian Mexican artifacts. Prof. H. G. M. Edwards and co-workers at the University of Bradford (United Kingdom) identified cinnabar and lazurite pigments in wall paintings and frescoes.

Raman spectroscopy provides information about the vibrations of groups of atoms in a mineral or compound; because of this, it can be used to provide fundamental information on gem- and gem-related-minerals. Dr. Giancarlo Parodi and Prof. Smith used Raman spectroscopy to describe the structures of the Fe^{3+} analog of beryl—the new mineral stoppaniite—and a kimzeyite (titanium-zirconium-rich garnet), both from Latium, Italy. Prof. Smith also has interpreted systematics among the

Raman spectra of over 100 garnets from the pyrope-almandine-spessartine and grossular-andradite-uvarovite subgroups. Dr. Shiv Sharma, of the University of Hawaii, Honolulu, Hawaii, obtained structural details of natural amphibole crystals. By using a special technique called resonance Raman spectroscopy, Dr. Mikhail Ostroumov, from the St. Petersburg School of Mines, found that $(SO_4)^{2-}$ ionic groups may play an important role in the coloration of lazurite, the main component of lapis lazuli.

Instrument improvements were discussed as well. The use of the confocal technique has proved invaluable for obtaining the spectrum of an inclusion separate from that of the surrounding host. Near-infrared lasers and Fourier-transform spectrometers do not excite visible luminescence (sometimes called "transmission luminescence") and so are ideal for running highly fluorescent materials. Also, Dr. Sharma and associates developed an oblique-illumination confocal microscope for the study of weakly (Raman) scattering materials, such as glasses.

The notion of a standard catalog of reliable Raman spectra is still being pursued, although at the time of the meeting too few individuals had subscribed to a proposed standard database that was unavoidably expensive. One additional difficulty is that Raman peak intensities—though not positions—may vary with crystallographic orientation, which could lead to misidentifications by uninformed users of such a catalog. Abstracts of the Georaman 96 conference are available as *Terra Abstracts*, Volume 8, supplement number 2 of *Terra Nova*, a Blackwell Science, London, journal. The next Georaman meeting is planned for 1999 in Valladolid, Spain.

MISCELLANEOUS

Synthetic sapphire assemblage with a gold "fractal" design. In triplets, the material of greatest interest is often that in the interlayer. In opal triplets, for example, a fragile piece of opal with a desirable play-of-color is protected by a backing material and a cover plate made of a durable transparent substance, such as quartz or glass (see Fall 1996 Lab Notes, pp. 209–210). Recently, the editors became aware of a different type of patterned assemblage (figure 18), in which a microscopically detailed design is etched on the back of a single crystal of Czochralski-pulled synthetic sapphire; the pattern is then deposited with gold. The front surface of the transparent crystal protects the design. The piece is then "backed" by another material. This assemblage is by Refractal Designs, of Danvers, Massachusetts.

According to Refractal Designs president Rick Becker, a proprietary technique (patent pending) photolithographically deposits the 18k gold on a specially prepared surface. With this technique, extremely intricate designs can be created, some 10 times finer than a human hair.

A fractal is the physical representation of a very complicated mathematical pattern that is "infinitely self-iterating," according to Mr. Becker. In effect, design elements visible in the overall view are also seen in the components of that design (figure 19), at (in theory) any magnification level. Mr. Becker reports clearly visible detail in the pattern at 1,000× with the proper instrumentation. Benoit Mandelbrot first brought these patterns to general attention over a decade ago (see, for instance, *The Fractal Geometry of Nature*, W. H. Freeman and Co., New York, 1982), but the complexity of the calculations made the representations very hard to produce until recently. Even with powerful desktop computers and special software, the generation of these images can take many hours.

The imaged crystal section is "R-plane" Czochralski-pulled synthetic sapphire from Union Carbide, according to Mr. Becker. We measured refractive indices consistent with this material (1.762–1.770). The blue background to the gold design is a metallic oxide that has also been deposited photolithographically. In the prototype sample we examined, glass was used as the backing material. Mr. Becker states that, in production runs, another piece of synthetic sapphire will be used. The

Figure 18. This 22-mm-diameter assemblage, called "Deep Sea Rising," consists of a piece of synthetic sapphire on one side of which a fractal design has been rendered in gold. The design is protected in the back by another slice of a transparent material. Courtesy of Refractal Designs; photo by Rudy DeLellis.

Figure 19. At 11× magnification, individual components of the fractal design in the assemblage shown in figure 18 can be seen to mimic the overall pattern. Photomicrograph by John I. Koivula.

Figure 20. The balloons in this glass block are completely contained by the surrounding glass; they were carved using a focused laser beam. Photo by Maha DeMaggio.

company is also developing processes to deposit more than one color of metal simultaneously. The designs reportedly can be deposited on many jewelry materials.

Completely internal "carving" of glass. At two shows during the last year, one of the editors (MLJ) encountered an unusual method for carving isotropic materials. The 78.25 × 50.2 × 49.8 mm sculpture in figure 20 was made from optical-quality (manufactured) glass. The balloons, and the ground below them, are completely internal to the glass block; they are actually patterns of short dashes that have been carved by a laser.

Richard Sittinger of WonderWorks, Cambria, California, provided some information about this cutting style. The sculptures, called "Erokhin Laser Glass Crystals," are made in Russia. For each piece, the three-dimensional design is created using computer graphics; a computer-controlled "focus laser-ray apparatus" then produces tiny energy bursts at specified points within the optical glass block. The laser ray actually passes through the glass and affects only the spot on which it is focused, according to information provided by Mr. Sittinger. Additional designs were available at both shows, including abstract geometric figures and sailboats.

When examined with magnification and polarized light, the glass showed areas of strain in the regions of the laser-etched pattern elements (figure 21). We see no obvious reason why this technique could not be applied to other isotropic substances, such as cubic zirconia—or even diamond.

Figure 21. When examined in polarized light, the areas of laser damage in the glass are seen to be surrounded by small regions of strain. Photomicrograph by John I. Koivula; magnified 15×.

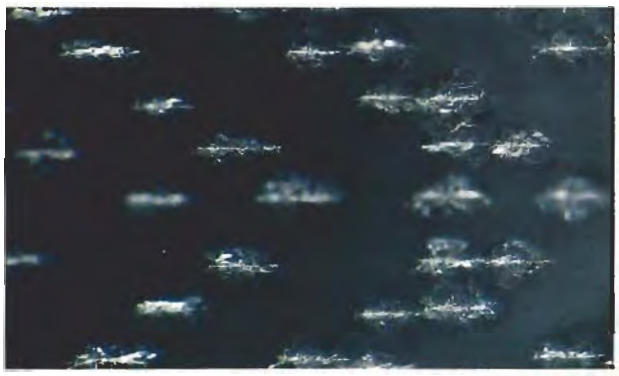

THE ROBERT C. KAMMERLING RESEARCH ENDOWMENT

The Gemological Institute of America has created The Robert C. Kammerling Research Endowment in honor of Bob and the work he cherished. The Endowment secures funds for qualified researchers worldwide who are engaged in applied gemological research, and ensures the continuation of Bob's unique and practical approach to gemology.

The following donors have contributed $100 or more to The Robert C. Kammerling Research Endowment for applied gemological research:

Anonymous
Mr. George Bosshart
Dr. G. V. Boukine
Mr. William E. Boyajian
Capalion Enterprise
Ms. Neola Caveny
Mr. George Crevoshay
Mr. G. Robert Crowningshield
Ms. Dona M. Dirlam
Mr. Richard B. Drucker
Mr. Robert A. Earnest
Ms. Nanette Forester
Dr. Neel K. French
Dr. Edward J. Gübelin
Gübelin Gemmological Laboratory
Dr. Gary R. Hansen
GIA Gem Trade Laboratory
Patricia D. Harris and John Connelly
Dr. Cornelius S. Hurlbut
Ms. Karin Hurwit
Dr. A. J. A. (Bram) Janse
Jeweler's Circular-Keystone
Mr. Alan Jobbins
Mr. Robert E. Kane
Ms. Alice S. Keller
Ms. Kathryn Kimmel
Ms. Gina Latendresse
Dr. Alfred A. Levinson
Mr. Richard T. Liddicoat
Mr. Philip Minsky
Dr. Oded Navon
Mr. David O. Ohlgisser
Ms. Judith A. Osmer
Mr. Mark Parisi and
Dr. Mary Johnson
Ms. H. Ruth Patchick
Ms. Anne Paul
Dr. Frederick H. Pough
Mr. Kenneth V. Scarratt
Dr. and Mrs. John Sinkankas
Stichting Nederlands
Edelsteen Laboratorium
Mr. Tay Thye Sun
Harold and Erica Van Pelt
Ms. Merle White
Mr. Raffaele Zancanella

The Robert C. Kammerling Research Endowment gives you the opportunity to help the Gemological Institute of America continue its efforts to secure the industry's future. Your commitment to the Endowment promotes the active advancement of gemological research, for the collective benefit of the industry.

For more information on how to support the Endowment, please contact Anna Lisa Johnston, GIA Associate Campaign Director. In the U.S. (800) 421-7250 ext. 274, outside the U.S. (310) 829-2991 ext. 274, fax (310) 829-2269, e-mail address ajohnsto@gia.org.

GEMSTONES OF AFGHANISTAN

By Gary W. Bowersox and Bonita E. Chamberlin, 220 pp., illus., publ. by Geoscience Press, Tucson, Arizona, 1995, US$60.00.*

While known for more than five millennia as the producer of the world's best lapis lazuli, Afghanistan has recently emerged as a premier locality for a variety of other fine gemstones. Today more than ever before, gemstones are playing a key role in Afghanistan's political development.

Bowersox and Chamberlin describe the history and current status of each of five types of gem deposits: lapis lazuli, spinel, ruby and sapphire, emerald, and pegmatite gems. For each category, the historical background establishes the role of the gems in the country's development, while generally excellent photography showcases the gems and the field areas. Maps are also included.

Following an introductory chapter on the general geography, geology, and tectonic setting, and a second on Afghanistan's history, each subsequent chapter focuses on one gem category. The first is lapis lazuli, which is mined from remote mountains in the Hindu Kush Range, about 300 km northeast of Kabul. Access to the mines is along steep and dangerous pathways, and mining methods are still relatively primitive. In addition to Description and Location of the mines, the chapter on lapis lazuli includes Legends and Lore, Geology and Topography, Historic Notes, Illustrations of Lapis Use and Trade, Mining Methods, Production Figures, Properties, and extensive references.

This chapter format is then followed for each of the other gem categories. For many years, spinel was mined in the far northeastern corner of Afghanistan, but there has been no recent production. This area was probably the source for such famous stones as the 170 ct Black Prince's "ruby" (now known to be spinel) in the Imperial State Crown of Great Britain. In contrast, true ruby and sapphire are mined today from white marble about 50 km southeast of Kabul, near Jegdalek, and about 32 km farther east, near Gandamak. Current production is limited, but the area has potential for more discoveries.

Emeralds of the Panjshir Valley are now world famous. Although noted in the literature as early as 250 years ago, there was apparently no reference to these deposits between 1891—when they were briefly mentioned in a report to the Geological Survey of India—and the 1970s. Today, more than 2,000 miners work nearly 100 mines under often-dangerous conditions. Although the geologic origin of these emeralds is not well understood, there appear to be many similarities with the Colombian deposits.

Gem-bearing pegmatites occur over a wide area in northeastern Afghanistan, part of a 3,000-km-long chain of pegmatites along the Himalayas. Evidence of gem beryl in Badakhshan archeological sites indicates that these gems were discovered thousands of years ago. However, contemporary mining has been active only since the 1970s. Many fine gems will undoubtedly emerge from this region (21 pegmatite fields have already been discovered).

A final chapter outlines the potential for mineral development in Afghanistan, and an appendix lists locations of many deposits by latitude and longitude (a valuable feature).

The text is very readable and coherent. Nevertheless, some typographical errors are apparent, such as the omission of the Cambrian period on the Geological Timetable (p. 15), and the incorrect age (600 million years rather than about 30 million years) assigned to the Oligocene Period (p.105). The book should be carefully edited for a second edition.

Because of the political upheaval that has plagued the country for many years, much of Afghanistan's infrastructure has been destroyed. Although gems are already being used by the mujahideen to finance their struggle, mining could play a key role in rebuilding the country. Books such as this raise international awareness of the region. This book is also a nice addition to any gemologist's library.

F. A. COOK, Ph.D.
University of Calgary
Calgary, Alberta, Canada

THE VOLCANIC EARTH

*By Lin Sutherland, 248 pp., illus., publ. by University of New South Wales Press, Sydney, NSW, Australia, 1995. US$45.95**

Volcanoes are the most visibly dramatic, as well as one of the most destructive (they have killed about 100,000 people this century), of all geologic processes. Dr. Sutherland has used the eye-catching physical features of volcanoes, and melded them with modern scientific concepts such as plate tectonics and geochronology, to produce a superb book.

Although the main emphasis is on the southwest Pacific region (Australia and New Zealand), there are enough examples from other parts of the world (e.g., Hawaii, North America, Iceland) that readers from all countries will be able to relate to the material covered. Of particular interest to gemologists is the fact that important sources of some gems—diamond, sapphire, ruby, zircon, peridot, garnet, feldspar, and quartz—are directly or indirectly related to volcanism. These may be brought up from great depths by volcanic magmas (e.g., diamonds, pyrope), may form within crystallizing magmas (e.g., peridot), or may form as secondary minerals within cavities in the hardened rocks (e.g., amethyst). Later geologic processes, such as weathering and erosion, may result in secondary gem deposits. Succinct discussions of these volcanic gems are presented.

This book is superbly illustrated in color throughout. I recommend it highly for gemologists at all levels.

ALFRED A. LEVINSON, Ph.D.
University of Calgary
Calgary, Alberta, Canada

**This book is available for purchase through the GIA Bookstore, 1660 Stewart Street, Santa Monica, CA 90404. Telephone: (800) 421-7250, ext. 282; outside the U.S. (310) 829-2991, ext. 282. Fax: (310) 449-1161.*

GEMOLOGICAL ABSTRACTS

C. W. FRYER, EDITOR

COLORED STONES AND ORGANIC MATERIALS

Common and rare colourless gemstones. D. Kent, *Journal of Gemmology*, Vol. 25, No. 2, 1996, pp. 87–89.

David Kent describes and illustrates his collection of 46 colorless faceted gem and collector minerals, which he uses in teaching gemology. A table provides useful R.I. and S.G. data for all 46 specimens—a bonus for gemologists compiling their own databases. *CMS*

Compositional characteristics of sapphires from a new find in Madagascar. C. C. Milisenda and U. Henn, *Journal of Gemmology*, Vol. 25, No. 3, 1996, pp. 177–184.

Blue sapphires from Andranondambo, Madagascar, have been well represented lately in the gemological literature. The first of two articles in this issue of *Journal of Gemmology* succinctly reports on the regional geology, physical properties, and internal features of these sapphires. The spectrum of a single sample was typical of sapphires from high-grade metasedimentary sources, with Fe^{3+} and Fe^{2+}/Ti^{4+} charge transfer evident. Common mineral inclusions are apatite, carbonates, and (tentatively) mica. A more detailed study of solid inclusions is being prepared. Color zoning, negative crystals, and fingerprint-type inclusions are also common. In general, Andranondambo sapphires resemble those from Burma and Sri Lanka. *CMS*

Emerald and green beryl from Central Nigeria. D. Schwarz, J. Kanis, and J. Kinnaird, *Journal of Gemmology*, Vol. 25, No. 2, 1996, pp. 117–141.

Central Nigeria is relatively well known as a source of aquamarine, but it also produces a limited quantity of emeralds and green beryl. This in-depth study reveals that these beryls formed under unusual geologic conditions which resulted in a suite of mineral inclusions that appears to be unique to emeralds and green beryls from this geographic region: albite, fluorides (fluorite, "boldyrevite," and ralstonite), F-silicate, Fe-rich mica, ilmenite, and monazite. "Boldyrevite" and ralstonite have not been reported previously in emeralds from any locality. Inclusions were iden-

This section is designed to provide as complete a record as practical of the recent literature on gems and gemology. Articles are selected for abstracting solely at the discretion of the section editor and his reviewers, and space limitations may require that we include only those articles that we feel will be of greatest interest to our readership.

Inquiries for reprints of articles abstracted must be addressed to the author or publisher of the original material.

The reviewer of each article is identified by his or her initials at the end of each abstract. Guest reviewers are identified by their full names. Opinions expressed in an abstract belong to the abstracter and in no way reflect the position of Gems & Gemology *or GIA.*

tified by SEM-EDS. Microprobe chemical analyses of the emeralds themselves revealed unusually low Mg and Na contents—another reflection of this material's environment of formation. Unfortunate from a gemological viewpoint is the low-Cr, low-V, and high-Fe chemistry of these emeralds. Distinct Fe^{2+} absorptions in their optical spectra will distinguish these emeralds from Colombian material when inclusions do not. *CMS*

The genesis of emeralds and their host rocks from Swat, northwestern Pakistan: A stable isotope investigation. M. Arif, A. E. Fallick, and C. J. Moon, *Mineralium Deposita*, Vol. 31, No. 4, 1996, pp. 255–268.

Emeralds in this area, locally associated with other Cr-bearing silicates (Cr-dravite and fuchsite mica), occur in veins with quartz, filling fractures in talc-magnesite and quartz-magnesite. The close spatial relationship and relatively narrow range of $\delta^{18}O$ values suggest that all the investigated phases (emerald, quartz, fuchsite, and tourmaline) are genetically related. The δD composition of channel water (released at >800°C) from emerald and that calculated for fuchsite and tourmaline are consistent with both magmatic and metamorphic origin, but a magmatic origin is favored. Relative to pegmatitic and other magmatic minerals from elsewhere, the $\delta^{18}O$ values of the minerals all show a strong enrichment in ^{18}O; the relatively high fluid $\delta^{18}O$ (calc.) suggests extensive interaction with ^{18}O-rich crustal (metasedimentary) rocks. The $\delta^{13}C$ and $\delta^{18}O$ values of the magnesite are remarkably uniform; their relatively low $\delta^{18}O$ values suggest formation at a high temperature. The CO_2-bearing fluids responsible for the carbonation were probably metamorphic in origin. *RAH*

Interesting gems from north-east Tasmania. B. Sweeney, *Australian Gemmologist*, Vol. 19, No. 6, 1996, pp. 264–267.

Author Boyd Sweeney describes and illustrates gems found by fossickers in northeast Tasmania, indicating the potential for future production there. Significant gem minerals recovered to date include sapphire, ruby, spinel, zircon, topaz, quartz, chrysoberyl, and tourmaline. A 900 ct sapphire was found in a paddock at Weldborough; sapphire reportedly is more abundant in the Weld River area. According to the author, most Tasmanian sapphires are found as clean, conchoidal fragments of trigonal crystals. Faceting-quality sapphires range from near-colorless to cornflower blue. More common are dark green sapphires and sapphires of a very dark, "ink" blue. Opaque Tasmanian sapphires commonly are pale blue to dark brown.

Opaque spinel from this area is "steel" gray with a vitreous luster and provides a good alternative to black onyx.

The author's discovery of a 2.95 ct ruby crystal helps disprove the misconception that there are no rubies in Tasmania. Zircon typically ranges from bright red to dark reddish brown, in sizes from 3 to 10 ct. Because the rough usually is extensively fractured, only small fragments can be faceted. Paler Tasmanian zircons, however, yield fashioned stones of good clarity and high dispersion. Much of the topaz from Weld River is found as colorless, waterworn pebbles. Only about 10% of all topaz rough occurs in pale shades of blue. The areas around Gladstone, Pioneer, South Mt. Cameron, and Derby are renowned for their yield of high-quality smoky quartz. Chrysoberyl is relatively common in the Weld River alluvial gravels. Colors range from a satiny "creamy" green to "grass" green; some rough cuts good cat's-eyes. Black tourmaline, with some gem potential, is also found in the rivers of northeast Tasmania. *MD*

Mangatobangy: Amethyst-zepter aus Madagaskar (Mangatobangy: Amethyst scepters from Madagascar). F. Pezotta, *Lapis*, Vol. 21, No. 9, 1996, pp. 32–35.

Madagascar has been an important source of amethyst, generally from numerous small mines. This article briefly describes one such locality near Mangatobangy, about 40 km (26 miles) west of Fianarantsoa. This mine is especially interesting because it produces amethyst scepter crystals of extraordinary size and beauty. Most range from 5 to 20 cm (2–8 inches), but at least one was 60 cm (24 inches). They are usually well formed, with amethyst caps on milky to colorless quartz crystals; sometimes they are doubly terminated. Six color photos show the open-pit mining site and amethyst scepter specimens. *RT*

Mintabie opal field. *Australian Gold Gem & Treasure*, Vol. 11, No. 1, January 1996, pp. 68–72.

This article is a first-person report (strangely lacking a byline) on a visit to the mostly depleted opal fields at Mintabie, South Australia, 400 km by road south of Alice Springs. Techniques used there to mine opal are described.

The article is written in the breezy style of the magazine: for instance, "Like chooks on a compost heap, we started to investigate the rubble, finding parts of the potch band and cracking them open with our geopicks." The claims are primarily strip-mined by bulldozer. On one claim visited, spotters behind the bulldozer had found table-top-sized seams of opal (showing green play-of-color, and worth eventually Aus$350,000). The matrix sandstone is cemented together by strongly silicified bands of blue potch opal; jackhammers remove patches showing color. Some miners say that opal is often found in horizontal bands a few meters away from strong vertical faults. The Mintabie fields are due for a revival, as relocation of the airfield will free up many promising opal areas. *MLJ*

Ribbonstone. H. Bracewell, *Australian Gold Gem & Treasure*, Vol. 11, No. 1, January 1996, p. 44.

Ribbonstone is a variety of chert, a cryptocrystalline quartz. It is distinguished by its pattern of fine banding: characteristic swirls that are partly concentric, the result of widespread cracking that was subsequently cemented by silica. This ornamental material is found at several localities in the Barkly Tableland of Australia's Northern Territory, with

the best material coming from the Anthony's Lagoon area. The ribbonstone was formed as a large, sheet-like deposit along a subsurface water table, probably in Tertiary times; the banded nature reflects changing rates of silica deposition with seasonal changes in ground moisture. *MLJ*

Sapphire—"a funny place." P. O'Brien, *Australian Gold Gem & Treasure*, Vol. 11, No. 1, January 1996, pp. 22–25, 58, 60–61.

The town of Sapphire, in the Anakie gemfields of Central Queensland, Australia, is colorfully profiled. Gem-quality sapphire was first found in the Anakie district in 1878, and the Anakie gemfields were officially named in 1902. By 1907, at least 500 people were digging at Anakie: One carrier shipped two tons of blue sapphires to the railhead that year. At that time, sapphire of any color other than blue was discarded as worthless, so yellow, green, and parti-colored sapphires were left on the dumps for more recent collectors.

Several colorful characters populate the legends of Sapphire. Perhaps most notable was Darky Garnet, who entered the Anakie district with all his worldly possessions in a wheelbarrow, and eventually left the same way—after winning and losing a couple of fortunes. (A 19 km wheelbarrow race, starting at the local pub, annually perpetuates his memory.) A resurgence of sapphire mining occurred following World War II. Today the district supports both professional mining and tourism, including "fossicking," as amateur collecting is known in Australia. *MLJ*

Sapphires from Andranondambo area, Madagascar. L. Kiefert, K. Schmetzer, M. S. Krzemnicki, H.-J. Bernhardt, and H. A. Hänni, *Journal of Gemmology*, Vol. 25, No. 3, 1996, pp. 185–209.

The second article on Andranondambo sapphires in this issue of *Journal of Gemmology* is more extensive, covering locality, geologic origin, crystallography, microscopic growth features, and detailed chemical and spectral analyses. The study collection contained more than 300 samples of both rough and cut stones that ranged from light to dark blue. Three types were distinguished on the basis of crystal habit: dipyramidal to barrel-shaped, prismatic, and tabular to short-prismatic dipyramidal. Internal growth features and color zoning are described in detail and illustrated extensively. Microscopic features and inclusions are discussed by sapphire type. Many solid inclusions were identified by Raman spectroscopy: apatite, calcite, and spinel (type I); apatite accompanied by tubes (type II); and apatite, zircon, calcite, and three-phase inclusions (liquid and gaseous CO_2 with diaspore needles; type III). Healed feathers were observed in types I and II. Apatite and calcite crystals were often surrounded by rosette-like fissures in both heated and unheated type I samples, but only the heated specimens contained fissures with a dendritic pattern containing an unknown filler. EDXRF and electron microprobe data document the chemical variability and zoning in this material. UV-visible spectra of samples before and after heat treatment reveal behavior similar to geuda-type material from Sri Lanka. Infrared spectra reveal features typical of most corundum. *CMS*

Shape, structure and colours of Polynesian pearls. J.-P. Cuif, Y. Dauphin, C. Stoppa, and S. Beeck, *Australian Gemmologist*, Vol. 19, No. 5, 1996, pp. 205–209 (translated from *Revue de Gemmologie*, March 1993).

Described are the processes that determine nacre quality and color in bead-nucleated cultured pearls from *Pinctada margaritifera*, the black-lipped pearl oyster of French Polynesia. Biological researchers want to control these characteristics to achieve a greater yield of superior gem-quality cultured black pearls.

The successful insertion of the shell-bead nucleus and mantle graft into the oyster will affect the shape and color of the resultant cultured pearl. The nacre produced is the result of a change in function of the epithelial cells that secrete calcium carbonate from the mantle. Essentially, calcite secretions are replaced by aragonite during formation. The final tile-like layer is caused by an ordered, rhythmic secretion of aragonite platelets; it yields the outer nacre that gives the cultured pearl its beauty and orient. The formation of "circle" pearls (undesirable cultured pearls that are typically of inhomogeneous color, with circumferential depressions) is also discussed.

The periphery of the mantle has the greatest pigmentation for creating the color of the pearl, but it also has the highest concentration of calcite-secreting cells. The paler "inner" mantle tissue contains the cells necessary for aragonite secretion and, thus, a thick nacre. The grafter risks producing cultured pearls with a thin nacre if he chooses to implant the darker epithelium that is restricted to the outer periphery of the mantle.

The authors analyzed the pigment of Polynesian cultured pearls using low-pressure chromatography, spectrophotometric techniques, and reflectance spectroscopy. Reflectance spectroscopy allows determination of statistical distributions of color in pearl populations. With such data, the influence on color distribution of factors such as changes in the geographic distribution of species or in production methods could be monitored—and possibly controlled.

Understanding nacre and color formation in pearls—and monitoring it with statistical techniques—is a significant step toward greater control in the production of higher-quality Polynesian black cultured pearls.

Cheryl Y. Wentzell

DIAMONDS

Automation: Still the key word. C. Hourmouzios, *Diamond International*, January/February 1996, pp. 73–74, 76, 78–80.

Mr. Hourmouzios does an excellent job of explaining the technology and machinery now available in the diamond-cutting industry. He describes a diamond-cutting laser that is accurate to 0.4 microns, 40 times more precise than the previous model. The bruting machine can stop automatically when the stone reaches the preset diameter. There is

a centering machine that plans, centers, and marks the stone. The blocking machine contains a diamond scaife that has boosted production 50%–75% in some areas of India. The polishing machine can polish excellent to ideal cuts from two points up to 18 ct and has an accuracy to 2.5 microns. Finally, he describes a girdle-faceting machine that can polish from 40–200 girdle facets on rounds and fancies as small as 50 points to as large as 10 ct.

This technology did not exist 25 years ago. At that time, Sir Philip Oppenheimer said, "Automation can only be an addition to the diamond industry." Still, technological progress for the diamond-cutting industry has been slow compared to other industries. *AMB*

A crustal mineral in a mantle diamond. L. R. M. Daniels, J. J. Gurney, and B. Harte, *Nature*, January 11, 1996, pp. 153–156.

Recent studies of diamonds, their inclusions, and related rocks provide evidence for the origin of some of these materials in the Earth's crust. Much of this evidence is isotopic, especially that involving isotopes of oxygen, sulfur, lead, and carbon. This article is the first report of staurolite, a metamorphic mineral that occurs in crustal rocks, as an inclusion in diamond.

The diamond that contained the staurolite inclusion came from the Dokolwayo kimberlite, one of a series of kimberlites that erupted about 200 million years ago in what is now northeastern Swaziland. Included minerals in Dokolwayo diamonds are consistent in composition and abundance with inclusions in diamonds from kimberlites—except for the relatively high contents of coesite, a high-pressure polymorph of quartz. The diamond studied was over 3 mm in its largest dimension; the staurolite inclusion, a discrete crystal about 0.08 mm, was completely enclosed by the diamond, with no cracks leading to it. Graphite was also included in the diamond; the diamond's carbon isotopic signature, $\delta^{13}C$ value of –5.0 per mil, was typical for mantle carbon without a crustal isotopic component.

Staurolite is a metamorphic silicate mineral that is typically found in metamorphosed sediments of clay-rich composition, derived from continental sources, which crystallized under conditions of moderate temperature and moderate-to-high pressure within the crust. However, other Dokolwayo diamonds contain silica (coesite) inclusions, and staurolite is not stable at the pressure-temperature conditions at which diamonds form if silica is present. (Magnesium-rich staurolites are stable at higher pressures and temperatures, but this specimen did not contain sufficient magnesium for this to be a factor.) The authors suggest that this inclusion formed under crustal conditions, before or during subduction of its source material; the staurolite survived as a relict grain in the diamond because it was not in contact with any silica phases. Unfortunately, the inclusion has been misplaced, precluding further study. *MLJ*

The diamond mining quarries of East Siberia as a factor affecting surficial water quality. V. N. Borisov, S. V. Alexeev, and V. A. Pleshevenkova; in Y. K. Kharaka and O. V. Chudaev, Eds., *Water-Rock Interaction, Proceedings of the 8th International Symposium on Water-Rock Interaction*, WRI 8, Vladivostok, Russia, August 1995, published by A. A. Balkema, Rotterdam, Netherlands, pp. 863–866.

The development of diamond mines in the arctic climate of Siberia, which has been ongoing since about 1960, has resulted in severe environmental problems. The nature and extent of these problems are only now being discussed openly in the scientific literature. This particular paper describes the effect that mining of the Udachnaya kimberlite pipe has had on the quality of surficial waters, specifically in the Markha River system. The same conditions are present at other mining locations, such as Mirny and Aikhal. The detrimental environmental effects are caused by:

1. High chloride brines: When the open-pit mine at Udachnaya penetrated the permafrost (permanently frozen zone), which occurs here at depths of 150–600 m, highly saline groundwaters began to infiltrate the pit. These brines came from porous and permeable sedimentary rocks surrounding the pit. The brines are predominantly of the chloride type, with associated Ca, Na, Mg, and K. Especially serious, however, are the dangerously high levels of bromide they contain.

At first, the brines were discharged directly into the river system or released onto the surface. Because these practices had such a negative impact on the environment, in recent years the brines have been injected into the permafrost zones. However, this latter method has potential problems. For example, the brines may leak onto the surface, again leading to severe pollution.

2. Tailings: The material that remains after diamond recovery generally includes finely ground kimberlite and chemicals from the separation process, which are stored in tailings piles on the surface. These piles are very susceptible to leaching by water from rain and snow, a process that adds more undesirable chemical phases to surface waters. Leakages from the tailings have been recorded for more than 10 years.

3. Spoil heaps from stripped rocks: Open-pit mining requires the removal (stripping) of large volumes of rock surrounding the pipe. These rocks are placed in spoil heaps that typically cover huge areas and are over 80 m high. Most of the stripped rocks are sedimentary (e.g., limestones), and so are readily leached, adding more undesirable chemical constituents to the environment. In addition, these rocks have been used to build roads and for other industrial purposes, resulting in a "ubiquitous salting of [the] soil landscape."

Using background (baseline) values for chemical parameters in the Markha River system that were taken in 1979–1980, the authors show that pollution now can be detected as far as 700 km downstream from the Udachnaya mine!

[Abstracter's Note: Environmental pollution of the type described in this paper will not occur in the proposed diamond mining area of Canada's Northwest Territories,

although the climate there is similar. In this area, the kimberlite pipes have intruded into metamorphic rocks that contain no brines or easily leachable sedimentary rocks.] *AAL*

Greenland: Country supplement. *Advertisement Supplement to Mining Journal, London,* March 1, 1996, 24 pp.

The discovery of diamond-bearing kimberlites in Canada's Northwest Territories has led to a reappraisal of similar rocks in Greenland. Some 500 potentially diamondiferous occurrences have been found in Precambrian rocks in West Greenland, between 60°N and 72°N (west of the permanent ice cap). Diamond indicator minerals have been found in stream sediments within the West Greenland Archaean craton, and microdiamonds have been found in kimberlite dike swarms at both the northern and southern margins of the craton. Exploration is proceeding on the Bjørnesund, Inglefield Land, Itillii, Kobberminebugt, Narsarsuaq, and Qaqortoq properties/license areas. *MLJ*

Magnesite-bearing inclusion assemblage in natural diamond. A. Wang, J. D. Pasteris, H. O. A. Meyer, and M. L. Dele-Duboi, *Earth and Planetary Science Letters,* Vol. 141, No. 1–4, 1996, pp. 293–306.

An inclusion in a diamond from the Finsch kimberlite pipe, South Africa, contains a euhedral rhombohedron-shaped crystal (~30 μm) of magnesite coexisting with several idiomorphic olivine (Fo_{93}) grains (~80 μm); many tiny anatase particles (~2–5 μm) and microcrystallites of diamond (<1 μm) and disordered graphite are attached to the surface of the magnesite grain. The occurrence of this syngenetic multiphase inclusion assemblage—that is, a group of many minerals that formed at the same time, before or during the growth of the host—in a natural diamond provides unambiguous evidence for the existence in the Earth's mantle of magnesite, which some have suggested is a major carbon reservoir in most of the mantle.

This inclusion assemblage suggests that two reactions involving the decomposition of the carbonates in mantle peridotite may occur during decompression. The P-T-fO_2 conditions defined by the inclusion are represented by the intersection of the graphite-diamond transition curve with the enstatite-magnesite-olivine-diamond buffer; they represent the highest oxidation state under which a mantle diamond can be stabilized in a peridotite environment. This indicates that the conditions for diamond formation are very limited if carbonates are major carbon sources for diamonds. It also suggests that, given the extremely low relative amounts of free oxygen inferred for portions of the Earth's mantle, carbonates may surely occur in peridotites, and much of the carbon in the mantle may be locked in reduced phases. *RAH*

NWT Diamonds Project. *Report of the Environmental Assessment Panel.* Canadian Environmental Assessment Agency, Hull, Quebec, June 1996, 88 pp.

BHP/Dia Met proposes to establish a diamond mine to draw ore from five kimberlite pipes in the Lac de Gras area of the Northwest Territories. They plan to use a combination of open-pit and underground methods over a 25-year period. The extremely fragile environment in the Canadian Arctic has been a major concern with respect to this project. Further, there are economic, social, and cultural factors that require consideration (e.g., the welfare of aboriginal peoples).

In December 1994, a four-member federal environmental assessment panel was appointed to review all aspects of the proposed project, as documented by BHP in a series of impact statements. The panel's report, published in this volume, concludes that the "environmental effects of the Project are largely predictable and mitigable." Further, the potential economic benefits from the project are large, and the socio-cultural effects are likely to be both positive and negative (the latter to be addressed in the future). Thus, the panel advocates approval by the Canadian government provided 28 recommendations are met.

The recommendations cover a wide spectrum of subjects, including: quick and equitable settlement of aboriginal land claims; annual reports on monitored air and water quality; detailed monitoring of caribou herds and bird populations; cash compensation for the loss of fish habitat; monitoring of socio-economic conditions and trends resulting from the project; and establishment by the government of procedures for diamond evaluation before full production starts.

This report, which has been approved by the federal cabinet, is a major step toward establishing a significant diamond-mining industry in Canada. The first rough diamonds may appear as soon as late 1998 (annual production is projected to reach 5,000,000 carats within five years). It also sets environmental, cultural, and sociological standards for future diamond-mining projects in northern Canada. *AAL*

Review of diamond resources in South Australia. I. J. Townsend, B. J. Morris, and M. G. Farrand, *Australian Gemmologist,* Vol. 19, No. 5, 1996, pp. 233–236.

Although most people associate Australian diamonds with the highly productive Argyle lamproite pipe found in 1979 in the northwest of the country, diamonds were found much earlier in the east, in 1851 in New South Wales, and in the south, in 1859 in South Australia. In both cases, the diamonds were alluvial and were found by gold panners. This paper briefly describes the original (in the Echunga Goldfield) and all subsequent South Australian diamond occurrences, none of which is economic.

Occurrences in which 100–200 stones have been reported include the Echunga Goldfield (the largest recorded stone weighed 5.25 ct), the Springfield Basin, and kimberlite dikes near Eurelia. The dikes are the only proven primary source of diamonds; 140 microdiamonds have been recovered from them.

Ten other localities, widely scattered throughout South Australia, have yielded up to 10 stones from gravels (e.g., gold placers), soils, or occasionally from rocks of recycled secondary origin (e.g., sandstone). A number of zones with kimberlitic indicator minerals have been defined.

All of these diamond occurrences are on—or adjacent to—the Gawler Craton, so this part of South Australia has the basic geologic requirement for primary diamond deposits. Accordingly, extensive exploration has been undertaken in recent years. Despite the use of various techniques (such as aeromagnetic geophysical surveys), no economic deposits have been reported. *AAL*

Subduction model for the origin of some diamonds in the Phanerozoic of eastern New South Wales. L. M. Barron, S. R. Lishmund, G. M. Oakes, B. J. Barron, and F. L. Sutherland, *Australian Journal of Earth Sciences*, Vol. 43, No. 3, 1996, pp. 257–267.

Eastern New South Wales, Australia, has produced more than 500,000 carats of alluvial diamonds, mostly from the Copeton-Bingara area. A local source is indicated by the diamonds' distinct character and lack of surface damage; their $\delta^{13}C$ values and suite of mineral inclusions are unlike those in diamonds from conventional diamond-producing areas, and their Phanerozoic setting is more than 1,000 km from the nearest craton. A subduction model has been developed to explain the origin and geology of these diamonds. This model involves prolonged subduction of mature oceanic crust, resulting in the development of a low-temperature metamorphic window into the diamond stability field within the downgoing slab, at half the depth required by conventional models.

The diamonds are preserved at depth by the termination of subduction, and they are brought to the surface by overriding lithospheric plates or by entrainment in suitable magmas. The type of diamond formed depends on the original source rock. This model predicts that the New South Wales diamonds are young (Phanerozoic) and that their features, age, associated minerals, and geographic distribution relate to the New South Wales tectonic provinces. The subduction diamond model extends the range of indicator minerals to include corundum and Na-bearing garnet, with a new series of carrier magmas (basanite, nephelinite, leucitite). *RAH*

World diamond production increases in '95. R. Shor, *Jewelers' Circular-Keystone*, Vol. 167, No. 10, October 1996, pp. 104–108.

World diamond production in 1995 increased by less than 1% over 1994, to a total of 107.9 million carats (Mct). Australia is still the world's largest producer by volume (40.8 Mct), followed by Zaire (20 Mct), Botswana (16.8 Mct), Russia (12.5 Mct), and South Africa (10.1 Mct). These five countries accounted for 92.8% by weight of the world's 1995 diamond production. Angola and Namibia produced about 1.8% and 1.2% of the world's diamonds, respectively; and about a dozen other countries, mainly in West Africa and South America, shared the remaining 4.2%. By value, the top-producing countries were (in decreasing order): Botswana, Russia, South Africa, Angola, Zaire, Namibia, and Australia.

This paper gives the current status of mining and production from all important diamond-producing countries, including selected details on production from important mines, recent changes in mine recovery operations, insight into exploration activities, and plans of certain companies for specific mines (e.g., De Beers is converting the presently dormant Mwadui [Williamson] mine in Tanzania into a smaller, low-cost operation). Of particular interest is the fact that the Argyle mine stopped recovering stones smaller than 1.5 mm, resulting in a production decrease of 3 Mct but a revenue increase of $15 million.

Mention is made of a small diamond mine now operating at Kelsey Lake, Colorado [see also the Gem News entry in this issue, pp. 282–283], the first in the United States since the 1930s, when the Prairie Creek pipe near Murfreesboro, Arkansas, ceased commercial operation. According to Mr. Shor, the Kelsey Lake mine is projected to produce 100,000 to 150,000 carats per year, which will barely register in future worldwide statistics. However, a mine in the Northwest Territories of Canada, expected to be fully operational in 1998, is projected to produce about 2% of the world's diamonds in the near future. *AAL*

INSTRUMENTS AND TECHNIQUES

The Adamas Advantage Gem Identification Kit 1.2e—a review. P. G. Read, *Journal of Gemmology*, Vol. 25, No. 3, 1996, pp. 219–224.

The author of one well-known gem identification software package reviews a competitor's product: the Adamas Advantage Gem Identification Kit (version 1.2e for Microsoft Windows). This subset of the larger Adamas Advantage program is relatively easy to use and, with 524 gem materials in its database, will satisfy the needs of most gemologists. Following a description of how to use the program, Mr. Read points out a few of its shortcomings. Although these "bugs" are not sufficient to deter potential buyers, users should be aware of them. The article closes with recommendations for improvements and an address where the kit can be obtained. *CMS*

The Bailey light source. T. Linton, R. Beattie, and G. Brown, *Australian Gemmologist*, Vol. 19, No. 6, 1996, pp. 250–251.

The Bailey light source, a refractometer light source developed and manufactured by South Australian gemologist Tony Bailey, was assessed by the Brisbane Instrument Evaluation Committee. Mr. Bailey came up with the idea in 1992, in response to the high cost of conventional sodium-vapor light sources. The Bailey product has three components: an LED light source (with six LEDs), a stained wooden base, and alternative sources of power (either a 240-volt power pack or a nine-volt dry-cell battery).

Although the mean wavelength of 580 nm that is emitted by the LEDs closely approximates the sodium-vapor emission doublet, the measured luminance of the six LEDs was only 18% that of the sodium lamp. The accuracy of the Bailey light source was evaluated on a Topcon refractometer; no significant differences were seen in the refractive indices determined by either the Bailey or the

sodium-vapor light source. However, the Bailey light source, with its essentially horizontally directed yellow light beam, relies on the output of its six LEDs, rather than any slight increase in their angle of emission, to produce a bright scale. A significant increase in the brightness of the scale can be accomplished by either altering the orientation of the LEDs a few degrees upward or by placing the wooden base on an angle.

The evaluation committee found the Bailey device to be a very economical alternative light source for the gem refractometer. However, the committee suggested that a more efficient array of LEDs be considered when this light is used with refractometers of Rayner or Topcon design, which produce brighter scales in their eyepieces when light is angled upward into their light-emitting portals. *MD*

Fade testing: Has the time come? K. Nassau, *Jewelers' Circular-Keystone*, Vol. 167, No. 9, September 1996, pp. 116–117.

This article, by noted author Kurt Nassau, raises an interesting question: Should fade testing be used routinely to check the permanence of color in certain gem materials? Although fade testing can be slightly destructive, sometimes it is needed to complete a difficult gemological identification.

Here, Dr. Nassau concentrates primarily on yellow-orange-brown sapphires and yellow-orange-brown topaz. A technique for fade testing is described that permits the rapid and reliable identification of rapid-fading color in some gem species. A simple, inexpensive fade testing apparatus is also described. It can be built and used easily—with negligible effect on colorfast or slowly fading material. A good suggestion by the author is that a person submitting material for a fade test should sign a disclaimer acknowledging the potential for color loss. *JEC*

JEWELRY HISTORY

Antique Cameos. O. Y. Neverov, *World of Stone*, No. 7, 1995, pp. 29–32.

In this interesting article, more technical than many, the author proves to be extremely knowledgeable about antique cameos.

Antique cameos are distinctive works in miniature. Long known as exquisite, impeccable jewels, many ancient cameos served a different purpose: They were tributes to the strength and power of a worshipped sovereign, his military accomplishments, and his dynasty—subjects very different from those used in today's cameos. In some ways, the art of cameo carving was similar to that of making medals—it served to document the life of an important figure.

The author discusses minerals used during specific time periods and provides historical background on some well-preserved cameos. There is also information on the cameo carvers themselves.

For those fascinated with cameos (for pleasure or profession), this article is essential. *AMB*

Roots of the turquoise trade. S. E. Thompson, *Lapidary Journal*, Vol. 50, No. 3, June 1996, pp. 57–60.

A thousand years ago, turquoise was "so valuable, a man could carry on his back a fortune in turquoise. It was like carrying your weight in diamonds."

So says Dr. Garman Harbottle, who—along with Phil C. Weigand—has spent 20 years piecing together turquoise trade routes between central Mexico and what is today the American southwest in an effort to discover where the Mesoamericans got their turquoise. By using an essentially nondestructive technique called neutron-activation analysis, Dr. Harbottle and Mr. Weigand have shown that samples recovered from individual mines have specific chemical profiles, and that these profiles are different for different mines. With this information, the two have been able to analyze samples from ancient Mexican artifacts and match the profiles to those of known samples from specific mines in the southwest.

The historical perspectives are fascinating, as are the conclusions attained through analytical means. Far from being a purely scientific report, the article conjures images of resolute ancients. To think of the hardships endured a thousand years ago to travel hundreds of miles in search of a blue stone makes one realize how much humans are willing to sacrifice for objects of wealth or worship. *JM*

PRECIOUS METALS

Improved wear resistance with electroplated gold containing diamond dispersions. A. R. Zielonka, *Gold Technology*, No. 16, July 1995, pp 16–20

This article reports the results of a research project funded by the World Gold Council and conducted by the Precious Metals Research Institute in Germany. Electroplating gold with a conventional cyanide gold electrolyte containing a fine homogeneous diamond power improved (as one would expect) the wear resistance of gold jewelry. Almost all of the relevant details of the electrolyte composition and the operation are presented: Auruna 556 electrolyte, 0.25 micron diamond powder, deposition rate of 0.5 microns per minute, turbulent flow, and so on. The diamond content of the electrolyte—and, therefore, the electroplated layers—was varied up to 200 grams per liter and 2.76%, respectively. Wear tests using "grinding" paper showed that wear resistance increased three-fold over that of pure gold, making the finished product almost twice as resistant to wear as copper but still only one-fifth as resistant as pure nickel. The additional cost to coat a ring would be a matter of pennies. *CEA*

INDEX TO VOLUME 32

NUMBERS 1–4 1996

SUBJECT INDEX

This index gives the first author (in parentheses), the issue, and the first page (plus "ff") of the article in which the indexed subject occurs. For Gem News (GN), Gem Trade Lab Notes (GTLN), and Letters (Let) sections, inclusive pages are given for the subject item. The reader is referred to the Author Index at the end of this section for the full title and the coauthors, where appropriate, of the articles cited. The pages covered by each issue are as follows: Spring (1–78), Summer (79–152), Fall (153–230), Winter (231–308).

D

E

AUTHOR INDEX

This index lists, in alphabetical order, the names of authors of all articles that appeared in the four issues of Volume 32 of *Gems & Gemology*, together with the inclusive page numbers and the specific isssue (in parentheses). Full citation is provided under the first author only, with reference made from joint authors.